Unfolded protein responses in models of Motor Neuron Disease

Alice Wing Sze Kwok

The Queen's College

University of Oxford

Submitted for the Degree of Doctor of Philosophy

Michaelmas Term 2010

Abstract

Unfolded protein responses in models of Motor Neuron Disease

Alice Wing Sze Kwok
The Queen's College, University of Oxford
Thesis submitted for the Degree of Doctor of Philosophy
Michaelmas Term 2010

Motor neuron disorders are a heterogeneous group of diseases characterized by the selective degeneration of motor neurons leading to muscle wasting and atrophy. Amyotrophic Lateral Sclerosis (ALS) is the most common amongst these disorders and is characterized by the selective loss of both upper and lower motor neurons in the brain and spinal cord. 20% of familial cases of ALS are caused by mutations in the Cu, Zn-superoxide dismutase gene (SOD1), a ubiquitously expressed enzyme responsible for scavenging superoxide radicals. The exact mechanisms underlying mutant SOD1-mediated neurotoxicity are unknown. Misfolded mutant SOD1 accumulates in the cytosol and mitochondrial intermembrane space (IMS) indicating the involvement of unfolded protein responses in ALS pathogenesis.

Unfolded protein responses (UPRs) are complex signal transduction cascades which detect perturbations in protein folding and couple them to the expression of protein quality control machinery thereby allowing individual compartments to adapt to stress. In the cytosol, this study has shown that HspB8 was upregulated by SOD1 mutants, where it induced the clearance of aggregates by macroautophagy. This is a protective mechanism, as overexpression of HspB8 suppressed mutant-SOD1 mediated toxicity. In contrast, HspB8 mutants were impaired in macroautophagy and are toxic to NSC-34 cells.

The mechanisms for the IMS-UPR have not been previously identified. To address this issue, a model for the accumulation of misfolded mutant SOD1 within the IMS was created and candidate proteins involved in protein quality control within the IMS were explored at the transcriptional level and at the level of protein expression. Preliminary results revealed some possible candidates that may have a role in the adaptation to mitochondrial stress. Interestingly, increased mitophagy was also found in IMS-G93A expressing cells, advocating the central role of macroautophagy in eliminating protein aggregates and damaged mitochondria in SOD1-FALS.

Declaration

All research reported in this thesis was performed by the author in the Department of Physiology, Anatomy, and Genetics, University of Oxford. Except where acknowledgement is made, all the work presented is my own and has not been submitted for any other degree in this or any other University or Institute of learning.

Acknowledgements

I am very grateful to my supervisors, Professor Kevin Talbot and Dr. Vishwas Agashe, for their supervision and advice throughout my years as a graduate student. It has truly been an enjoyable learning experience and one which I have greatly benefited from. I am also very grateful to Professor Kay Davies for allowing me to working in the laboratory. In addition, I would like to thank all past and present members of the Davies and Talbot labs for their advice and contributions throughout the years. In particular, I am very appreciative to Dr. Bradley Turner, who despite being in Melbourne, has provided lots of advice for the work presented in this thesis. I am also grateful to Dr. Neza Alfazema for all the animal work and Miss Annie Raw for performing the early in-situ work on HspB8. In addition, I would like to thank all the collaborators: Dr. Kanchan Phadwal and Dr. Katja Simon at the Nuffield Department of Medicine for their expertise with the Imagestream experiments; Miss Rebecca Dragovic at the Nuffield Department of Obstetrics and Gynecology for performing the FACS experiments; and Dr. Karl Morton also at the NDOG for advice on the oxygen clark electrode experiments. I would like to thank Miss Mattea Finelli, Mr. Alastair Crisp, Miss Anna Dulneva, Mr. Jun Jie Tan, Dr. Jing-Huan Li, and Dr. Carmen Coxon for livening up the atmosphere and making it a fun and engaging experience for the past 3 years. I am also very appreciative to all my friends from college and the department, who have supported and encouraged me throughout my years here.

Last but by no means least, I am most grateful to my wonderful parents, who have always supported me in all my pursuits and have provided me with every opportunity to learn and grow. My father, whose passion for mathematics and learning is truly inspirational and something I hope to emulate. I am also extremely grateful to my mother and siblings who never cease to amaze me and whose expressed support throughout my years at Oxford was encouraging and motivational to say the least. This thesis is dedicated to my family.

Contents

List of abbreviations

AIF	Apoptosis-inducing factor
ALS	Amyotrophic Lateral Sclerosis
ALS2	Alsin
ANG	Angiogenin
ATF4	Activating transcription factor 4
ATF6	Activating transcription factor 6
Bag3	Bcl2-associated athanogene 3
Bcl2	B cell lymphoma 2
BiP	Immunoglobulin heavy chain binding protein
C/EBPβ	CCAAT enhancer binding protein beta
CCS	Copper chaperone for SOD1
Chchd4	Coiled-coil-coiled-coil-helix domain containing 4
CHIP	Carboxy terminus of Hsc70-interacting protein
CHOP	c/EBP homologous protein
ClpP	Proteolytic subunit of Casinolytic protease
CMT	Charcot Marie Tooth Disease
DegP	Degradative protease P
DegS	Degradative protease S
dHMN	Distal Hereditary Motor Neuropathy
DNAJ	DNA J homolog
eIF2α	Eukaryotic initation factor 2 alpha
ER	Endoplasmic reticulum
ERAD	ER-associated degradation
Erv1	Essential for respiration and viability 1
FALS	Familial ALS
FUS	Fused in sarcoma
GAPDH	Glyceraldehyde 3-phosphate dehydrogenase
GEF	Guanine-nucleotide exchange factor

Gfer	Growth factor, augmenter of liver regeneration
GrpE	Glucose-related protein E
HSE	Heat shock element
HSR	Heat shock response
Hsf1	Heat shock factor 1
Hsps	Heat shock proteins
HtrA2	High temperature requirement protein A2
IMM	Inner mitochondrial membrane
IMS	Intermembrane space
IRE1	Inositol requiring enzyme 1
LC3	Microtubule-associated protein light chain 3
Lon	DNA-binding ATP-dependent protease La
Map1LC3A	Microtubule-associated protein light chain 3A
MIA	Mitochondrial intermembrane space assembly
mtHsp70	Mitochondrial Hsp70
NFκB	Nuclear factor kappa-light chain-enhancer of activated B cells
NMJ	Neuromuscular junction
OMM	Outer mitochondrial membrane
OPTN	Optineurin
OTC	Ornithine transcarbamylase
PBMCs	Peripheral blood mononuclear cells
PERK	Protein kinase-like ER kinase
PI3K	Phosphatidylinositol 3 kinase
PINK1	PTEN-induced putative kinase 1
ROS	Reactive oxygen species
SALS	Sporadic ALS
SCF	Skp-Cullin F box
SETX	Senataxin
sHsps	Small Heat Shock proteins
SOD1	Cu/Zn superoxide dismutase 1

TCL	Total cell lysates
TDP-43	TAR DNA-binding protein
Tim9	Translocase of the inner mitochondrial membrane 9
Tim10	Translocase of the inner mitochondrial membrane 10
UPR	Unfolded protein response
UPR^{ER}	Unfolded protein response of the endoplasmic reticulum
UPR^{mt}	Unfolded protein response of the mitochondrial matrix
UPS	Ubiquitin proteasome system
VAPB	Vesicle associated membrane protein B
VCP	Valosin-containing protein
VDAC1	Voltage-dependent anion channel 1
XBP1	X-box binding protein 1
Yme1L1	Yeast mitochondrial escape 1 like-1 protein

List of Figures

List of Tables

Introduction

Motor neuron disorders are a heterogeneous group of diseases characterized by the selective degeneration of motor neurons leading to muscle weakness and atrophy. Two groups of motor neurons are affected: lower motor neurons which originate in the spinal cord and brainstem nuclei and whose axons directly contact and innervate skeletal muscles, and upper motor neurons which originate in the cerebral cortex and whose direct connection with lower motor neurons (or interneurons that synapse with lower motor neurons) is necessary for controlling voluntary movement. Upper motor neurons are clustered together to form descending tracts in the brain and the spinal cord. In anthropoid primates, the largest and most important of these tracts is the corticospinal tract, in which direct corticomotoneuronal synapses are found and is required for the development of 'skilled' motor capacities, such as enhanced dexterity of distal musculature, particularly in humans (Heffner and Masterton, 1975, Heffner and Masterton, 1983, Bortoff and Strick, 1993). Direct corticomotoneuronal connections appear to be a unique feature in primates and there is little evidence of a major role of the corticospinal tract in non-primate mammals (Eisen, 2009). Motor neuron disorders are broadly divided into three main groups: those that affect upper motor neurons only such as Primary Lateral Sclerosis and Hereditary Spastic Paraplegia, pure lower motor neuron disorders such as Spinal Muscular Atrophy and Progressive muscular atrophy, and those that affect a combination of upper and lower motor neurons such as Progressive Bulbar Palsy and Amyotrophic Lateral Sclerosis (ALS).

Recent advances in our understanding of the genetics of motor neuron disorders have provided valuable insights into the reasons for the selective vulnerability of motor neurons in sporadic and familial forms of these diseases. Motor neurons are highly adapted to their functions and it is likely that these specialized features leave them particularly vulnerable to cell death. A major feature of motor neurons is their large volume (up to 5000 times that of a typical cell) and extreme polarity; in addition to the soma (~50-60μm), motor neurons also have extensive dendritic trees (up to ~1000 μm in extent) and a long axon that can extend up to a metre away from the soma [reviewed in (Nicholson et al., 2000)]. Consequently, motor neurons are very reliant on (i) the integrity of the cytoskeleton for shape and tensile strength as well as providing the means by which materials are transported around cells and (ii) mitochondria to meet the high metabolic demands of the cell. Oxidative phosphorylation in mitochondria provides much of the ATP required for maintaining membrane potentials across the axon, protein synthesis and degradation, and retrograde and anterograde transport. Motor neurons also have high thresholds for activation of the heat shock response, thus compromising their ability to protect against damage during cell stress (Batulan et al., 2003). To illustrate the involvement of some of these processes in motor neuron degeneration, this thesis will primarily focus on the familial ALS model that is based on mutations in Cu/Zn superoxide dismutase 1 (SOD1). A section of the thesis will also relate to motor neuron disorders of the peripheral nervous system, Distal Hereditary Motor Neuropathy (dHMN) and Charcot Marie Tooth Disease (CMT).

1.1 Amyotrophic Lateral Sclerosis

ALS is a debilitating neurodegenerative disorder characterized by the relentless loss of upper and lower motor neurons in the cortex, brainstem and spinal cord leading to progressive muscle weakness and atrophy, with associated spasticity and brisk tendon reflexes. ALS typically develops between 50-70 years of age and initial motor symptoms appear focally in either one limb (often referred to as spinal onset) or in the muscles of speech and swallowing (referred to as bulbar onset) (Talbot, 2002, Ravits et al., 2007). Motor involvement becomes progressively more diffuse as disease progresses [reviewed in (Ravits and La Spada, 2009)]. In affected motor neurons, ubiquitinated proteinaceous inclusions, abnormal mitochondria, and neurofilament aggregates are found at autopsy. Neighbouring glial cells are also affected, and evidence from transgenic models suggests that the release of inflammatory mediators from activated glia may contribute to the spread of degeneration from one focal point to another. It is not yet clear if glial involvement contributes to ALS pathogenesis or occurs secondary to disease in humans [reviewed in (McGeer and McGeer, 2002)]. The rate of disease progression is generally rapid and most patients die within 2-3 years of symptom onset, usually as a result of respiratory failure. Only 8-22% of ALS patients survive for at least 10 years [reviewed in (Talbot, 2009)]. There is currently no cure or preventative treatment for ALS; the only prescription drug available is Riluzole, a glutamate antagonist that delays the onset of ventilator-dependence and extends life by 3-5 months in a subset of patients (Miller et al., 2003, Traynor et al., 2003, Talbot, 2009).

With an annual incidence rate of 1-2 per 100,000 in most populations and a prevalence of 4 per 100,000, ALS is the most common of adult-onset motor neuron disorders. Higher incidences of ALS-like syndromes have been reported in 3 foci in the Western Pacific, namely in Western Pacific of Guam (Koerner, 1952, Arnold et al., 1953, Kurland and Mulder, 1954), the Kii Peninsula of Japan (Hirano et al., 1966), and Western New Guinea (Gajdusek, 1963, 1982, Gajdusek and Salazar, 1982). These 3 diseases appear to be the same and have characteristic tau pathology that distinguishes them from ubiquitin-related ALS (Ikemoto et al., 2000). 95% of ALS cases are sporadic (SALS) with mostly unknown etiology although genetic predisposition is likely to be involved. A large number of candidate genetic susceptibility or modifier genes including angiogenin, ciliary neurotrophic factor, neurofilament heavy chain, peripherin, monoamine oxidase B, survival motor neuron, and vascular endothelial growth factor have been identified through association studies although these have not yet been confirmed in repeated studies [reviewed in (Schymick et al., 2007, Beleza-Meireles and Al-Chalabi, 2009)]. The remaining 5% of ALS cases are inherited and are referred to as familial ALS (FALS) (Byrne et al., 2010). So far, 9 genes with a mendelian inheritance pattern have been identified in ALS, though for several of these the clinical features are highly atypical and probably should not be considered as having direct relevance to most cases of FALS and SALS (ALS2 due to mutations in alsin, ALS4 due to senataxin and ALS8 due to VAPB). Familial and sporadic forms of ALS are clinically indistinguishable from each other and both affect motor neurons with a similar pathology although cytoplasmic TAR DNA binding protein (TDP-43) inclusion bodies are absent in FALS cases associated with Cu/Zn superoxide dismutase (SOD1) (Mackenzie et al., 2007).

1.2 Genetics of FALS

In 1993, the first gene linked to familial ALS was identified in 13 families (Rosen, 1993). Located on chromosome 21q22.1, this gene encodes a ubiquitously expressed free radical scavenging enzyme Cu/Zn superoxide dismutase 1 (SOD1). SOD1 mutations account for 1% of all ALS cases and 20% of all FALS cases (Cleveland and Rothstein, 2001).

Since then, several other causative genes associated with diverse range of cellular processes including RNA processing, membrane trafficking, and axonal transport have been identified (reviewed in Table 1.1). Mutations in TAR DNA-binding protein (TDP-43) (Neumann et al., 2006, Kabashi et al., 2008), fused in sarcoma (FUS) (Kwiatkowski et al., 2009, Vance et al., 2009), and angiogenin (ANG) (Greenway et al., 2006) all give rise to autosomal dominant, adult-onset ALS, although these occur less frequently than SOD1 mutations. A recessively inherited, juvenile-onset form of ALS that progresses more slowly compared to classical ALS has been attributed to mutations in alsin – a gene encoding a putative activator of small G-proteins of the Ras superfamily (Hadano et al., 2001). Mutations in the vesicle trafficking protein, vesicle-associated membrane protein B (VAPB), are associated with an atypical, slowly progressive form of ALS (Nishimura et al., 2004). Mutations in the gene encoding optineurin (OPTN) have also been identified in 3 Japanese families with ALS (Maruyama et al., 2010). Although precise functions have yet to be elucidated, optineurin is suggested to be involved in nuclear factor kappa-light

Table 1.1 Genetics of FALS [adapted from (Dion et al., 2009)]

Locus	Gene	Linkage	Disease and inheritance pattern	Known Gene Function(s)	References
ALS1	SOD1	21q22.11	Mainly autosomal dominant with the exception of D90A and N85S	Free radical scavenger	(Rosen, 1993)
ALS2	ALS2	2q33.2	Autosomal recessive juvenile ALS	Predicted to be a regulator of GTPase based on its three putative guanine-nucleotide exchange factor (GEF) domains	(Hadano et al., 2001, Yang et al., 2001)
ALS3	Unknown	18q21	Autosomal dominant	Unknown	(Hand et al., 2002)
ALS4	SETX	9q34	Autosomal dominant juvenile ALS	DNA and RNA metabolism	(Chen et al., 2004)
ALS5	Unknown	15q15.1-21.1	Autosomal recessive	Unknown	(Hentati et al., 1998)
ALS6	FUS	16p11.2	Autosomal dominant	DNA repair; regulation of transcription; RNA splicing and transport	(Kwiatkowski et al., 2009, Vance et al., 2009)
ALS7	Unknown	20p13	Autosomal dominant	Unknown	(Sapp et al., 2003)
ALS8	VAPB	20q13.33	Autosomal dominant, slowly progressive ALS	Axonal transport; vesicle trafficking	(Nishimura et al., 2004)
ALS9	ANG	14q11.1	Autosomal dominant	Neovascularization	(Greenway et al., 2006)
ALS10	TARDBP (TDP-43)	21q22.11	Autosomal dominant; ALS with FTD	RNA binding and splicing	(Neumann et al., 2006, Mackenzie et al., 2007)
ALS	DCTN1	2p13	Autosomal dominant	Microtubule binding; axonal transport	(Puls et al., 2003)
ALS	OPTN	10p13	Autosomal recessive and dominant	NF-κB signaling, golgi maintenance and trafficking	(Maruyama et al., 2010)
ALS	VCP	9p13.3	Autosomal dominant	Proteostasis; cell cycling; cell signaling, organelle biogenesis; autophagy	(Johnson et al., 2010)

chain-enhancer of activated B cells (NF-κB) signaling, as well as golgi maintenance and trafficking (Maruyama et al., 2010). More recently however, mutations in valosin-containing protein (VCP) have been identified in FALS individuals by whole exome sequencing (Johnson et al., 2010). VCP is a highly conserved AAA+ ATPase involved in the removal of selected proteins from their complexes for recycling and degradation in an ubiquitin-dependent manner (Halawani and Latterich, 2006, Ju et al., 2009). As such, VCP has an important role in maintaining proteostasis in cells through the ubiquitin proteasome system (UPS) and autophagy pathways. Causative genes have still yet to be identified in the ALS3, ALS7, ALSX loci, on chromosomes 18 and 20 and the X chromosome respectively.

The variety of genes that cause or predispose to ALS illustrates the heterogeneous and complex nature of this disease. Moreover, it indicates that motor neuron degeneration in ALS derives from multiple interconnected pathways and susceptibility factors.

1.3 Hereditary peripheral motor neuropathies

Distal hereditary motor neuropathies (dHMN) are a spectrum of diseases characterised by motor neuron degeneration in the peripheral nervous system (Harding, 1993). Symptom onset usually occurs during childhood or adolescence and begins with weakness and progressive wasting of extensor muscles of the toes and feet. As the disease progresses, weakness and atrophy can also occur in proximal muscles of the lower limb and distal upper limbs. dHMN closely resembles another peripheral motor neuropathy, Charcot Marie Tooth disease, except that there is no sensory involvement (Harding and

Thomas, 1980). CMT is most common of peripheral motor neuropathies and is subdivided into two types: CMT1 is a demyelinating disorder and CMT2 is classed as an axonopathy (Dyck and Lambert, 1968a, b). In general, it is difficult to distinguish between dHMN and CMT2 because sensory signs are often lacking in CMT2 patients and as such, electrophysiological examinations are required to confirm diagnosis (Harding and Thomas, 1980).

1.3.1 Small heat shock proteins HspB1 and HspB8

Small heat shock proteins (sHsps) are a subclass of Hsps that are induced in response to a variety of stress stimuli. Ranging from 12-43kDa, all ten members of the sHsp family share a common central α-crystallin domain, that is required for assembly into higher oligomers. The formation of homo- or heterooligomeric complexes is obligatory for sHsp chaperone functions (Kim et al., 1998, van Montfort et al., 2001, Van Montfort et al., 2002). As they lack intrinsic ATP activity, sHsps mainly serve to prevent the aggregation of folding intermediates and misfolded proteins (Horwitz, 1992, Ehrnsperger et al., 1997, Lee et al., 1997).

The importance of sHsps for the survival of motor and sensory neurons is exemplified by mutations in small heat shock protein B1 (HspB1; also known as Hsp27) and small heat shock protein B8 (HspB8; also known as Hsp22) genes found in dHMN and CMT2 families (Evgrafov et al., 2004, Irobi et al., 2004). Six missense mutations have been identified in HspB1 of which four mutations (R127W, S135F, R136W and T151)

were found in the highly conserved α-crystallin domain (Evgrafov et al., 2004, Liu et al., 2005b). The remaining two mutations both result in a substitution of the proline residue at position 182 in the C-terminal region (Kijima et al., 2005). Likewise, two missense mutations have been identified in the α-crystallin domain of HspB8 in European, Chinese and Japanese CMT2L and dHMN families (Irobi et al., 2004, Tang et al., 2004, Tang et al., 2005). Both mutations result in a substitution of the lysine residue at position 141 (K141E and K141N) (Irobi et al., 2004). These mutations are associated with a toxic gain-of-function of the chaperone.

The majority of mutations in HspB1 and HspB8 target amino acids in the α-crystallin domain resulting in reduced conformational stability and an increased tendency of the mutant chaperone to aggregate (Ackerley et al., 2006). As described below, SOD1 mutants also demonstrate increased aggregation propensity suggesting that the combination of protein misfolding and impaired protein quality control may be common pathogenic mechanisms in motor neuron disorders.

1.4 Structure and functions of SOD1

1.4.1 Structure

SOD1 is a highly conserved 153 amino acid homodimeric metalloenzyme. Each subunit consists of an 8-stranded, anti-parallel Greek-key β-barrel motif that normally binds a catalytic copper ion at its active site and a zinc ion that is essential for the structural stability of the enzyme (Tainer et al., 1982, Bertini et al., 1998). Histidine residues link the

Cu^{2+} and Zn^{2+} ions in each subunit; a direct bridge is formed between the ions via His-63, whilst an extended secondary bridge is formed via His-46 (a copper ligand) and His-71 (a zinc ligand) with Asp-125. The subunits are held together through hydrophobic contacts and whilst the dimer interface is predominantly hydrophobic, there is also a significant (30%) proportion of the interface that is hydrophilic. The fully metallated (holo) protein is extremely stable, melting at temperatures of 85-95^{0}C (Roe et al., 1988) and retaining its catalytic activity in 8 M urea or 4 % SDS (Forman and Fridovic.I, 1973).

The stability of the SOD1 enzyme is dependent on a series of post-translation maturation steps including copper and zinc binding, disulphide bond formation and N-terminal acetylation of each subunit. Copper binding occurs first and is assisted by the chaperone, copper chaperone for SOD1 (CCS) (Culotta et al., 1997). During copper acquisition, a temporary heterodimer between SOD1 and CCS is formed via an intermolecular disulphide bond; the bond is broken and CCS is released upon copper acquisition and intramolecular disulphide bond formation in SOD1 (Field et al., 2003). The mechanism for zinc acquisition in SOD1 has not yet been identified.

An unusual feature of the native SOD1 holoenzyme is the presence of an intramolecular disulphide bond that is maintained despite the highly reducing chemical environment of the cytosol. Normally, disulphide bonds are only maintained in extracellular proteins, where the prevailing redox conditions are highly favourable to their formation, and their formation greatly increases the stability of these proteins (Derman et al., 1993, Battistoni et al., 1999). Similarly in SOD1, the disulphide bond between cysteines 57 and 146 (Bordo et al., 1994) confers exceptionally high thermostability of the

holoenzyme and also serves to promote the homodimerization of SOD1 monomers that is necessary for catalytic activity. The formation of the intrasubunit disulphide bond is driven by the coordination of Cu^{2+} and Zn^{2+} ions within the active site and may be assisted by CCS.

1.4.2 Enzymatic activity

Superoxides ($O_2\bullet^-$) are potent oxidizing agents that must be scavenged by cells to prevent any oxidative damage to protein, DNA or lipids. Traditionally regarded as by-products of aerobic metabolism, the majority of intracellular superoxides are generated by the escape of electrons from mitochondrial respiratory chain complexes. These electrons then react with molecular oxygen to form superoxides. As much as 2% of oxygen consumed by the mitochondria is converted into superoxides by this process (Chance et al., 1979). As such, cells have evolved dismutases to protect against and limit oxidative damage. SOD1 is one such enzyme catalysing the dismutation of superoxide radicals to hydrogen peroxide and oxygen ($2O_2\bullet^- + 2H^+ \rightarrow O_2 + H_2O_2$) (McCord and Fridovich, 1969); this reaction proceeds through a 'ping-pong' mechanism and requires oxidation/reduction of the copper ion within the active site. SOD1 is present within the cytoplasm (Weisiger and Fridovich, 1973) and mitochondria (Sturtz et al., 2001, Field et al., 2003) and whilst the role of cytoplasmic SOD1 in scavenging free radicals is well established, the functions of mitochondrial SOD1 are unknown. Neuronal tissues generate high levels of reactive oxygen species (ROS) compared to other cell types and the high proportion of SOD1 in the

brain (accounts for 1% of total brain protein) indicates the importance of SOD1 activity within these cells (Pardo et al., 1995, Shaw and Eggett, 2000).

1.5 SOD1 variants and mechanisms of toxicity

1.5.1 SOD1 mutations

The past decade of research into SOD1 has found over 150 disease-associated mutations (http://alsod.iop.kcl.ac.uk). These mutations are spread across all 5 exons although a small number can also be found in the 3' untranslated region (3' UTR) and introns [reviewed in (Orrell, 2000)]. Most of the mutations lie in exons 4 and 5 with some codons more susceptible than others. In particular, the glycine residue at position 93 is most susceptible with 6 substitution mutations identified so far. The vast majority of these mutations are missense, although a small number of deletion and insertion mutations are also found [reviewed in (Turner and Talbot, 2008)]. All mutations are dominantly inherited with the exception of D90A and N85S which can also be recessively inherited (Andersen et al., 1995, Andersen et al., 1996, Andersen et al., 1997). Interestingly, the penetrance and phenotype of the D90A mutant allele is believed to be dependent on a cis-acting modifying factor after studies showed that all recessive D90A pedigrees derive from a single common ancestor whereas dominantly inherited D90A families originated from several unrelated ancestors (Al-Chalabi et al., 1998, Parton et al., 2002). Hitherto the putative protection factor has not been identified. A de novo mutation, H80R, has also been identified in a

single Irish SALS patient and is the only de novo mutation verified to date (Alexander et al., 2002).

In general, the association between genotype and phenotype is not clearly defined for the vast majority of SOD1 mutations. Clinical characteristics, age of onset, and rate of disease progression varies widely both within and between families carrying the same mutation making accurate predictions of disease phenotype with mutation difficult. However, there are a few mutations in which disease progression can be reliably predicted. The A4V mutation is most prevalent in North America and is associated with a rather severe and rapidly progressing form (<2yr) of ALS (Rosen et al., 1994, Cudkowicz et al., 1997). The H46R mutation is associated with a protracted disease course with patients surviving an average of 16-18 years following symptom onset (Arisato et al., 2003). D90A is the most prevalent mutation in Europe and is also associated with mildly progressive ALS (average disease duration is 16yr) (Andersen et al., 1996).

SOD1 mutants are believed to result in toxic gain-of-function of the enzyme for several reasons: (i) transgenic mice expressing SOD1 mutants develop the typical clinical and pathological features that are found in human ALS, even in the presence of the endogenous enzyme (Gurney et al., 1994); (ii) overexpression of human wildtype SOD1 did not affect disease progression in transgenic mice expressing mutant G85R or G86R (Bruijn et al., 1998, Audet et al., 2010) but exacerbated disease in G93A and L126Z transgenic mice (Deng et al., 2006); (iii) SOD1 knockout mice do not develop ALS, despite the toxicity of the free radicals (Reaume et al., 1996) and; (iv) several human SOD1 mutations retain dismutase activity despite patients developing the disease (Borchelt et al.,

1994, Bowling et al., 1995). However, despite intensive research, the exact mechanisms underlying mutant-SOD1 cell death remain unknown.

1.5.2 Protein misfolding and aggregation

One of the prevailing hypotheses for mutant SOD1-induced toxicity is related to the propensity of mutant SOD1 to form noxious misfolded protein species and aggregates. Inclusions containing SOD1 aggregates have been found in motor neurons and astrocytes of SALS and FALS patients harbouring SOD1 mutations (Shibata et al., 1996, Ince et al., 1998, Kato et al., 1999, Kokubo et al., 1999), in all transgenic SOD1 mouse models (Dalcanto and Gurney, 1994, Wong et al., 1995, Bruijn et al., 1998) and in neuronal cells expressing mutant SOD1 (Durham et al., 1997). In transgenic models, inclusions appear concomitantly with symptom onset and accumulate markedly towards end stage (Johnston et al., 2000, Wang et al., 2002).

Aggregation of SOD1 requires monomerization, demetallation and oligomerization of the mutant protein. Many, if not all, disease-related mutants can accelerate this process through destabilization of SOD1 structure. For instance, mutations may alter metal binding affinities of mutant SOD1 (Crow et al., 1997, Hayward et al., 2002), increase susceptibility of the mutant protein to disulphide reduction (Tiwari and Hayward, 2003) or other oxidative modifications, alter the net surface charge of the protein [reviewed in (Shaw and Valentine, 2007)] or destabilize the dimer interface (Lindberg et al., 2005) such that they promote monomerization or oligomerization of mutant SOD1. It is not yet known which of the species – soluble monomeric species, oligomers or SOD1 aggregates – confers toxicity

in cells. It has been recently shown that SOD1 mutants that demonstrate a greater propensity to monomerize and aggregate (e.g. A4V) are associated with a much shorter disease course in ALS patients compared to mutations that exhibit a more moderate rate of aggregation (e.g. H46R) indicating that aggregation may influence the progression of disease (Prudencio et al., 2009). Misfolded mutant SOD1 might conceivably cause toxicity by: (i) blocking essential cellular functions or by entrapment of soluble cellular proteins including chaperones and proteasome components; (ii) mitochondrial dysfunction or; (iii) impairing axonal transport. Alternatively, mutant SOD1 aggregates may represent a failure of protein quality control machinery in motor neurons.

1.5.2.1 Heat shock proteins

Heat shock proteins (Hsps) are an evolutionarily conserved family of molecular chaperones that have key roles in the folding of proteins to the native state, preventing protein aggregation, and facilitating the elimination of aberrant proteins (Morimoto et al., 1997, Hartl and Hayer-Hartl, 2002). The age-dependent rise in detergent-insoluble mutant SOD1 species in transgenic mice may result from impairments in chaperone activities within motor neurons. Consistent with this hypothesis, overall chaperoning capacities were reduced in the lumbar region of the spinal cord prior to symptom onset in G85R and G93A mice (Tummala et al., 2005). This could occur by aggregate-induced chaperone sequestration which would reduce the overall pool of available chaperones required for other essential functions. Indeed, several Hsps including Hsp70, Hsp40, Hsp25 and αB-crystallin co-fractionated with mutant SOD1 in the detergent-insoluble fraction of spinal

cord from G93A and H46R/H48Q/H63G/H120G (Shinder et al., 2001, Wang et al., 2003). A direct interaction of mutant SOD1 with chaperones was also confirmed in transfected NSC34 and N2A cells (Okado-Matsumoto and Fridovich, 2002). Increasing chaperone activities through overexpression of Hsp70 suppressed mutant SOD1 aggregation and toxicity in N2A cells (Takeuchi et al., 2002b), but did not have an effect on disease onset nor lifespan in transgenic mice when delivered alone (Liu et al., 2005a). However, genetic delivery of Hsp70 and HspB1 in combination offered more protection to dorsal root ganglion neurons transduced to express mutant SOD1 suggesting that multiple Hsps are required for protection (Patel et al., 2005b). In support of this theory, administration of arimoclomol, a drug that upregulates multiple Hsps though activation of heat shock factor 1 (HSF1), improved muscle performance, motor neuron survival and extended survival in G93A mice (Kieran et al., 2004a). Arimoclomol is currently in phase II clinical trials.

1.5.2.2 Proteolytic machinery

The UPS is the main proteolytic system within the cytosol to degrade misfolded or aberrant proteins. *In vitro* studies have shown that mutant SOD1 is polyubiquitinated and degraded by the proteasome (Urushitani et al., 2002). E3 ligases such as CHIP recognize Hsp70-mutant SOD1 complexes and tag them for proteasomal degradation by ubiquitylation (Urushitani et al., 2004). Initial studies *in vitro* revealed that overall proteasome activity is reduced in mutant SOD1 expressing cells. Furthermore, treating cells with proteasome inhibitors promoted mutant SOD1 insolubility as well as the formation of large SOD1-containing inclusion bodies that resemble those observed in ALS patients and transgenic mice expressing mutant SOD1 leading to the suggestion that

proteasome activity may be compromised *in vivo* (Durham et al., 1997, Puttaparthi et al., 2003). By exploiting a mouse model which allows the monitoring of UPS activity *in vivo*, impairment of UPS activities were observed only in the ventral spinal cord and the brainstem motor nuclei at symptomatic stages of G93A mice (Cheroni et al., 2009). UPS dysfunction was not observed in astrocytes and microglia. In another study, reduced proteasome activities were also observed in spinal cord, but not liver homogenates of G93A mice at symptomatic stages and correlated to a reduction in 20S β5- and 20Sα-proteasome subunits in lumbar motor neurons (Kabashi et al., 2004).

A second proteolytic pathway, autophagy, is complementary to the UPS and is responsible for the bulk degradation of long-lived proteins, dysfunctional organelles, and protein aggregates in the cytosol (Rideout et al., 2004, Bernales et al., 2006, Monastyrska and Klionsky, 2006, Kim et al., 2007). The importance of autophagy in neuronal homeostasis is underscored by the finding that mice deficient in constitutive autophagy showed extensive loss of CNS neurons before dying prematurely, 4 weeks after birth (Hara et al., 2006, Komatsu et al., 2006). Moreover, degenerating neurons were marked by ubiquitin-containing inclusion bodies and protein aggregates similar to those found in neurodegenerative diseases (Hara et al., 2006, Komatsu et al., 2006). Little is known about role of autophagy in SOD1-FALS, except that mutant SOD1 is degraded by autophagy *in vitro* (Kabuta et al., 2006) and that upregulation of macroautophagy was observed in spinal cords of G93A mice in late symptomatic stages (Morimoto et al., 2007). Chaperones such as HspB8 assist in the recognition of mutant SOD1 by the autophagy machinery (Crippa et al., 2010).

1.5.3 Mitochondrial Dysfunction

The initial indications that mitochondria could be involved in the pathogenesis of ALS came from histological observations of vacuolated and disorganized mitochondria in motor neurons and muscle from sporadic and familial ALS patients (Hirano et al., 1984, Sasaki and Iwata, 1996, 2007). Similar morphological abnormalities were also present in motor neurons axons and dendrites in dismutase-active mice (Dalcanto and Gurney, 1994, Wong et al., 1995, Kong and Xu, 1998) but absent in dismutase-inactive mutants (Bruijn et al., 1997). In G37R and G93A transgenic mice, mitochondrial morphological abnormalities present prior to symptom onset and are amongst the earliest pathological changes observed (Dalcanto and Gurney, 1994, Wong et al., 1995, Kong and Xu, 1998). Swollen and fragmented mitochondria were also observed in NSC34 cells constitutively expressing G93A (Menzies et al., 2002a, Raimondi et al., 2006).

Although predominantly a cytoplasmic protein, mutant SOD1 has also been detected in enriched mitochondrial fractions derived from affected, but not unaffected tissues, in several mutant SOD1 mouse models (Mattiazzi et al., 2002, Liu et al., 2004, Bergemalm et al., 2006, Vande Velde et al., 2008). Mutant SOD1 accumulation in the intermembrane space (IMS) and on the cytosolic leaflet of the outer mitochondrial membrane is associated with mitochondrial dysfunction. Several studies have found reduced mitochondrial Ca^{2+} uptake, complex I and IV activities, and ATP production in G93A mutant mice and in neuronal cells expressing SOD1 mutants (Jung et al., 2002, Mattiazzi et al., 2002, Kirkinezos et al., 2005, Damiano et al., 2006). Mutant SOD1 may also prevent protein import by obstructing translocases situated on the outer mitochondrial

membrane (OMM) (Liu et al., 2004). More recently, misfolded G85R and G93A mutants were found to bind to and directly impair the conductance of the voltage-dependent anion channel (VDAC1) in spinal cord motor neurons (Israelson et al., 2010). VDAC1 is located on OMM and has important roles in regulating ATP/ADP exchanges between the cytosol and mitochondrial matrix, transport of Ca^{2+} and other metabolites across the OMM, mitophagy, and apoptosis.

Mitochondria-mediated apoptosis plays a key role in motor neuron degeneration in mouse models of ALS. Alterations in the expression of pro- and anti-apoptotic genes, activation of caspases and release of cytochrome c have been found in the spinal cord of SOD1G93A transgenic mice (Vukosavic et al., 1999, Guegan et al., 2001, Ishigaki et al., 2002, Takeuchi et al., 2002a, Pasinelli et al., 2004, Kirkinezos et al., 2005, Tanaka et al., 2006). In addition, disease onset and mortality can be delayed in G93A mice by treatment with caspase inhibitors such as zVAD-fmk (Li et al., 2000), or with cytochrome c release inhibitors such as monocycline (Zhu et al., 2002) or through overexpression of Bcl2 (Kostic et al., 1997). Interestingly, Bax deletion in G93A mice prevented motor neuron cell death but not mitochondrial vacuolization and denervation at the neuromuscular junction (NMJ) demonstrating that mitochondrial dysfunction in distal synapses and subsequent retraction of the distal axon from the NMJ is sufficient to trigger the clinical symptoms (Gould et al., 2006). This may involve the release of pro-apoptotic factors such as cytochrome c and apoptosis-inducing factor (AIF) from damaged mitochondria in minute amounts such that they trigger the loss of distal synapses but is insufficient to trigger immediate cell death [reviewed in (Manfredi and Xu, 2005)]. Consistent with this dying

back hypothesis, 40% of the NMJ were denervated in early presymptomatic stages prior to final motor neuron cell death at 100 days (post-symptomatic) in G93A mice (Fischer et al., 2004).

1.5.4 Unfolded protein response

As outlined above, the deposition of misfolded mutant SOD1 proteins in the cytosol and mitochondria causes dysfunction and reduces cell viability. To guard against the accumulation of misfolded or unfolded proteins, cells have evolved elaborate signal transduction cascades which detect perturbations in protein folding status within each compartment and couples this to the expression of chaperones and proteolytic machinery. These signalling mechanisms are collectively known as the unfolded protein response (UPR) and allow individual compartments to adapt to cellular stress and enhance protein folding and degradation capacities when necessary. As such, transient activation of UPR is primarily cytoprotective and allows cells to function during adverse conditions.

1.5.4.1 Heat Shock Response

The cytosolic UPR is the heat shock response and is primarily controlled by the transcription factor, heat shock factor 1 (Hsf1), in vertebrates. Normally the activities of Hsf1 are inhibited by cytosolic sequestration of the Hsf1 monomer by Hsp90 and Hsp70. However, during cellular stress, Hsp70 and Hsp90 dissociate from Hsf1 thus allowing the transcription factor to translocate to the nucleus where it binds as a trimer to heat shock

elements (HSE). Subsequent hyperphosphorylation of Hsf1 allows recruitment of cofactors and RNA polymerase II to initiate transcription of target genes (Morimoto, 1998). The majority of genes encode Hsps and components of the UPS, although a small subset also encodes proteins involved in the ER stress response (Morimoto, 1998, Liu and Chang, 2008). Although the heat shock response is a ubiquitous phenomenon, neurons particularly motor neurons, exhibit high thresholds for Hsf1 activation and thus are generally unresponsive to cellular stressors such as heat shock, glutamate exposure, or protein aggregation (Batulan et al., 2003). Defects in regulation of Hsf1 are thought to be the cause of compromised Hsf1 activation and could underlie the selective vulnerability of motor neurons to mutant-SOD1 toxicity (Batulan et al., 2003). Therefore, agents that increase Hsf1 activities are likely to be protective against mutant SOD1 toxicity. In line with this hypothesis, both arimoclomol and celastrol demonstrate efficacy in the G93A mouse model of ALS (Kieran et al., 2004a, Kiaei et al., 2005). Moreover, enhanced Hsf1 activation through celastrol treatment reduced lipid peroxidation in mitochondrial membranes indicating that activation of the heat shock response can have a protective effect on mitochondrial function (Sassa et al., 1990). The glutamate antagonist, riluzole, may also exert protective effects in ALS patients by reducing chaperone-mediated autophagy of Hsf1 and thus prolonging the heat shock response (Yang et al., 2008). Activation of Hsf1 can also protect cells against chronic ER stress (UPR^{ER}) by promoting the translocation of nascent peptides into the ER and enhancing ER-associated degradation (ERAD) (Liu and Chang, 2008).

1.5.4.2 Unfolded protein response of the endoplasmic reticulum

The UPR^{ER} is a multifaceted signaling mechanism induced by the accumulation of unfolded proteins in the ER lumen. Initiation of the UPR^{ER} involves sequential activation of three pathways – protein kinase-like ER kinase (PERK), activating transcription factor 6 (ATF6), and inositol requiring enzyme 1 (IRE1) – leading to translational attenuation and increased transcription of ER chaperones and ERAD genes to restore protein homeostasis in the compartment [reviewed in (Rutkowski and Kaufman, 2004)]. The three pathways are linked by a unifying luminal chaperone, immunoglobulin heavy chain binding protein (BiP), which binds to the ER stress sensors, PERK, ATF6 and IRE1, and regulates them in a dominant negative manner. Binding of BiP to misfolded and unfolded proteins in the ER lumen releases the sensor proteins thus activating the ER stress response [reviewed in (Kaufman, 1999)].

SOD1 is not typically associated with the ER, however, the discovery of mutant SOD1 in microsomal fractions along with the finding that mutant, but not wildtype, SOD1 interacts with BiP in spinal cord motor neurons of transgenic SOD1 mice suggests that a small proportion of the mutant enzyme may at least be aberrantly localized to this compartment (Kikuchi et al., 2006). Moreover, the finding that UPR^{ER} is induced in cell culture and transgenic models of SOD1-FALS also lends support to the idea that mutant SOD1 does reside in the ER in a subset of cells. In G85R and G93A transgenic mice, upregulated expression of UPR^{ER} markers including phosphorylated eukaryotic initiation factor 2α (p-eIF2α), PERK, BiP, and activating transcription factor 4 (ATF4) were found in motor neurons at presymptomatic stages indicating that activation of the UPR^{ER} at these early stages is a protective measure to counteract the aggregation of mutant SOD1 within

this compartment (Tobisawa et al., 2003, Wate et al., 2005, Saxena et al., 2009). However, as disease progresses and the protein quality control machinery becomes increasingly overwhelmed by mutant SOD1, the UPR^{ER} switches from being pro-survival to pro-apoptotic through activation of c/EBP homologous protein (CHOP) and ER-localized caspase -12 (Nakagawa et al., 2000, Urano et al., 2000). Additional ER stress at these stages can also occur through mutant SOD1-mediated mitochondrial dysfunction. Increased ROS production and subsequent oxidative damage can result in the build-up of misfolded proteins within the ER leading to ER stress. Alternatively, increased Ca^{2+} uptake into the mitochondria can deplete ER Ca^{2+} thus leading to ER dysfunction and stress (Berridge, 2002).

1.5.4.3 Mitochondrial UPR

Each subcompartment of the mitochondrion contains its own repertoire of molecular chaperones and proteolytic machinery. Disturbances to homeostasis in any of these subcompartments may trigger an UPR to increase the expression of chaperones and proteases necessary to restore the balance. So far, a stress response has been identified for the mitochondrial matrix (UPR^{mt}) but not for the IMS or OMM. Analogous to UPR^{ER}, the accumulation of misfolded or unfolded protein in the mitochondrial matrix activates CHOP and CCAAT-enhancer binding protein β (C/EBPβ) transcription factors which bind to UPR^{mt} elements to induce the transcription of genes involved in protein quality control in the matrix. These include mitochondrial Hsp70 (mtHsp70) which drives the import of unfolded proteins across the inner membrane, cofactors [matrix DNAJ homolog (DnaJ) and

glucose-related protein E (GrpE)], chaperonins (Hsp60 and Hsp10), and ATP-dependent proteases [DNA-binding ATP-dependent protease La (Lon) and proteolytic subunit of Casinolytic protease (ClpP)].

It is currently unknown whether a stress response in the mitochondrial matrix is triggered by mutant SOD1. As the majority of mitochondrial mutant SOD1 is concentrated in the IMS and to a lesser extent the OMM, an UPR^{mt} may not be as apparent as IMS or OMM stress responses.

Progress in identifying stress responses in the IMS or OMM have been slow due to the fact that very little is known about the quality control mechanisms within these compartments. Despite this, several proteins have been implicated. One of these proteins is the ATP-dependent metalloprotease of the i-AAA family, yeast mitochondrial escape 1 like-1 protein (Yme1L1). Yme1L1, resides in the inner membrane with its protease domain facing the IMS where it is involved in the degradation of unassembled membrane complexes (Weber et al., 1996). These proteolytic activities are essential for mitochondrial integrity as Yme1L1 mutants in yeast display morphological and functional abnormalities in mitochondria (Campbell and Thorsness, 1998). In addition, a recent study has found Yme1L1 to be responsive to UPR^{mt} induced by a deletion mutant of the mitochondrial matrix enzyme ornithine transcarbamylase (OTC); upregulation of Yme1L1 during UPR^{mt} is dependent on CHOP binding (Aldridge et al., 2007). It is not yet known whether Yme1L1 is similarly upregulated to protein misfolding in the IMS.

Another attractive candidate for the IMS stress response is the serine protease, high temperature requirement protein A2 (HtrA2, also known as Omi), which has dual anti-

apoptotic and pro-apoptotic functions. Bacterial orthologues of HtrA2 [degradative proteases P (DegP) and S (DegS)] have roles in transducing stress adaptive signals (DegS) and degrading unfolded protein (DegP) suggesting that HtrA2 may also perform these protective functions in mammalian cells [reviewed in (Young and Hartl, 2003)]. Moreover, HtrA2 activity is regulated by the PTEN-induced putative kinase 1 (PINK1) indicating a potential signalling mechanism between the mitochondria and cytosol (Plun-Favreau et al., 2007). Interestingly, HtrA2 co-stained with inclusion bodies in anterior horn cells in autopsied spinal cords from SALS and SOD1-related FALS patients although it is not clear whether this derives from the release of HtrA2 into the cytosol during mitochondria-mediated apoptosis (Kawamoto et al., 2010).

The degradation of proteins on the OMM is believed to operate in an ERAD-analogous manner and under the control of the ubiquitin conjugation system. Consistent with this idea, RING-finger E3 ubiquitin ligases and Skp-Cullin F box (SCF) ubiquitin ligases have been shown to mediate ubiquitylation of OMM components thus targeting them to the 26S proteasome for destruction (Neutzner et al., 2008). Recently, an OMM ubiquitin ligase, mitol, has been found to interact with and ubiquitinate G85R and G93A mutants on the OMM. Overexpression of mitol reduced the amount of mitochondrial mutant SOD1 and this correlated with decreased ROS production and increased survival of N2A cells (Yonashiro et al., 2009). Therefore, upregulation of protein quality control machinery in the OMM is likely to be protective by attenuating mutant SOD1 damage to the mitochondria. It is not yet known whether mitol is upregulated in mutant SOD1 mice to protect mitochondria under stressful conditions.

1.5.5 Autophagy

Insufficient clearance of misfolded mutant SOD1 in the mitochondria and ER can cause irreparable damage leading to apoptosis through the release of pro-apoptotic effectors. Thus to prevent this from occurring, cells can enhance autophagy to eliminate any dysfunctional organelles before they can release pro-apoptotic mediators. Macroautophagy is the major autophagic pathway and is responsible for the elimination of the majority of long-lived proteins, and excess or dysfunctional organelles. Macroautophagy is also the principle mechanism employed by cells to dispose of misfolded proteins and aggregates that are too large to be degraded by the proteasome. In this pathway, regions of the cytoplasm are sequestered within a double membrane envelope (phagophore membrane) to form a structure known as the autophagosome. Autophagosomes and their contents are then eliminated by fusion with late endosomes and lysosomes containing acid hydrolases (Fig. 1.1) (Berg et al., 1998). Normally, autophagy occurs constitutively at basal levels to facilitate the degradation of aged or damaged organelles but further increases in autophagy flux can be induced by cellular stressors including nutrient deprivation, high temperatures, accumulation of protein aggregates, or inflammation (Hara et al., 2006, Nakai et al., 2007). The stimulus will determine the nature of autophagy induced. In selective autophagy, the signal for biogenesis of the phagophore membrane originates from the targeted protein or organelle whereas in non-selective autophagy, the signal comes from the direct activation of the autophagy machinery.

The induction of autophagy reduced the toxicity of mutant SOD1 aggregates in cell culture (Kabuta et al., 2006). Enhanced autophagy as observed by increased levels of

microtubule-associated protein light chain 3 II (LC3II) and cathepsins were also found in spinal cords from symptomatic G93A mice and indicates a possible protective mechanism for autophagy *in vivo* (Wootz et al., 2006, Morimoto et al., 2007). Recently, HspB8 was found to be upregulated in cell culture and animal models of SOD1-FALS; this was mediated by Hsf1 indicating a close relationship between Hsf1-mediated activation of the macroautophagy machinery and neuroprotection (Crippa et al., 2010). Aside from clearing mutant SOD1 aggregates, Hsf1-induced autophagy can also promote cell survival by eliminating dysfunctional ER and reducing chronic UPR^{ER} activation. A link between UPR^{ER} and autophagy is supported by studies in which genetic ablation of X-box binding protein 1 (XBP1), a transcription factor downstream of the ATF6 pathway, increases autophagy and protects against mutant SOD1 toxicity in cell culture and in the G93A transgenic mouse (Hetz et al., 2009). Clearance of dysfunctional mitochondria through macroautophagy can also protect cells through its effects on ROS generation and Ca^{2+} signaling. Therefore, the final outcome may depend on duration of cell stress and how effective UPR mechanisms are in removing misfolded SOD1 from cellular compartments and preventing toxicity (Fig. 1.2).

1.6 Aims of work presented in this thesis

The broad aims of this study are to understand how misfolded, mutant SOD1 in different cellular compartments can cause toxicity and to identify the proteins that may process mutant SOD1 in the cytosol and mitochondria. Specifically, the aims of each chapter are:

Chapter 3: To determine the roles of HspB8 in autophagy of mutant SOD1 and whether this is able to suppress mutant SOD1-mediated toxicity.

Chapter 4: To create a NSC-34 cell culture model in which hSOD1 is targeted into the IMS.

Chapter 5: To identify proteins which are likely to be involved in the IMS stress response using the model created in Chapter 4.

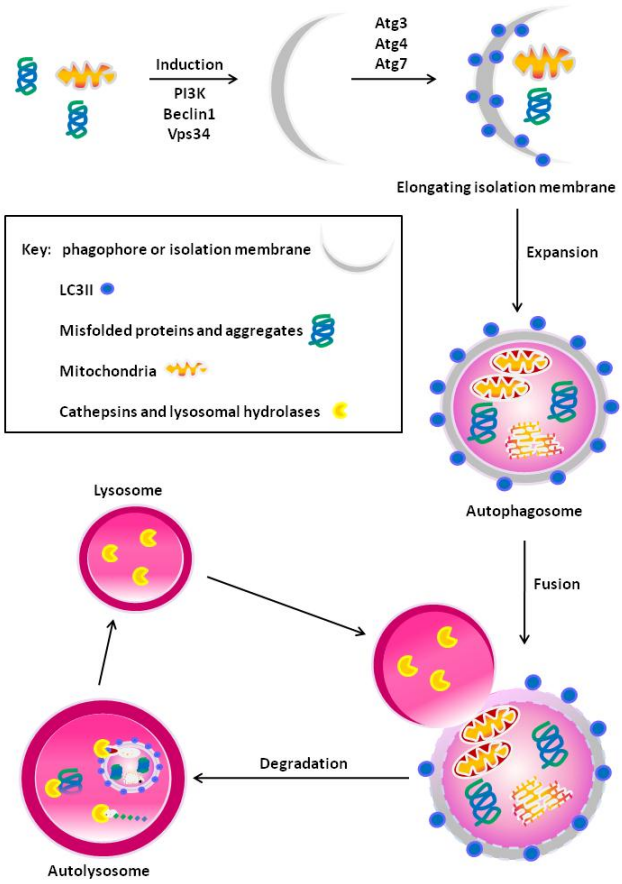

Fig.1.1 Schematic diagram of the steps involved in macroautophagy. After induction of macroautophagy by cellular stress signals such as the accumulation of misfolded proteins, phagophore or isolation membranes form at the ER or mitochondrial OMM in mammalian cells. Kinase complexes involving autophagy-specific phosphatidylinositol-3-kinase (PI3K), vacuole sorting protein 34 (Vsp34), and beclin1 proteins are required for the initiation of the isolation membrane. Initiation and elongation of the isolation membrane also requires lipidation of LC3I to LC3II; this is mediated by 2 ubiquitin-like conjugation systems. First, the cysteine protease autophagy-related gene 4 (Atg 4) cleaves LC3I. LC3I is then subsequently activated by Atg7 and transferred to Atg3, an E2- homologous enzyme, which conjugates phosphatidylethanolamine to LC3I to form LC3II. The lipidated LC3II molecule is associated with autophagic membranes or vesicles and thus is commonly used as a marker for autophagy. Following its formation, autophagosomes receive lysosomal constituents such as proton pumps from late endosomes via vesicle-mediated transport. Fusion of the outer membrane of the autophagosome with the late endosome or lysosome (autolysosome) allows autophagosome contents to be degraded by cathepsins and other acidic lysosomal hydrolases. Adapted from (Glick et al., 2010).

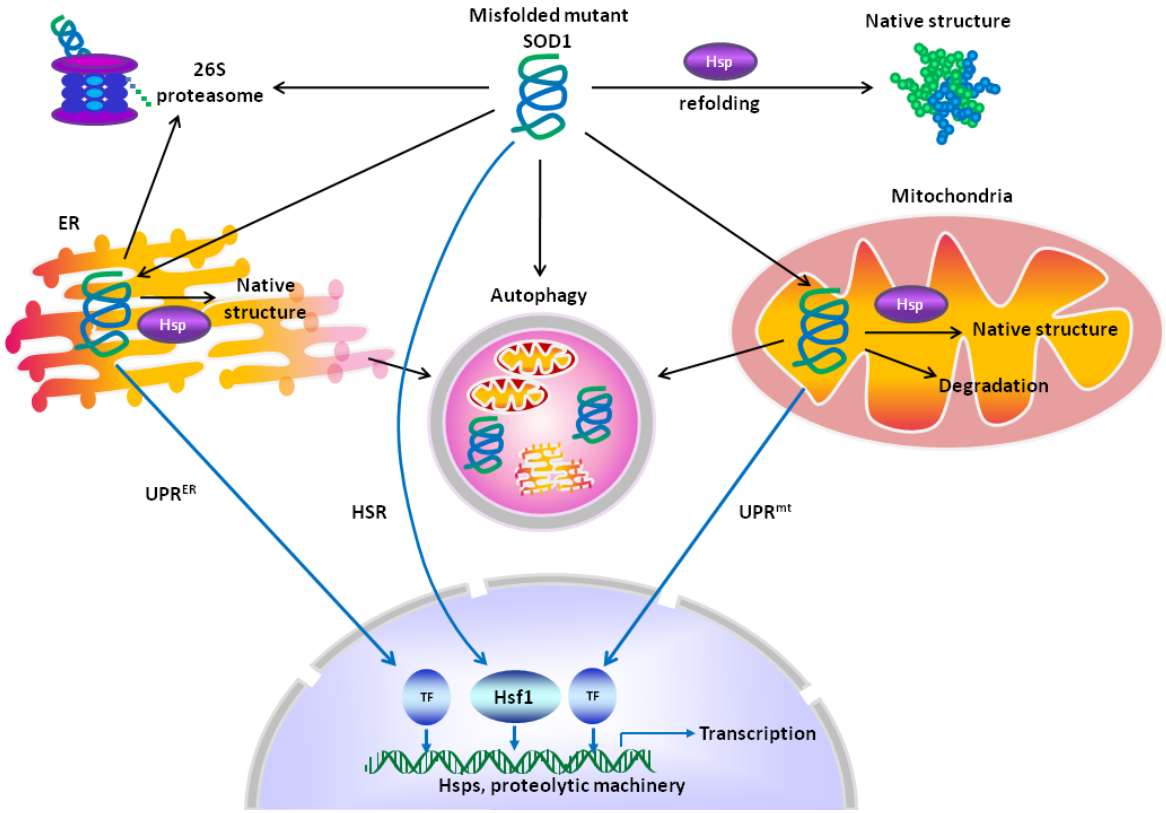

Fig. 1.2 Mechanisms for preventing the toxicity misfolded mutant SOD1. Mutant SOD1 misfolds and aggregates in the cytosol, endoplasmic reticulum (ER) and mitochondria causing motor neuron cell death. In the cytosol, heat shock proteins (Hsps) recognize and bind to exposed hydrophobic regions on mutant SOD1 to prevent their aggregation and in some cases, to assist their refolding to the native state. Hsps also facilitate the removal of misfolded mutant SOD1 species by the 26S proteasome or autophagy. Similarly, chaperones and proteases in the mitochondria and ER process misfolded SOD1 to prevent dysfunction in these compartments. As the ER does not contain proteases, misfolded proteins are exported to the cytosol by the ER-associated degradation (ERAD) machinery for degradation by the proteasome. The buildup of mutant SOD1 also triggers a stress response within the cytosol (heat shock response; HSR), endoplasmic reticulum (UPR^{ER}), and mitochondria (UPR^{mt}), leading to transcription of genes required to restore protein homeostasis within these compartments. Autophagy is also activated to eliminate dysfunctional mitochondria and ER to prevent apoptosis through the release of pro-apoptotic mediators.

2. Materials and Methods

2.1 Animals

Transgenic mice expressing high copy numbers of human SOD1 carrying the G93A mutation were purchased from Jax Laboratories (stock number, 004435; strain designation: B6.Cg-Tg (SOD1-G93A)1Gur/J). In some experiments, mice that express equivalent levels of wildtype human SOD1 were used. Transgenic mice were maintained in the hemizygous state by mating G93A males with non-transgenic C57BL/6J females. Carrier females are not fertile and thus cannot be used for the mating. All mice were derived and maintained by Dr. Neza Alfazema and Dr. Bradley Turner.

2.1.1 Tissue preparation

In this study, G93A mice at P30, P100, and P150 corresponding to presymptomatic, symptomatic, and end stages, respectively, of disease were sacrificed by carbon dioxide; death was verified by exsanguination. Symptomatic G93A mice were characterized by weakness in the hind limbs, rolling gait and hunched posture. Age-matched wtSOD1 or Ntg mice were used as controls. Both brain and spinal cord tissues were isolated from each of the mice. For mice below P60, spinal cords were ejected from the cervical end of the vertical column by exerting pressure through a syringe plunger mounted on an 18-guage hypodermic needle at the caudal end of the spinal canal (Meikle and Martin, 1981). Released spinal cords were immediately washed with PBS, placed in cryotubes and frozen

on dry ice. For mice above P60, laminectomy was used to remove spinal cord from the vertebral canal. The brain was harvested by decapitation; an incision was made at the base of the brain, and the skull peeled away to expose the brain for removal. Isolated brains were immediately washed with PBS, placed in cryotubes and frozen on dry ice. Tissue samples were stored at -80ºC for long-term storage. All animal procedures were approved by the Home Office and performed by Dr. Neza Alfazema and Dr. Bradley turner.

2.2 Patient samples

2.2.1 Collection of blood

Three age-matched healthy individuals and one CMT2L patient harboring the pathogenic K141E mutation were recruited for the study. Informed consent was obtained from all individuals and 50ml of peripheral blood was obtained was collected from each of the individuals in ten EDTA tubes at the John Radcliffe Hospital, Oxford.

2.2.2 Isolation of peripheral blood mononuclear cells (PBMCs)

For isolation of PBMCs, 45ml of whole blood from patients and healthy donors were separated by Lymphoprep gradient centrifugation. PBMCs collected in the white layer were then washed thrice with Roswell Park Memorial Institute-1640 (RPMI-1640; Gibco) to remove remaining plasma before resuspending in R10 medium. R10 medium consists of RPMI-1640 supplemented with 100U/ml penicillin, 10μg/ml streptomycin, 2mM L-glutamine, and 10% (v/v) FCS (Gibco). The number of PBMCs from each

individual was counted in a hemocytometer and the sample then divided into three equal groups for subsequent treatments. All samples were processed for ImageStream on the same day.

2.2.3 Treatments

To induce autophagy, freshly isolated PBMCS were starved in Hanks buffered salt solution (HBSS) media for 2 hours prior to antigen labeling and fixation. For the inhibited samples, PBMCs were treated with 10μM 2S,3S-trans-(Ethoxycarbonyloxirane-2-carbonyl)-L-leucine-(3-methylbutyl) amide (E64d; Sigma) and 10μM pepstatin A (Sigma) in HBSS (Invitrogen) for 2 hours.

2.3 Construction of expression plasmids

2.3.1 HspB8 constructs

The human HSPB8 coding sequence was generously provided by Dr. Vincent Timmerman (University of Antwerp) and subcloned into the pCAGGs expression vector. A hemagglutinin (HA)-tag was incorporated at the C-terminus to facilitate subsequent analyses.

The HSPB8 point mutation 423G→C (resulting in amino acid substitution K141N) was introduced using the following primers 5’-ctaagaacttcacaaacaaaatccagcttcctgcag-3’ and 5’-ctgcaggaagctggattttgtttgtgaagttcttag-3’, and the QuikChange site-directed

mutagenesis kit (Stratagene). All constructs were verified by DNA sequencing (Geneservice at the Department of Biochemistry, University of Oxford).

2.3.2 hSOD1 constructs

2.3.2.1 pcDNA3-hSOD1 and EGFP-hSOD1 constructs

Wild-type and mutant hSOD1 (A4V, G37R, G85R, and G93A) cDNA were previously subcloned into pEGFP-N1 (Clontech) or pcDNA3 (Invitrogen) vectors by Dr. Bradley Turner. All sequences were confirmed by DNA sequencing.

2.3.2.2 IMS-SOD1 constructs

To direct the expression of hSOD1 in the IMS, a fusion protein consisting of hSOD1 and an N-terminal IMS-targeting sequence was needed. The bipartite targeting sequence chosen was that of HtrA2, an apoptotic protein that normally resides in the IMS and is only released into the cytosol when an apoptotic signal is received. The cDNA encoding mouse HtrA2 (accession number BC049880.1) was obtained from the I.M.A.G.E consortium (MRC geneservice, UK) and the first 399 nucleotides of the open reading frame was amplified using primers 5'- GCAAAGCTTATGGCTGCGCTGAAAGCGGGG-3' and 5'-GCCTTCGTGGCAGCCAGCACCGTG-3' thus creating a HtrA2 half-product encoding only the bipartite sequence. Amplification of wildtype and mutant hSOD1 cDNA created the second half product with a HA tag incorporated at the 3' end. The HtrA2 and SOD1 half products were combined in a final PCR reaction to create the fusion cDNA: HtrA2-

wtSOD, HtrA2-G85R, and HtrA2-G93A. This fusion cDNA was then EcoRI/HindIII digested and subcloned into pcDNA3. These vectors were then designated IMS-wtSOD1, IMS-G85R, and IMS-G93A respectively. All constructs were confirmed by DNA sequence analysis (Geneservice, Department of Biochemistry, University of Oxford).

2.4 Cell culture

2.4.1 Cell lines

Mouse neuroblastoma x spinal cord (NSC-34) cells and HEK293T cells were cultured in Dulbecco's Modified Eagle Medium (DMEM) supplemented with 10% (v/v) fetal calf serum (FCS) and 1% (v/v) penicillin-streptomycin and maintained at 37°C in a 5% (v/v) CO_2 humidified incubator. Once confluent, cells were harvested in trypsin-EDTA (Invitrogen) and plated at various densities for subsequent experiments: 2.5 x 10^4 cells/well in 24-well tissue culture plates (Falcon) containing autoclaved coverslips for immunocytochemistry experiments; 2.5 x 10^5 cells/well in 6-well plates (Falcon) for RNA extraction, protein extraction, or flow cytometry experiments; 2.5 x 10^6 cells/10cm dish (Falcon) for co-immunoprecipitation experiments and; 10^6 cells/35mm glass bottom dishes (MakTek) for live imaging. For mitochondrial fractionation experiments, cells were pooled from multiple confluent T75 flasks (Falcon).

2.4.2 Transient transfections

Cells were transfected with constructs using Lipofectamine 2000 (Invitrogen) according to manufacturer's recommendations. The amount of DNA used to transfect cells ranged from 500ng for 24-well plates, 1μg for 6-well plates, and 7μg for 10cm dishes. The transfection efficiency for single transfection of HspB8 or hSOD1 constructs in NSC-34 cells was 70-80%, whilst efficiency for SOD1 and HspB8 co-transfections was slightly lower at 60-65%.

2.4.3 Stable transfections

NSC-34 cells constitutively over-expressing hSOD1 in the mitochondrial IMS were created by transfection with IMS-SOD1 constructs (as above) and after 72h, selection was started with G418 (Sigma). Selection was carried out for a period of two weeks before colonies were picked and the levels of hSOD1 determined by western blotting analyses. Colonies expressing similar levels of hSOD1 were constantly maintained in complete DMEM in the presence of 50 μg/ml of G418 (Sigma). Except where indicated, all experiments performed using IMS-SOD1 stable cell lines were performed with only a subset of selected clones, namely IMS-wtSOD1 clone 1, IMS-G85R clone A and IMS-G93A clone 1.

2.4.4 Treatments

2.4.4.1 Proteasome inhibition

NSC-34 cells transfected with EGFP-hSOD1 constructs were treated with 10μM MG132 (Sigma) for 7h prior to harvesting. The 7h incubation was chosen to avoid mass cell death due to toxicity of MG132.

2.4.4.2 Inhibition of autophagy

48h after transfection with hSOD1 and HspB8 constructs, NSC-34 cells were treated with 10μM of E64d (Sigma) and 10μM pepstatin A (Sigma) or 10μM 3-methyladenine (3-MA; Sigma) for the times indicated prior to harvesting.

2.4.4.2 Nutrient deprivation

For cell stress experiments, NSC-34 cells were maintained in serum-free DMEM for 72h immediately after transfection of hSOD1 constructs. NSC-34 cells constitutively expressing IMS-hSOD1 constructs were also subjected to metabolic stress by culturing in no-glucose DMEM (Invitrogen) supplemented with 10% FCS and 1% (v/v) penicillin-streptomycin, or no-glucose DMEM supplemented with 10μM galactose (Sigma), 10% FCS , and 1% (v/v) penicillin-streptomycin, for 4 days prior to the fluorescence-activated cell sorting (FACS) experiment.

2.5 Imaging and microscopy

2.5.1 Live imaging

2.5.1.1 Analysis of SOD1-EGFP aggregates

The number of aggregate-positive cells was counted and compared to the number of total positive transfectants in each well to determine the aggregation potential. A minimum of 300 transfected cells were counted. Aggregates were defined as bright non-homogenous structures within the cytosol. Cells were imaged with a Axiovert 200M inverted microscope (Carl Zeiss) using x20 objectives.

2.5.1.2 Mitochondrial morphology

For imaging mitochondria, NSC34 cells were plated onto poly-D-lysine-coated 35mm glass bottom dishes (MakTek) and later transfected with mito-DsRed2 (Clontech). MakTek dishes were placed into the humidified incubation chamber set at 37°C with 5% (v/v) CO_2 and mitochondrial morphology in 20 cells were recorded with the Zeiss LSM 510 Meta confocal microscope (Carl Zeiss) using x63 oil objectives.

2.5.2 Immunohistochemistry

Frozen 14μM lumbar spinal cord sections of adult mice were air dried and fixed in 4% (w/v) paraformaldehyde (PFA) for 10 minutes at room temperature. After washing in PBS, sections were permeabilized by incubation with 0.1% (v/v) Triton-X100 in PBS for

10 minutes at room temperature. Sections were subsequently blocked in 5% FCS in PBS for 1 hour after which goat anti-HspB8 antibody (Abcam; 1:500) was added to the blocking solution for overnight incubation at 4^0C. Excess antibody was removed by washing thrice in PBS and sections were subsequently incubated with Alexafluor 488 dye-conjugated donkey anti-goat IgG (Invitrogen; 1:1000) for 1h. After 3 PBS washes, sections were mounted with Vectashield (Vector Laboratories) and slides were visualized for HspB8 using AxioPlan 2 micrscope (Carl Zeiss) equipped with an AxioCam MRm camera and using AxioVision 4.5 software.

2.5.3 Immunocytochemistry

NSC-34 cells were grown on coverslips one-day prior to transfection with hSOD1 and/or HA-tagged HspB8 constructs or mito-DsRed2 (Clontech). 72 hours later, coverslips were washed with PBS, fixed with 4% PFA for 15 min, washed again with PBS, and permeabilized with 0.2% Triton X-100 for 10 min. Coverslips were then blocked with 5% (v/v) milk in PBS for 30 min before incubation with polyclonal rabbit anti-HA (Sigma; 1:1000) at 4^0C overnight. Proteins of interest were visualized by subsequent incubation with the appropriate AlexaFluor dye-conjugated IgG (Invitrogen; 1:1000) for 2 hours at room temperature. Images were collected using a LSM 510 Meta confocal laser scanning microscope (Carl Zeiss Inc.) with x40 or x63 objectives.

2.6 RTPCR

Total RNA was extracted from cells using Trizol Reagent (Invitrogen) or mouse spinal cord using Qiagen RNeasy Minikit (Qiagen), following manufacturer's recommendations. 10μg of RNA was Turbo DNase treated (Ambion) and 1μg of this RNA was used for cDNA synthesis using the High Capacity cDNA Reverse Transcription Kit (Applied Biosystems), according to manufacturer's recommendations.

Quantitative real time PCR (qPCR) was carried out on StepOnePlus Real time PCR system (Applied Biosystems) using 1:10 diluted samples of cDNA, 1x SYBR Green PCR Master Mix (Applied Biosystems) and optimized concentrations of forward and reverse primers (Table 2.1), in a total volume of 20μl and in triplicate for each sample. The following cycling conditions was used for all genes: denaturation at 95°C for 10 min, followed by product amplification by 40 cycles of 95°C for 15 s and 60°C for 1 min. The comparative ΔΔCT method was used to determine the relative levels of each target in the samples; GAPDH or β-actin was used as a reference to normalize expression levels.

Table 2.1 Primer design for qPCR

Target ID	Target Name	Forward primer sequence (5'-3')	Reverse primer sequence (5'-3')	References
HspB8	Heat Shock protein B8	GCACGCTGGGGCTCC AGTC	CAGTGATCTCCACCACGC CTTC	N/A
GAPDH	Glyceraldehyde 3-phosphate dehydrogenase	AACTTTGGCATTGTGG AAGG	ACACATTGGGGGTAGGAA CA	N/A

β-actin	Beta-actin	TCCCCCAACTTGAGATGTATGAAG	AACTGGTCTCAAGTCAGTGTACAGG	(Ding et al., 2009)
Tim9	Translocase of the inner mitochondrial membrane 9	TCAGAGGCGAGATCCTGTGGC	GTGCCCCGCCTTCTGCTTGT	N/A
Tim10	Translocase of the inner mitochondrial membrane 10	AAGTTGGGGACGTTGCGGGA	TGGGCTCTGAGCGGATCCAT	N/A
Gfer	Growth factor, augmenter of liver regeneration	AGAACAACAACAGGATATGGC	AAAATCAGGCTTGCCCAG	(Santti et al., 2005)
PINK1	PTEN induced putative kinase 1	GGACACGAGACGCTTGCA	TTACCAATGGACTGCCCTATCA	(Franks et al., 2008)
HtrA2	High temperature requirement protein A2	CCCCGGATCTCTGGGCACGATTGAAT	ATCCCCGCTAGGCAGCCTCACTCGTA	(Martins et al., 2004)
Yme1L1	Yeast mitochondrial escape 1 like-1	ATGCCTCGAGGGCCAACACT	ATCTGTGCAAGCAGCTGGGC	N/A

2.7 In-situ hybridization

cDNA encoding exon 1 of mouse HspB8 was subcloned into pCR4-TOPO (Invitrogen) and isolated clones were verified by sequencing. cDNA-containing plasmids were linearized by digestion with PstI and NotI restriction enzymes, gel purified, and used as templates for *in vitro* transcription of HspB8 digoxigenin (DIG)-labeled RNA probes. The transcription mixture included 500ng of linearized DNA, DIG labeling mix (Roche), polymerase buffer, RNasin (Promega) and RNA polymerase. Transcription was carried out

for 2h at 37°C. HspB8 riboprobes were purified by precipitation by addition of 9µl 4M LiCl, 72µl Tris-ethylenediaminetetraacetic acid (TE) (10:1) and 270µl absolute EtOH and centrifugation for 20 min at 4°C. Purified DIG-labelled RNA products were verified by agarose gel electrophoresis and stored at -80°C.

For hybridization, frozen sections were air-dried and fixed in 4% PFA at room temperature for 10 min. After washing with PBS, sections were acetylated for 10 min during which 1ml of acetic anhydride was added dropwise for the first 4 min of incubation. Sections were again washed in PBS before prehybridization for 1h at room temperature with hybridization solution [50% (v/v) formamide, 10mg/ml E.coli tRNA, 1x Denhardt's solution, 200mM dextran sulphate, 600mM NaCl, 8.3 mM SDS, 1mM EDTA, pH 8.0] for 1h at room temperature. Probes were added to the hybridization mix (1ng/2.5µl) and pipetted directly onto the section. Hybridization was carried out for 16-20h at 60°C. To prevent evaporation during the hybridization step, slides were placed in a box saturated with 5x standard sodium citrate (SSC) and 50% (w/v) formamide solution. After incubation, slides were washed in 0.2x SSC for 1h at 70°C, washed for 5 min in 0.2x SSC at room temperature and equilibrated in Buffer 1 solution (100mM Tris-HCl, 150mM NaCl, pH 7.6) for 5 min at room temperature. Sections were blocked with blocking powder (Roche) in Buffer 1 for 1h at room temperature before incubation with anti-DIG antibody (Roche; 1:5000) in blocking solution overnight at 4°C. Sections were washed thrice in buffer 1, equilibrated in Buffer 2 (100mM Tris-HCl, 100mM NaCl, 50mM $MgCl_2$ pH 9.5) for 5 min, and incubated with nitro-blue tetrazolium chloride/ 5-bromo-4-chloro-3'-indolyphosphate-p-toludine salt solution (NBT/BCIP; Roche) for 12-48h in the dark room.

Following development of slides, the staining reaction was stopped by washing slides in PBS. Slides were mounted in 90% (v/v) glycerol and sealed with nail varnish. All *in-situ's* were performed by Miss Annie Raw.

2.8 Gel Electrophoresis and Immunoblotting

2.8.1 Preparation of protein extracts

Transfected NSC-34 cells were lysed on ice in Tris-EDTA-NaCl (TEN) buffer containing 10mM Tris-HCl, pH 8.0, 1mM EDTA, 100mM NaCl, 0.5% (v/v) Nonidet P-40 (NP-40) and 1% (v/v) protease inhibitor cocktail (Roche). Collected lysates were centrifuged to obtain NP40- soluble (supernatant) and –insoluble (pellet) fractions. Pellets were washed twice in lysis buffer, solubilized by addition of TEN buffer containing 10mM Tris-HCl, pH 8.0, 1mM EDTA, 100mM NaCl, 0.5% (v/v) NP-40, 1% (v/v) protease inhibitor cocktail (Roche) and 1% (w/v) sodium dodecyl sulphate (SDS) then sonicated at 50% output for 15 seconds. Sonicated samples were then centrifuged and the supernatant (SDS-soluble fraction; P1) and pellet (SDS-insoluble fraction; P2) were prepared for gel electrophoresis.

Mouse lumbar spinal cords were dissected, snap frozen and sonicated in RIPA lysis buffer [50mM Tris-Cl, pH 7.5, 150mM NaCl, 0.1% (w/v) SDS, 1% (v/v) sodium deoxycholate, 1% (v/v) TX-100) and 1% (v/v) protease inhibitors]. Homogenates were clarified by centrifugation at 17,500 xg for 20min at 4^{o}C to obtain soluble and insoluble protein fractions. Proteins from the insoluble fraction were extracted by sonication in RIPA

lysis buffer containing 2% (w/v) SDS followed by centrifugation at 17,500 xg for 20min at 4°C.

2.8.2 Isolation of mitochondrial fraction

NSC-34 cell lines were homogenized in ice-cold 0.1M Tris-MOPS buffer containing 1mM ethylene glycol tetraacetic acid (EGTA)/Tris and 200mM sucrose using a Teflon pestle. Homogenates were centrifuged at 600 xg for 10 min at 4°C. The supernatant was collected and subjected to another round of centrifugation at 7000 xg for 10min at 4°C. The supernatant was discarded and the pellet washed twice to remove contaminating cytosolic proteins. Finally, the mitochondria-containing pellet was resuspended in 0.1M Tris-MOPS buffer containing 1mM EGTA/Tris, 200mM sucrose and 1% NP-40.

2.8.3 Western blotting analysis

The concentration of protein extracts was measured using the bicinchoninic acid (BCA) kit (Pierce). Protein samples were prepared for gel electrophoresis by dissolving in 2X SDS-sample buffer [4% (w/v) SDS, 100mM Tris-HCl, pH 6.8, 200mM dithiolthreitol, 0.2% (w/v) bromophenol blue, 20% (v/v) glycerol] and boiled at 100°C for 5 min. 20μg of protein samples were resolved on a 12.5% SDS-PAGE gel and transferred to nitrocellulose membrane (Millipore). The membrane was then blocked with 5% (w/v) skimmed-milk in Tris-buffered Saline Tween-20 (TBST) for 1 hour before incubation with the primary antibody at 4°C overnight. Blots were developed using appropriate horse radish peroxidase

(HRP)-conjugated antibodies (GE healthcare; 1:10000) and enhanced chemiluminescence (ECL) (Amersham).

2.8.4 Primary antibodies

Primary antibodies used for this study were: sheep anti-SOD1 (Calbiochem; 1:1000), goat anti-HspB8 (Abcam; 1:1000), rabbit anti- β-actin (Sigma; 1:1000), rabbit anti-HA (Sigma; 1:1000), rabbit 20S β1 proteasome subunit (Santa Cruz Biotechnology rabbit anti – microtubule-associated protein light chain 3A (Map1LC3A) (Epitomics; 1:1000), goat anti-PINK1 (Santa Cruz Biotechnology; 1:1000), goat anti-Hsp60 (Santa Cruz Biotechnology; 1:1000), rabbit anti-Yme1L1 (Proteintech; 1:300), rabbit anti-GFER (Proteintech; 1:300).

2.8.5 Co-immunoprecipitation

100μg of protein samples were incubated with anti-SOD1 antibody and placed on a rotating wheel at 4°C overnight. The next day protein G sepharose (Invitrogen) was added to each sample and incubated on a rotating wheel for 1hr at 4°C. After centrifugation at 7000 xg for 2min, beads were washed thrice in TEN buffer. For western blotting, immunoprecipitates were released by incubation with SDS sample loading buffer.

2.9 Flow cytometry

2.9.1 ImageStream

2.9.1.1 NSC34 cells

NSC-34 cells co-transfected with hSOD1 and HA-tagged HspB8 constructs for 48 hours were trypsinized and incubated with Lyso-ID Red Detection Reagent (Enzo Life Sciences) for 15 min at 37°C. Cells were washed, then fixed with BD Cytofix Fixation buffer (BD Biosciences) and permeabilized with BD Perm/Wash Buffer (BD Biosciences) according to manufacturer's recommendations. Intracellular staining was performed by sequential incubation with the following antibodies for 1h at room temperature: sheep anti-SOD1 (Calbiochem; 1:1000) and rabbit anti-Map1LC3A (Epitomics; 1:200), followed by Alexafluor 405 dye-conjugated goat anti-rabbit IgG (Invitrogen; 1:1000), Alexafluor 488 dye-conjugated donkey anti-sheep IgG (Invitrogen; 1:1000), and finally mouse phycoerythrin-conjugated anti-HA (Santa Cruz; 10μg). 3 rounds of cell washes with BD Perm/Wash Buffer were carried out in between each round of antibody incubation. Stained cells were resuspended in PBS and analysed on ImageStream (Amnis).

For each sample, images of 25,000 cells were acquired after excitation with 405- and 488-nm laser light. Debris was eliminated from the data set by setting a minimum object area in channel 1 (laser scatter channel) of 120 pixels. Signals from Map1LC3A, SOD1, HA and LysoID, were detected by channels 2, 3, 4 and 6, respectively, while side scatter and brightfield images were collected in channels 1 and 5, respectively. For spectral compensation, images of unstained cells and of cells stained with a single antibody or fluorophore were acquired without brightfield illumination. Post-acquisition spectral

compensation and data analysis was performed using ImageStream Data Exploration and Analysis Software (IDEAS). To assess the autophagy of SOD1, spot counts were applied on single-cell populations that are in-focus and positively-stained for SOD1, Map1LC3A and Lyso-ID.

2.9.1.2 PBMCs

Cells were washed, incubated with Lyso-ID Red, fixed and permeabilized as described above. Intracellular staining for Map1Lc3A was carried out for 30 min at room temperature, after which cells were washed and incubated with Alexafluor 488 dye-conjugated goat anti-rabbit IgG (Invitrogen; 1:1000) for 30 min at room temperature. Stained cells were resuspended in PBS and analysed on Imagestream as described above. Data for 25,000 stained PBMCs were acquired for each sample.

2.9.2 Mitochondrial content

250,000 cells were incubated with 100nM MitoTracker Green FM (Invitrogen) for 1h at 37°C. After incubation, cells were washed twice in PBS before resuspending in PBS for FACs analyses on BD LSR II instrument (BD Biosciences). Using forward and side scatter to exclude dead cells from analysis, the mitochondrial content of 10,000 viable cells was measured. Except for the labeling of cells, the FACS experiment was performed by Miss Rebecca Dragovic (Nuffield Department of Obstetrics and Gynaecology, University of Oxford).

2.10 Cell viability test

2.10.1 MTT assays

72 hours post-transfection, NSC-34 cells were treated with 3-(4,5-dimethylthiazol-2-yl)-2,5-diphenyltetrazoloium bromide (MTT, 5mg/ml) (Sigma) in PBS and incubated at 37°C for 1 hour. The medium was aspirated from the wells and the MTT reaction was terminated by addition of dimethyl sulphoxide (DMSO) (Sigma). Absorbance was measured at 544nm in a microplate reader (FluoStar, BMG). All samples were assayed in quadruplets and the mean ± SD for each condition was calculated. The results were expressed as a percentage of cell viability of controls (pcAGGs/pcDNA3).

2.10.2 Live/Dead cell viability assays

4μM ethidium homodimer-1 and 2μM calcein acetoxymethyl ester (Live/Dead Viability/Cytotoxicity kit; Invitrogen) in PBS was added to transfected NSC-34 cells. After incubation for 45 min at room temperature, cells were washed and resuspended in warm HBSS. Cell viability (as a percentage of total cell number) was then assessed by counting at least 300 cells in each well on an Axiovert 200M inverted microscope (Carl Zeiss) using x20 objectives.

2.11 Clark oxygen electrode

$2x10^6$ cells were resuspended in complete DMEM or no-glucose DMEM containing 10% FCS before loading into the 37°C chamber of the Clark oxygen electrode also containing media. Respiration rates were then determined by measuring oxygen consumption over a period of at least 30min or until the oxygen had been depleted from the chamber.

2.12 Statistics

One-way and Two-way ANOVAs were used to determine statistical significance for datasets except where indicated. Multiple comparisons were performed with post-hoc Bonferroni t-test using GraphPad Prism 5 software.

3. Induction of HspB8 promotes autophagy in models of SOD1-FALS

3.1 Introduction

Mutations in SOD1 destabilize the enzyme leading to misfolding and aggregation in the cytosol and other cellular compartments in motor neurons and astrocytes of transgenic mice and in SOD1-related FALS cases (Dalcanto and Gurney, 1994, Shibata et al., 1996, Bruijn et al., 1998, Kato et al., 1999, Kokubo et al., 1999). These aggregates associate with a number of proteins including chaperones of the small heat shock protein (sHsps) family.

sHsps are a subclass of Hsps that are induced in response to a variety of stress stimuli. Ranging from 12-43kDa, all ten members of the sHsp family (HspB1-B10) share a common central α-crystallin domain, which is required for structural stability and assembly into higher oligomers. The formation of homo- or hetero-oligomeric complexes is obligatory for sHsp functions and the majority of sHsps are found in complexes ranging from 2 to >40 subunits (Kim et al., 1998, van Montfort et al., 2001, Van Montfort et al., 2002). sHsps lack ATPase activity and have a prominent role in preventing the aggregation of folding intermediates or misfolded proteins (Horwitz, 1992, Ehrnsperger et al., 1997, Lee et al., 1997).

HspB8 (also known HspB8, H11 kinase and E21G1) is a 22kDa chaperone of the sHsp family that was identified in a yeast two-hybrid screen for HspB1-binding partners (Benndorf et al., 2001). Expression of HspB8 is ubiquitous, but is most abundant in striated and smooth muscle, brain, and in some cancer cells such as melanoma and breast cancer

(Kappe et al., 2001). The ability of HspB8 to bind to misfolded proteins and prevent their aggregation in cell culture is well documented (Carra et al., 2005, Wilhelmus et al., 2006, Sanbe et al., 2007). More recently, a role for HspB8 in selective macroautophagy has been demonstrated (Carra et al., 2009, Arndt et al., 2010, Crippa et al., 2010). Two missense mutations resulting in a substitution of the lysine residue at position 141 (K141E and K141N) of HspB8 have been identified in families with Charcot Marie Tooth disease type 2 (CMT2) and distal hereditary motor neuropathies (dHMN) suggesting that HspB8 activities are crucial for the survival of motor and sensory neurons (Irobi et al., 2004, Tang et al., 2004, Tang et al., 2005). Both mutations are associated with a toxic gain-of-function or dominant-negative effect of the mutant chaperone and deleterious effects may arise through abnormal interactions with its binding partners. For instance, HspB8 mutants demonstrate an increased affinity for several proteins including HspB1, HspB5 and Ddx20 which may impact negatively on other cellular processes including axonal transport, spliceosome assembly, protein transcription and translation (Sun et al., 2004, Anderson et al., 2010).

3.1.1 Aims of Chapter 3

The aims of this study are to determine the roles of HspB8 in SOD1-FALS and to observe whether overexpression of this chaperone is able to alleviate the toxicity of mutant SOD1. In addition, it aims to establish the *in vivo* functions of HspB8.

3.2 Results

3.2.1 HspB8 is prominently expressed in cranial and spinal motor neurons

A To define the expression pattern of HspB8 within the CNS, *in situ* hybridization was performed on brain and spinal cord sections from adult non-transgenic mice (Ntg) (this work was carried out by a project student in the laboratory, A. Raw). In brain sagittal sections, HspB8 transcripts were restricted to the motor trigeminal nucleus (Mo5) (Fig. 3.1AII and AIII) where they were present in both cell bodies and axons (Fig. 3.1AIII). Likewise, HspB8 transcripts were also found in cell bodies and axons of motor neurons in the Rexed's lamina IX in spinal cord sections (Fig. 3.1BIII-BV). The expression pattern for HspB8 transcripts in the brain and spinal cord is consistent with those observed in the Allen Brain Atlas (http://www.brain-map.org/). Immunohistochemistry of adult lumbar spinal cord sections confirmed the presence of HspB8 protein in the Rexed's lamina IX (Fig. 3.1CI).

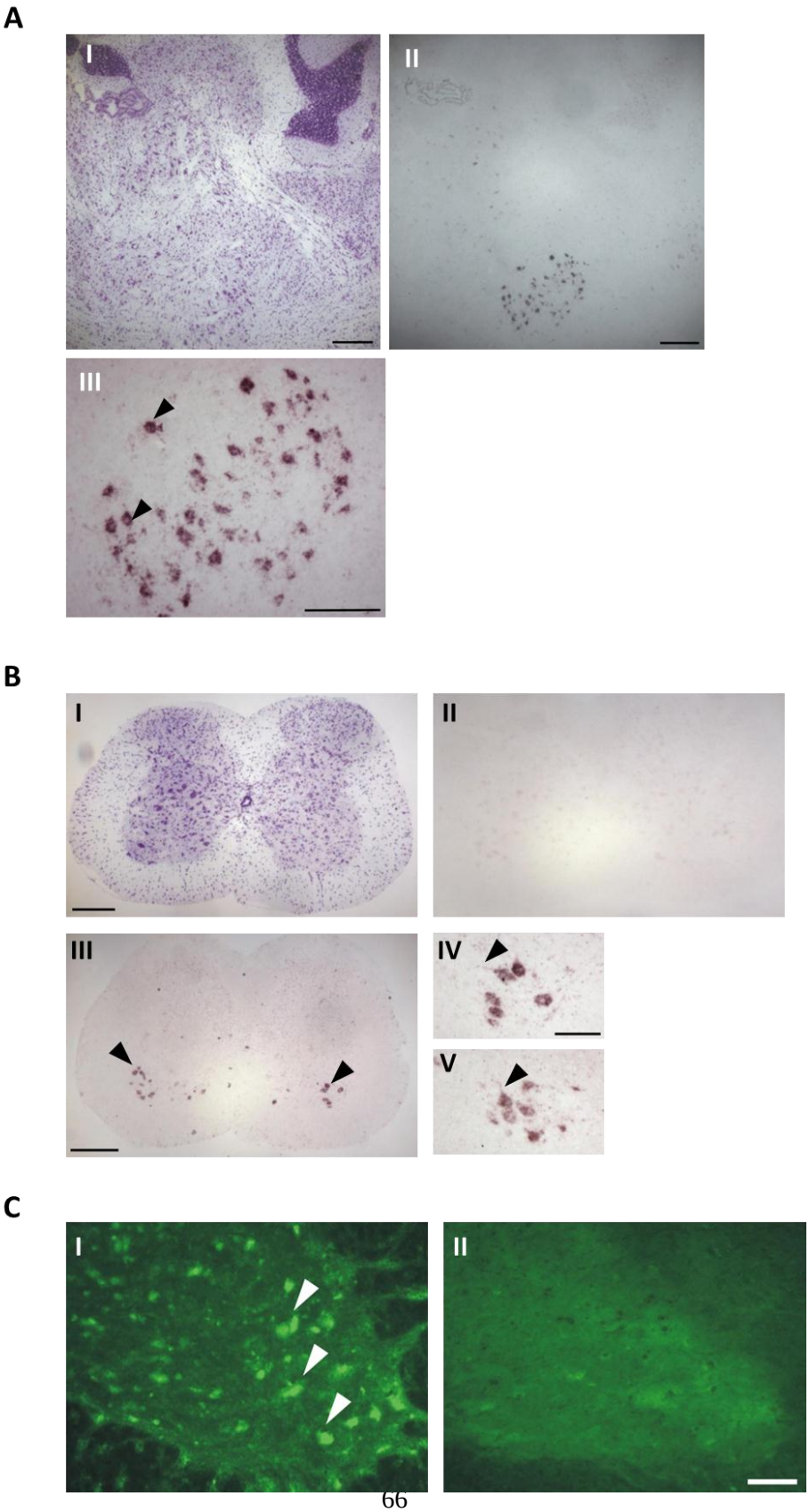
A
I
II
III
B
I
II
III
IV
V
C
I
II

Fig 3.1 Expression pattern of HspB8 in the CNS. (A) *In situ* hybridization of HspB8 in brain saggital sections of adult Ntg mice (AI) Cresyl violet stain (AII) *In situ* hybridisation using an antisense HspB8 probe, labels a group of cells positive for HspB8 mRNA (arrowheads). (AIII) The stained neurons shown at higher magnification were localised to the motor trigeminal nucleus (Mo5) (arrowheads) (AD). Scale bars, 500 mm (AI-AII), 100 mm (AIII). (B) HspB8 transcripts localise to anterior horn cells in adult mouse spinal cord. (Bi) Cresyl violet stain of spinal cord cell nuclei delineates grey and white matter. (BII) No signal was obtained with sense HspB8 probes. (BIII) The antisense HspB8 probe labels a subset of cells positive for HspB8 mRNA (arrowheads). These cells exhibit motor neuron morphology upon inspection at higher magnification (BIV, BV) and are located in the region of the Rexed's lamina IX. The presence of HspB8 protein within the axons of motor neurons is indicated by the arrowheads. Scale bars, 500 mm (BI-BIII), 100 mm (BIV, BV). (CI) Immunohistochemistry of adult mouse spinal cord section with an HspB8 antibody reveals expression in ventral horn cells (arrowheads), in contrast to (CII) the negative control with antibody omission. *In situs* and immunohistochemistry were performed by Miss Annie Raw.

3.2.2 Mutants G85R and G93A induce expression of HspB8 in NSC-34 cells via a post-transcriptional mechanism

Altered levels of heat shock proteins have been found in numerous models of SOD1-FALS. As HspB8 is prominently expressed in motor neurons in the spinal cord, this study investigated whether levels of this chaperone were also altered by transient overexpression of SOD1 mutants (A4V, G37R, G85R, G93A) in NSC-34 cells. Western blot analyses of cell lysates revealed that HspB8 levels were increased in G85R and G93A mutant-expressing cells when compared to wildtype or control. No changes in HspB8 levels were observed in A4V and G37R mutant expressing cells (Fig. 3.2A and 3.2BI). The effects of mutant SOD1 on levels of the 20S β1 proteasome subunit were also examined and shown to be comparable across all cell lines (Fig. 3.2A and 3.2BII). The association of chaperones with mutant SOD1 can lead to the redistribution of the chaperone to the detergent-insoluble fraction. Thus to examine this possibility, western blot analyses were also performed on the NP-40 insoluble fraction. Although, small amounts of HspB8 were

observed in this fraction in G37R, G85R and G93A mutant expressing cells, these were insignificant when compared with the control or wtSOD1 (Fig. 3.2D).

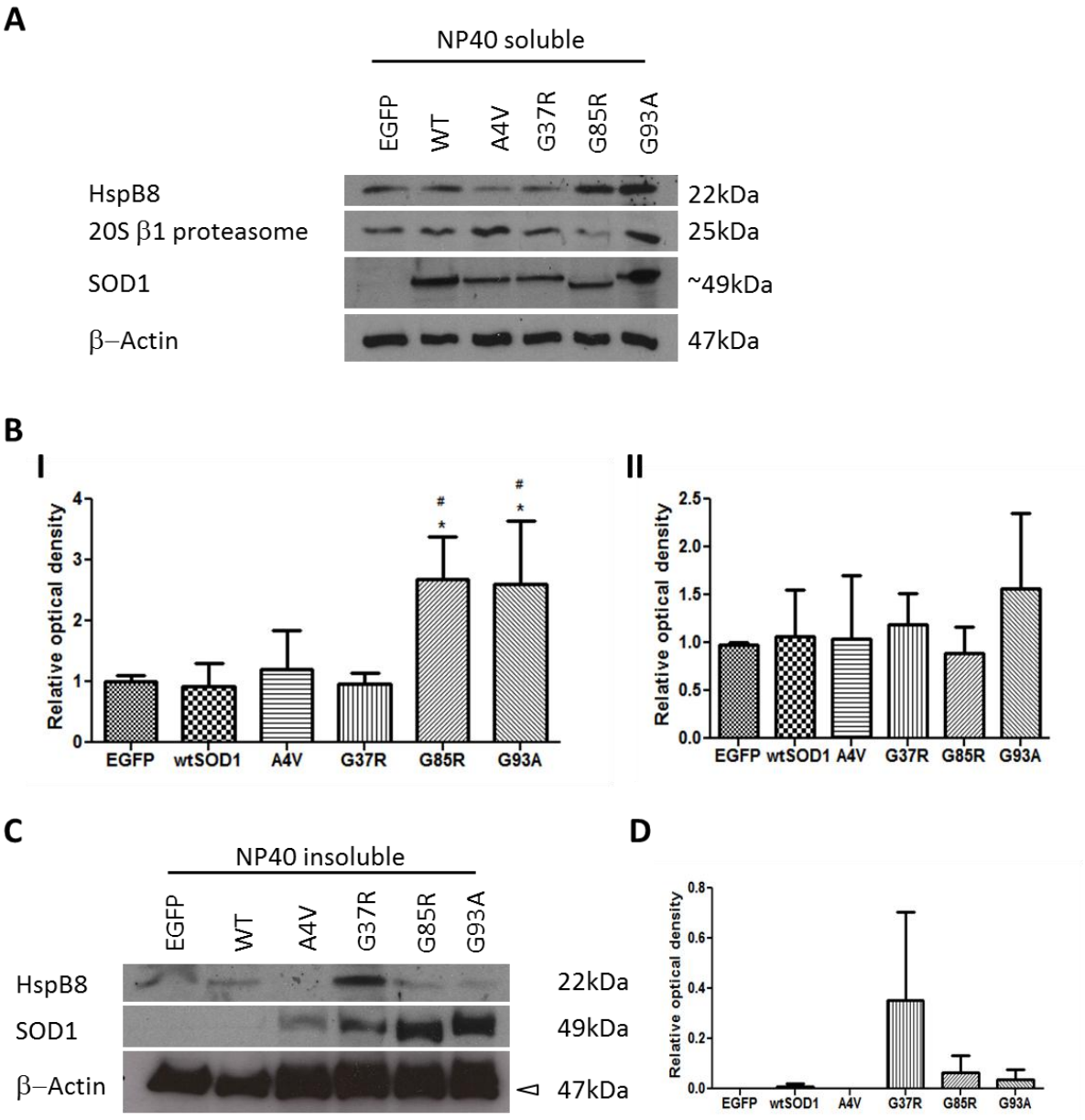

Fig 3.2 G85R and G93A mutants show marked upregulation of HspB8 in NSC-34 cells. NSC-34 cells transiently transfected with EGFP or EGFP-tagged wildtype and mutant (A4V, G37R, G85R and G93A) SOD1 were lysed in buffer containing NP-40 and centrifuged to obtain soluble and insoluble fractions. (A) Western blot analysis of HspB8 and 20S β1 proteasome subunit in the NP-40 soluble fraction. (B) Densitometric analysis for HspB8 (I) and 20S β1 proteasome subunit

(II) in NP-40 soluble fractions. Results are expressed relative to the intensities of EGFP, which were normalized to 1. *$p<0.05$ vs EGFP, $^{\#}p<0.05$ vs wtSOD1 (C) Western blot analysis of HspB8 in the NP-40 insoluble fraction. (D) Levels of HspB8 in insoluble fraction quantified by densitometry. Optical densities of HspB8 in the insoluble fraction were expressed relative to the levels of β-actin for each sample.

To examine whether increased HspB8 levels were associated with changes in transcript abundance, quantitative real-time PCR (qPCR) was performed on RNA extracted from NSC-34 cells expressing wildtype or mutant SOD1. As shown in Fig. 3.3, levels of HspB8 mRNA were comparable for all cell lines suggesting that post-transcriptional mechanisms were responsible for the observed increase in HspB8 expression.

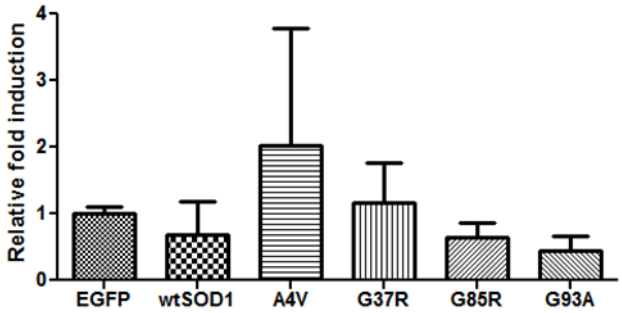

Fig. 3.3 Increased HspB8 protein levels not due to changes in transcript abundance. NSC-34 cells transiently transfected with EGFP or EGFP-tagged wildtype and mutant (A4V, G37R, G85R and G93A) SOD1 for 72h after which total mRNA was isolated. Quantitative real time PCR analysis of HspB8 mRNA showed constant levels across all cell lines, supporting a post-transcriptional mechanism for the increased HspB8 levels in G85R and G93A mutant cells. Data are mean ± SD of three independent experiments. Results are normalized to the EGFP control and expressed as relative fold induction.

Increased levels of chaperones including HspB8 can be brought about by cellular stress such as serum starvation, or through inhibition of the proteolytic machinery. To determine which of these mechanisms enhances HspB8 levels in NSC-34 cells expressing mutant SOD1, cells were either serum-starved, treated with MG132, a proteasome inhibitor or treated with a combination of lysosomal protease inhibitors, E64d and pepstatin A. The results showed that HspB8 levels were comparable within each treatment group (Fig. 3.4A and 3.4B). However, in EGFP and G93A expressing cells, treatment with E64d/pepstatin A led to significantly increased levels of HspB8 when compared with serum deprivation or MG132 treatment indicating the contrast in effects of autophagy inhibition on HspB8 levels compared to serum starvation or MG132 (Fig. 3.4A and 3.4B).

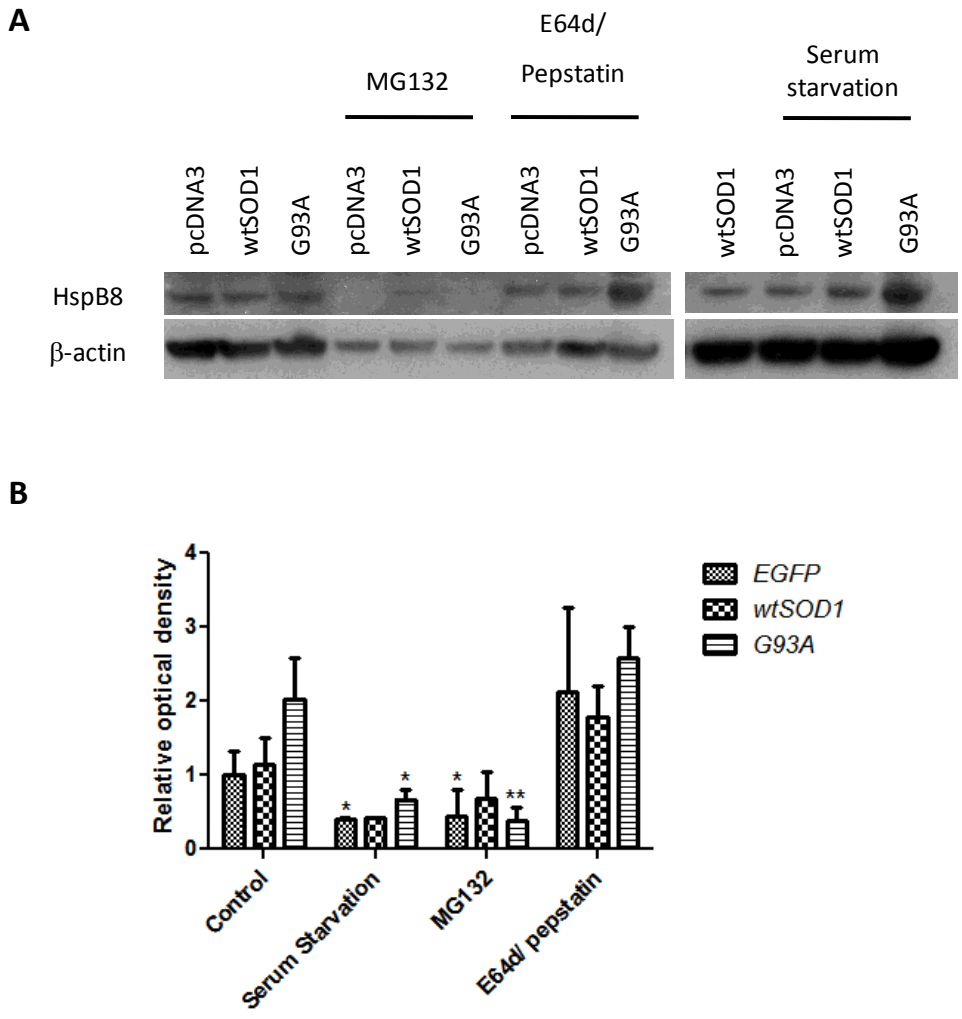

Fig 3.4 Effects of serum starvation, proteasome inhibition and autophagy inhibition on HspB8 levels in G93A expressing cells. NSC-34 cells transfected with EGFP, EGFP-wtSOD1, or EGFP-G93A were incubated with serum-free media, 10μM MG132, or 10μM E64d and 10μM pepstatin A for 4.5 hours before protein extraction. (A) Western blot analysis of HspB8 in cell lysates. (B) Optical density of HspB8 in relation to β-actin was measured for each sample in three independent experiments. All results were expressed relative to the untreated, EGFP-expressing control. *$p<0.05$ versus E64d/ pepstatin A.

3.2.3 Wildtype but not mutant HspB8 binds to mutant SOD1 to suppress aggregate formation

Two missense mutations, K141E and K141N, disrupt a highly conserved lysine residue in the α-crystallin domain of HspB8 and are associated with motor neuron degeneration in the peripheral nervous system (Irobi et al., 2004). As the α-crystallin domain is required for oligomer assembly and structural stability of sHsps, mutations in the domain are likely to cause misfolding and aggregation of the chaperone. Previous studies have shown HspB8 aggregates in cultured cells (Irobi et al., 2004). To confirm this finding in NSC-34 cells, the number of cells exhibiting aggregates was counted 72 hours after transfection with empty (pCAGGS), HspB8, or $HspB8^{K141N}$ vectors. The results show that $HspB8^{K141N}$ was more susceptible to aggregation compared to its wildtype counterpart (Fig. 3.5A and 3.5B). $HspB8^{wt}$ showed a diffuse staining pattern in the cytoplasm and the nucleus (Fig. 3.5A) with ~3% of cells exhibiting aggregates (Fig. 3.5B)

Next, the effect of HspB8 and $HspB8^{K141N}$ on mutant SOD1 aggregation was examined. Unlike wtSOD1, SOD1 mutants, G37R and G93A, were excluded from the nucleus (Fig. 3.5D) and demonstrate an increased propensity to aggregate when transfected alone in NSC-34 cells (Fig. 3.5C). However, co-expression of HspB8 with G37R or G93A reduced aggregate formation by more than 10% and 50% respectively and a diffuse cytosolic staining pattern for both the mutants was observed. Overexpression of HspB8 had no effect on wtSOD1. In contrast, overexpression of $HspB8^{K141N}$ exacerbated mutant SOD1 aggregation with larger aggregates observed in the cytosol (Fig. 3.5C and 3.5D).

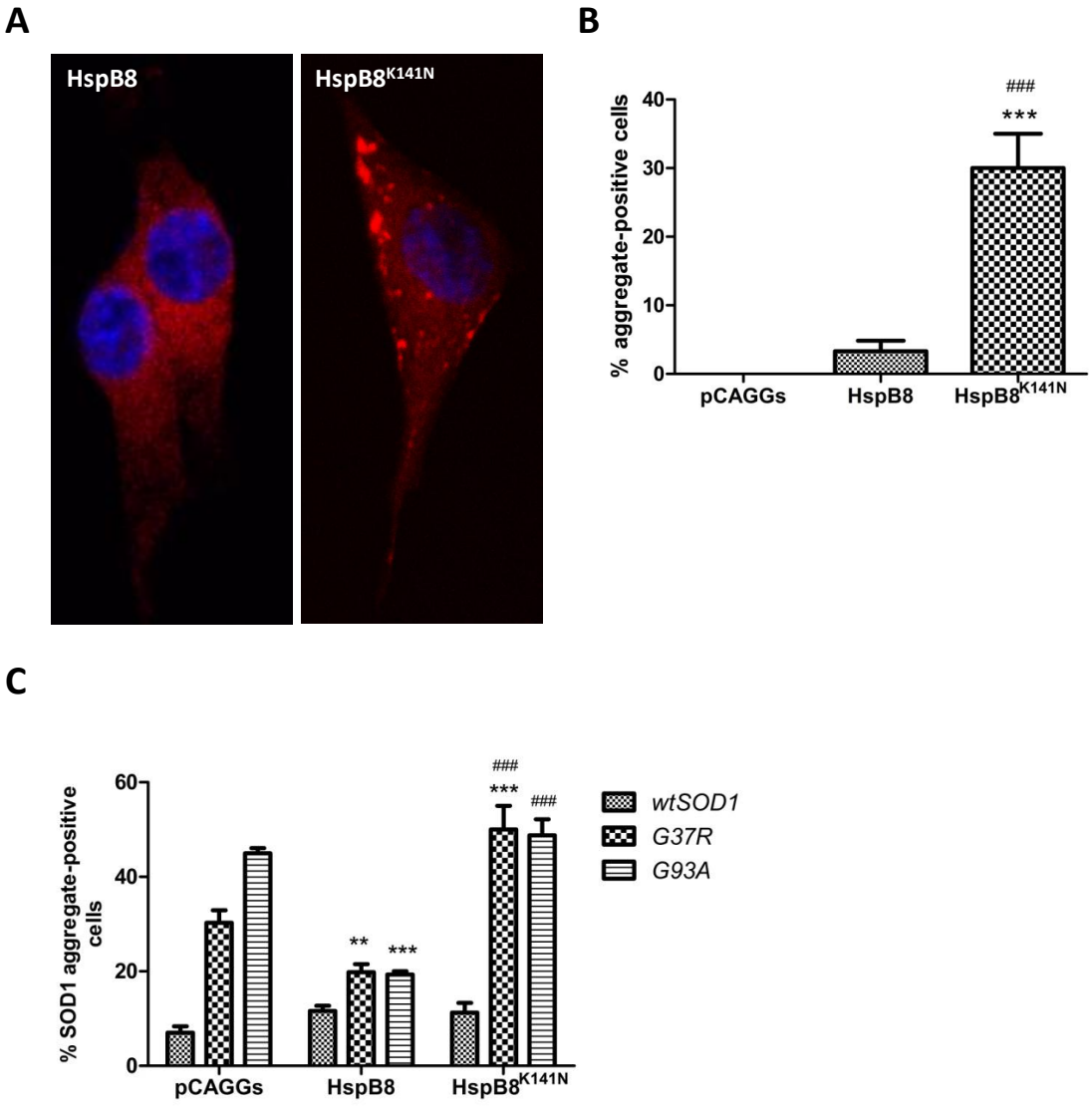
A
HspB8
HspB8K141N
B
% aggregate-positive cells
40
30
20
10
0
###
***
pCAGGs
HspB8
HspB8K141N
C
% SOD1 aggregate-positive cells
60
40
20
0
**
***
###
***
###
wtSOD1
G37R
G93A
pCAGGs
HspB8
HspB8K141N

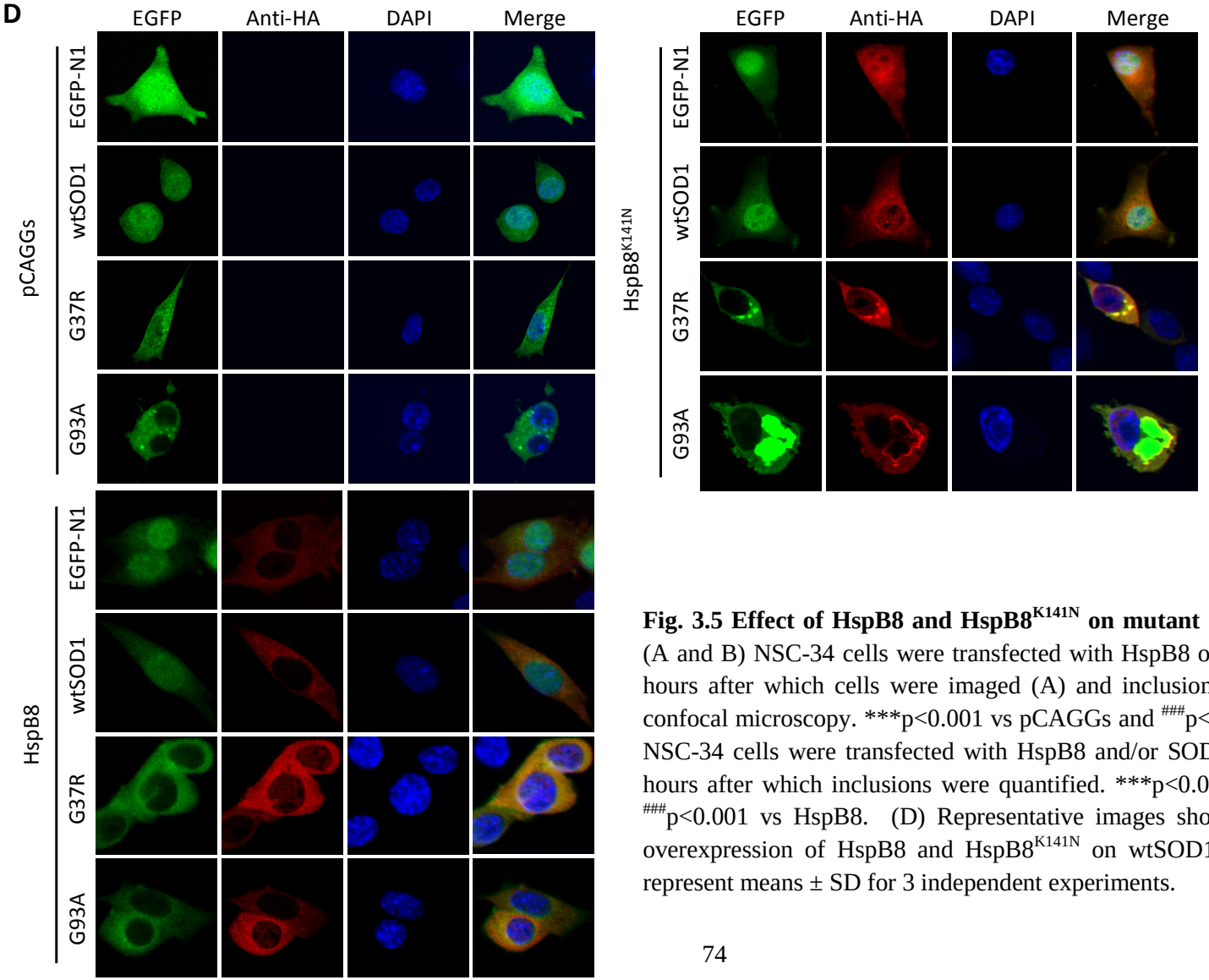

Fig. 3.5 Effect of HspB8 and HspB8^{K141N} on mutant SOD1 aggregation. (A and B) NSC-34 cells were transfected with HspB8 or HspB8^{K141N} for 72 hours after which cells were imaged (A) and inclusions quantified (B) by confocal microscopy. ***p<0.001 vs pCAGGs and $^{###}$p<0.001 vs HspB8 (C) NSC-34 cells were transfected with HspB8 and/or SOD1 constructs for 72 hours after which inclusions were quantified. ***p<0.001 vs pCAGGs and $^{###}$p<0.001 vs HspB8. (D) Representative images showing the effects of overexpression of HspB8 and HspB8^{K141N} on wtSOD1 and G93A. Data represent means ± SD for 3 independent experiments.

In order to correlate the cellular aggregation behaviour of mutant SOD1 with the biochemical changes in mutant SOD1 solubility, cell lysates were fractionated in NP-40-containing lysis buffer. Both NP-40-soluble and -insoluble fractions were analyzed by SDS-PAGE and western blotting. In the absence of transfected HspB8, most wtSOD1 was present in the NP-40 soluble fraction although a small amount was also observed in the insoluble fraction due to the high levels of overexpression. In contrast, G93A mutants were predominantly found in the NP-40-insoluble fraction (Fig. 3.6). Overexpression of HspB8 in G93A-expressing cells led to an increase in solubility of mutant G93A in NP-40. A corresponding decrease in the amount of mutant protein in the NP40-insoluble fraction was also observed. wtSOD1 levels were also reduced in the NP40-insoluble fraction after HspB8 overexpression. The absence of a corresponding increase in the levels of wtSOD1 protein in the NP40-soluble fraction indicates that HspB8 promotes the turnover of aggregated human SOD1 in NSC-34 cells. Compared with HspB8 or empty vector (pCAGGs) controls, overexpression of $HspB8^{K141N}$ reduced levels of wildtype and mutant SOD1 proteins in the NP-40 soluble fraction and increased human SOD1 protein levels in the NP-40 insoluble fractions. This suggests that mutant HspB8 alters the biochemical properties of these proteins such that they become more insoluble (Fig. 3.6).

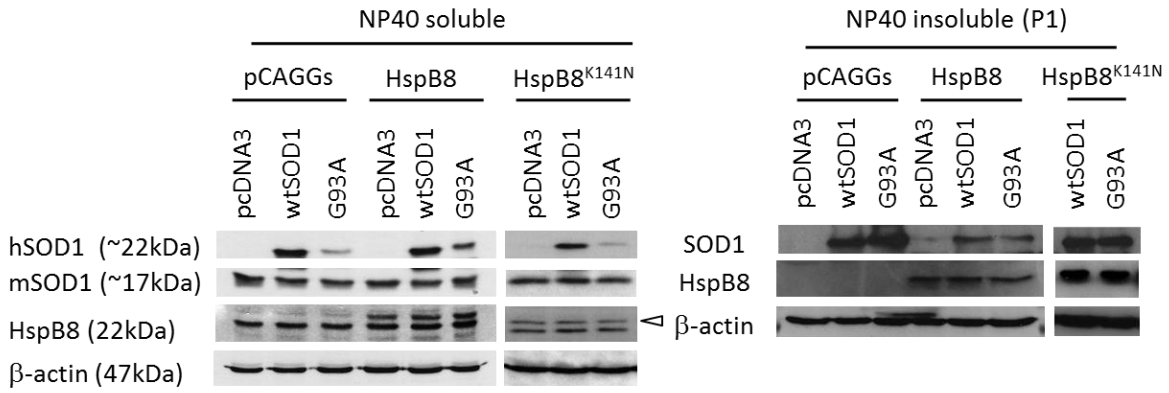

Fig. 3.6 Effect of HspB8 and HspB8^{K141N} on mutant SOD1 solubility. Western blot analysis of SOD1 proteins in NP-40 –soluble and –insoluble fractions 72h after co-transfection of SOD1 and HspB8 constructs in NSC-34 cells. Data represent means ± SD for 3 independent experiments.

To determine if HspB8 binds directly to mutant SOD1 to modulate its solubility, co-immunoprecipitation was performed on lysates from HspB8 and SOD1 co-transfected cells. Using anti-SOD1 for immunoprecipitation, HspB8 was found to bind to both wtSOD1 and G93A in NSC-34 cells (Fig. 3.7). A similar result was also obtained for HspB8^{K141N} indicating that the mutation in the α-crystallin domain does not disrupt chaperone-substrate interactions (Fig. 3.7). Interestingly, an interaction with β-actin was also found in G93A and HspB8^{K141N} co-expressing cells.

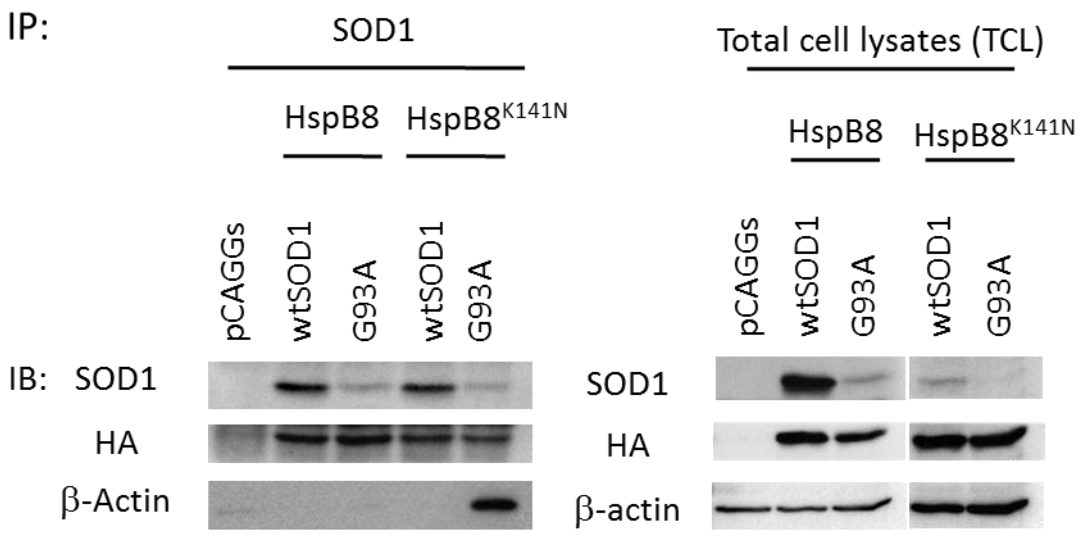

Fig. 3.7 K141N mutation does not prevent binding to mutant SOD1. NSC-34 cells were transfected with HspB8 and SOD1 constructs for 72h after which cells were harvested and prepared for co-immunoprecipitation. 100μg of protein were immunoprecipitated with anti-SOD1 antibody.

3.2.4 Wildtype but not mutant HspB8 promotes autophagy of mutant SOD1 and is associated with increased cell viability

HspB8 was recently shown to mediate macroautophagy of G93A in NSC-34 cells (Crippa et al., 2010). To confirm this finding and to demonstrate that other SOD1 variants can also be targeted for macroautophagy by HspB8, imaging flow cytometry (ImageStream; Amnis) was performed on SOD1/HspB8 co-transfected cells labelled with lyso-ID (a lysosome marker), anti-SOD1 and anti-LC3A. Colocalization between all 3 markers would then indicate the degradation of SOD1 by macroautophagy. As the SOD1 antibody also recognizes mouse SOD1, signals from pcDNA3 cells represent autophagy of the endogenous enzyme. Under control conditions, NSC-34 cells transfected with G93A mutant exhibited significantly higher levels of autophagy compared to cells transfected with wtSOD1 or empty vector. Overexpression of HspB8 led to a doubling of autophagy in

all cell lines with the greatest induction observed in G85R and G93A expressing cells indicating some specificity in the autophagic response (Fig. 3.8A). Reduced levels of LC3A in HspB8 transfected cells also indicate increased autophagy in these cells (Fig. 3.8B).

The autophagic activities of HspB8^{K141N} were also assessed. As shown in Fig. 3.8A, levels of autophagy in HspB8^{K141N} expressing cells were similar to the pCAGGs control indicating that the mutation blocks the ability of the chaperone to promote autophagy. Autophagy proceeds through a series of steps including induction, autophagosome formation, fusion of autophagosomes with lysosomes, and degradation and recycling of vesicle components, and HspB8^{K141N} could act at any of these steps to impair autophagy in cells (Kovacs et al., 1982, Takeshige et al., 1992, Tanida et al., 2005, Kiselyov et al., 2007). To determine whether HspB8^{K141N} impairs autophagy induction, levels of LC3A were measured by flow cytometry. Compared to control, significantly higher fluorescent intensities of LC3A were observed in HspB8^{K141N} expressing cells indicating that the ability to induce autophagy was not abolished by the mutation (Fig. 3.8B). Next, the ability of HspB8^{K141N} –mutant SOD1 complexes to localize to the autophagosome was examined by looking at colocalization between SOD1, HspB8, and LC3A proteins. Compared with HspB8, targeting of HspB8^{K141N} –mutant SOD1 to autophagosome membranes was much reduced in HspB8^{K141N} expressing cells thus indicating that defects in autophagy arise from inefficient targeting or incorporation of substrates into the autophagosome.

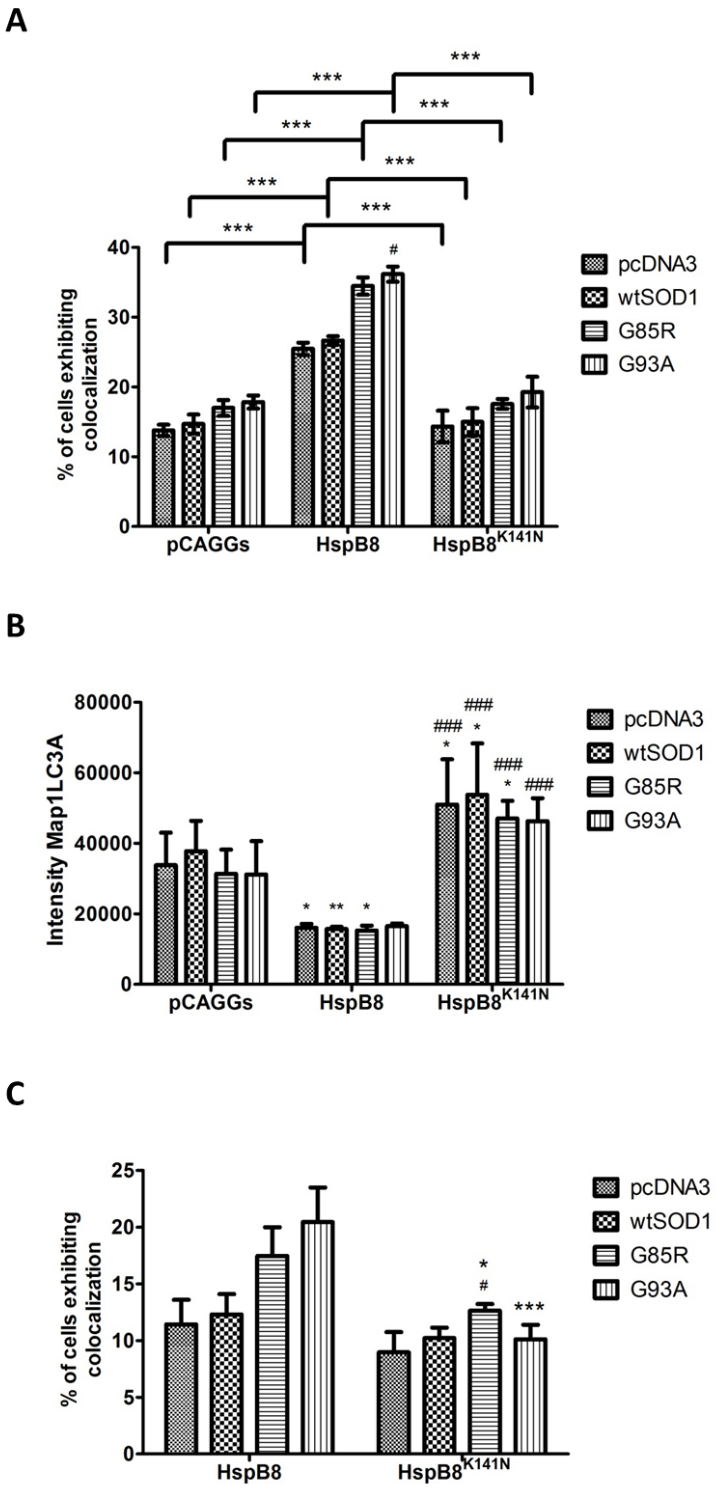

Fig. 3.8 Wildtype but not mutant HspB8 promotes autophagy of SOD1 in NSC-34 cells. NSC-34 cells were co-transfected with (i) pcDNA3 vectors containing no insert, human WT or mutant (G85R, G93A) SOD1 cDNAs and (ii) pCAGGs plasmids containing no insert or HA-tagged human HspB8 sequence or HspB8^{K141N} mutant for 48 hours after which cells were treated with LysoID

prior to fixation and permeabilization. Fixed cells were then subsequently immunostained with SOD1, phytoerythrin-conjugated HA, and LC3A antibodies and analysed by ImageStream. 25,000 cells were counted for each sample. (A) Autophagy of SOD1 was assessed by counting cells that display colocalization between SOD1, LC3A, and LysoID ***p<0.001, #p<0.05 vs pcDNA3 (B) Fluorescent intensity of LC3A in cells *p<0.05 vs pCAGGs, ###p<0.001 vs HspB8 (C) Delivery of HspB8-SOD1 complexes to the autophagosome was assessed by counting cells that show colocalization of HspB8, SOD1 and LC3A Data represent means ± SD for 3 independent experiments *p<0.05 vs HspB8, #p<0.05 vs pcDNA3.

To determine whether HspB8-induced autophagy of mutant SOD1 is able to protect against toxicity, cell viability assays were performed on HspB8/SOD1 co-transfected cells 72 hours post-transfection. Both G85R and G93A mutants were toxic with the vector alone but this toxicity was rescued by the overexpression of HspB8. Expression of $HspB8^{K141N}$ alone resulted in 25% cell toxicity in NSC-34 cells when compared to $HspB8^{WT}$ or control. As toxicity was not compounded in mutant SOD1 and $HspB8^{K141N}$ co-transfected cells, this suggests that the same cell death pathways are activated by SOD1 and HspB8 mutants (Fig. 3.9).

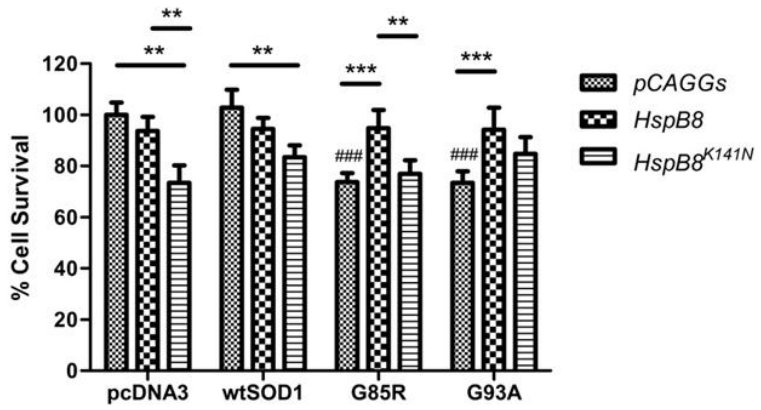

Fig. 3.9 Overexpression of wildtype HspB8 ameliorates mutant SOD1 cell death. NSC-34 cells were transiently co-transfected with HspB8 and SOD1 constructs for 72h after which cells were

treated with 3-(4,5-dimethylthiazol-2-yl)-2,5-diphenyltetrazoloium bromide (MTT, 5mg/ml) in PBS for 1h. The reaction was terminated by addition of absolute dimethyl sulphoxide and the absorbance was measured at 544nm in a microplate reader (FluoStar, BMG). Values were normalized to pcDNA3/pCAGGs co-transfected cells. Data represent means ± SD for 4 independent experiments **$p<0.01$, $^{\#}p<0.05$ vs pcDNA3.

3.2.5 Increased HspB8 protein levels observed in symptomatic G93A mice

To determine the role of HspB8 *in vivo*, western blots were performed on spinal cord lysates from G93A mice at presymptomatic (P30), symptomatic (P100), and terminal (P150) stages of the disease. Age-matched non-transgenic (Ntg) and wildtype SOD1 transgenic mice were used as controls. As shown in Fig. 3.10A, HspB8 levels fluctuated with disease with HspB8 levels peaking at P100. By end stage, HspB8 levels were decreased relative to the symptomatic stage, but were still increased relative to presymptomatic stages despite the loss of motor neurons at this advanced stage of the disease. Compared to Ntg or WT, HspB8 protein levels were greater in G93A mice at all ages (Fig. 3.10A and BI).

20S β1 proteasome subunit levels were also studied. In spinal cords from G93A transgenic mice, levels of the proteasome subunit increased with disease progression, with levels peaking at end stage. However, compared to Ntg or WT mice, levels of 20S β1 proteasome were reduced in G93A mice at all stages of the disease (Fig. 3.10A and BII). Although speculative, increased autophagy driven by high levels of HspB8 in the spinal cord of G93A may negatively regulate UPS systems to protect cells against excess protein degradation. This may occur through transcriptional regulation of proteasomal subunits or through increased degradation of UPS components.

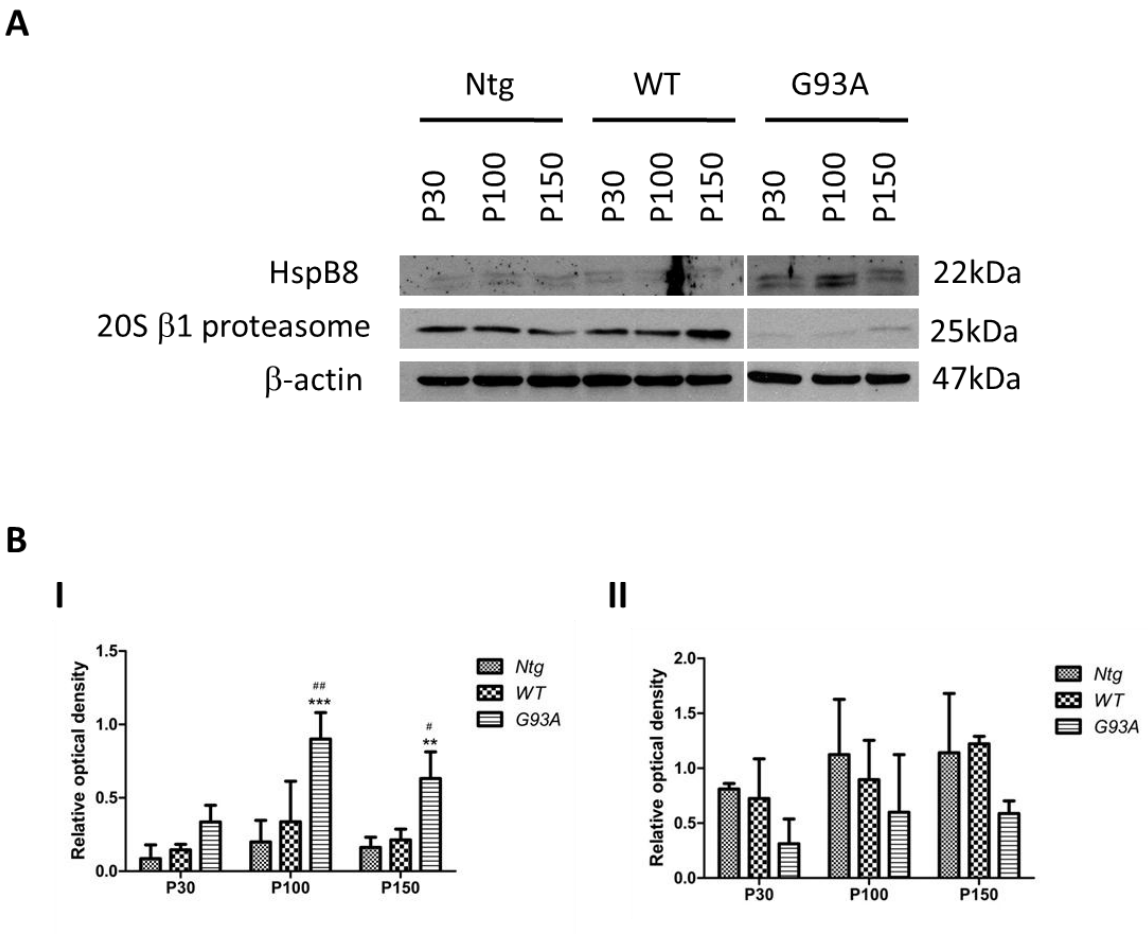

Fig. 3.10 Increased HspB8 in spinal cords of symptomatic G93A mice (A) Immunoblotting analysis of HspB8 and 20S β1 proteasome subunit in the spinal cord of pre-symptomatic (P30), symptomatic (P100) and end-stage (P150) transgenic $SOD1^{G93A}$ mice. A total of 50μg of protein was loaded into each lane. (B) Relative intensities of HspB8 (I) and 20S β1-proteasome subunit (II) at each stage. Optical densities for HspB8 and 20S β-1 proteasome subunits were measured relative to the optical densities observed for β-actin for each sample. n=3, bars represent mean ± SD, *$p<0.05$

3.2.6 Defective autophagy in peripheral blood mononuclear cells derived from distal HMN patient with HspB8 mutation K141E

The *in vitro* study showed that mutations in lysine 141 in HspB8 impair the autophagic activities of the chaperone. To confirm this finding *in vivo*, peripheral blood mononuclear cells (PBMCs) were isolated from a distal HMN patient harbouring the K141E mutation. To assess the degree of basal autophagy and induced autophagy, PBMCs were incubated with R10 and starvation media respectively. PBMCs were also incubated with E64d/pepstatin in starvation media. Autophagy was examined using the Imagestream instrument to observe colocalization between LC3A and lysosomal markers. As shown in Fig. 3.11A, basal autophagy was reduced in PBMCs from the patient. A similar trend was observed in patient PBMCs under starved and autophagy-inhibited conditions. Consistent with the *in vitro* findings, fluorescent intensities of LC3A in patient PBMCs were higher than those of healthy individuals under basal conditions indicating a lack of LC3A turnover (Fig. 3.11B). Altogether these findings support the role of HspB8 in autophagy *in vivo*.

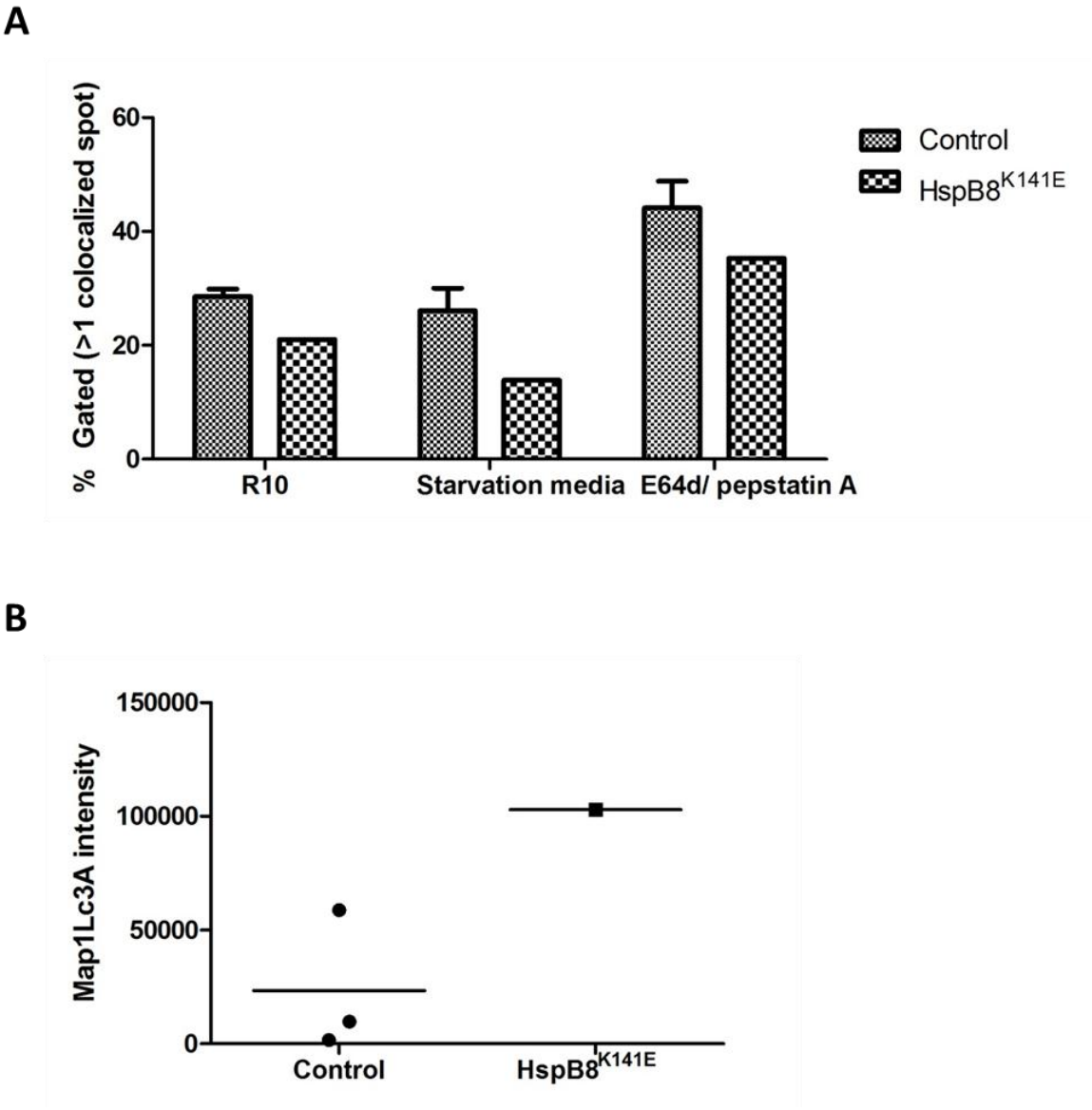

Fig. 3.11 Impaired autophagy in PBMCs from patient carrying K141E mutation. (A) PBMCs from 3 age-matched healthy controls and 1 patient carrying the HspB8^{K141E} mutation were fixed and stained with lysosome marker (lysoID), and LC3A. 25,000 cells were counted by ImageStream and autophagy was assessed by colocalization between lysoID and LC3A. (B) Fluorescent intensities of LC3A in PBMCs under basal conditions. n=3 for control and n=1 for patient groups

3.3 Discussion

Many cells respond to proteotoxic stress by inducing expression of heat shock proteins with a variety of chaperone activities. Upregulation of Hsp70 by mutant SOD1 attenuates protein aggregation and facilitates degradation of the mutant protein by association with CHIP (Bruening et al., 1999, Urushitani et al., 2004, Koyama et al., 2006). Similarly, the small heat shock protein, HspB1, is also upregulated by mutant SOD1 and protects against protein aggregation by maintaining mutant proteins in a folding-competent state (Vleminckx et al., 2002). In this study, the accumulation of mutant SOD1 within the cytosol was shown to induce HspB8 expression, which in turn was shown to promote the clearance of aggregates through autophagy. As overexpression of HspB8 promotes cell survival in mutant SOD1-expressing cells, this indicates that the upregulation of HspB8 *in vivo* is a protective measure to counter the toxic effects of SOD1 aggregates.

Large perinuclear aggregates containing mutant SOD1 are prominent pathological features in human post-mortem spinal cords, cell culture models, and mouse models of SOD1-FALS (Dalcanto and Gurney, 1994, Shibata et al., 1996, Bruijn et al., 1998). In SOD1 transgenic mouse models, detergent-insoluble inclusions appear after symptom onset and are associated with the abnormal expression of a number of stress-related chaperones. The results in this study show that HspB8 is upregulated in G85R and G93A-expressing cells and in spinal cords of G93A transgenic mice at symptom onset. In both cases, HspB8 induction coincides with the appearance of detergent-insoluble SOD1 aggregates indicating that its upregulation is dependent upon protein misfolding in the cytosol. As there was no change in HspB8 mRNA levels, upregulation of HspB8 does not appear to be Hsf1 driven and likely occurs via post-transcriptional mechanisms. Alternatively, cytosolic mutant

SOD1 initially induces Hsf1 activation, but this is later attenuated during chronic cellular stress.

In vitro, overexpression of HspB8 increased the solubility of mutant SOD1 aggregates through direct binding to the misfolded protein. In addition, HspB8 promoted autophagy of two different SOD1 mutants, G85R and G93A, suggesting that the effects of HspB8 are not variant specific. Although this study took a different approach to evaluate autophagy, the results obtained for the G93A mutant are consistent with the study by Crippa et al. (Crippa et al., 2010). In agreement with their data, reduced LC3A levels were observed in all HspB8 overexpressing cells indicating that HspB8 had an overall effect of stimulating autophagy in cells. However, as autophagy was greatest in mutant SOD1 co-expressing cells, this suggests that there is some specificity in the induction of this pathway. Increased autophagy was also observed in G93A cells presumably as a result of HspB8 upregulation. Interestingly, reduced levels of HspB8 were found in serum-deprived or MG132-treated cells. Since both serum deprivation and proteasome inhibition promotes aggregate formation, treating cells with these can exacerbate mutant SOD1 aggregation leading to enhanced HspB8 turnover through autophagy. As such, HspB8 upregulation is not dependent on proteasome inhibition – as was suggested in the study by Crippa et.al (Crippa et al., 2010) – but rather occurs directly as a result of mutant SOD1 misfolding and aggregation in the cytosol.

Several studies have shown HspB8 substrates are degraded through macroautophagy and is dependent on HspB8 binding to its co-chaperone, Bcl2-associated athanogene 3 (Bag3) (Arndt et al., 2010, Fuchs et al., 2010). Bag3 then recruits the

Hsc70/CHIP complex to allow ubiquitylation of the substrate which is required for recognition by the macroautophagy machinery (Arndt et al., 2010).

Autophagy plays a key role in the clearance of mutant SOD1 aggregates *in vivo*. Increased LC3II levels have been observed in post-mortem spinal cord samples from SALS and FALS patients and in spinal cords of symptomatic G93A mice (Morimoto et al., 2007, Hetz et al., 2009). The finding that HspB8 levels also peak in symptomatic G93A mice supports the role of HspB8 in autophagy *in vivo*. As HspB8 transcripts and proteins were found in both the axons and cell bodies of motor neurons in adult spinal cord sections, HspB8 is likely to be involved in the selective autophagy of proteins in these regions.

This study also found HspB8 mutants were impaired in autophagy in cell culture and *in vivo* using PBMCs derived from the dHMN patient harbouring the K141E mutation. Mutations at the K141 residue in HspB8 did not affect substrate binding, nor did they affect the ability to induce autophagy as observed by the high levels of LC3A in cells. Rather, HspB8 mutants affected a downstream step – perhaps through impaired Bag3 binding or through disruption of the microtubule network. Although HspB8 does not appear to interact with the cytoskeleton directly, HspB8 may mediate effects through its binding partner HspB1. Both HspB8^{K141E} and HspB8^{K141N} mutants demonstrate a greater affinity for HspB1 and sequestration of HspB1 can prevent its functions in the maintenance of the cytoskeleton (Fontaine et al., 2006). In agreement with this idea, beaded neurites have been observed in primary motor neuron cultures expressing HspB8 mutants indicating damage to the axonal cytoskeleton (Irobi et al., 2010). Interestingly, we have found that G93A also interacts with β-actin only in the presence of HspB8^{K141N} indicating that aberrant interactions with cytoskeletal proteins is likely to contribute to motor neuron cell death.

Contrary to previous findings, the results presented in this study suggest that HspB8 causes toxicity through the loss of function rather than a gain-of function. Autophagy was first described as a survival strategy in yeast to allow cells to degrade cytoplasmic contents for amino acids during starvation (Klionsky, 2007). However, extensive neurodegeneration and post-embryonic lethality have been observed in non-starved Atg-knockout mice, thus suggesting that in higher eukaryotes, autophagy has additional roles beyond that of starvation-induced survival (Hara et al., 2006, Komatsu et al., 2006). Indeed, the proteostatic functions of autophagy in neurons are particularly critical and the loss of such protective activities can have dire consequences for motor neuron function and survival. In particular, protein aggregates accumulating in the cytosol can sequester sHsps and other cellular proteins whose activities are crucial for motor neuron survival (Ackerley et al., 2006, Fontaine et al., 2006). Both of the HspB8 mutations target the evolutionarily conserved α-crystallin domain that is essential for HSPB8 stability, this destabilises the protein and results in aggregates that are associated with reduced cell viability. Since HspB8 is itself induced by protein aggregation, the formation of mutant HspB8 aggregates may prompt an increased expression of HspB8 mutant protein. This would aggravate the situation further with an increase in cellular stress and eventually cause activation of the cell death programs.

Chaperones are found to be potent modulators of neurotoxicity in models of ALS. *In vitro,* overexpression of Hsp27 and Hsp70 was protective against mutant SOD1 aggregates and prevented cell death (Patel et al., 2005a). Furthermore, pharmacological induction of the heat shock response by arimoclomol increased motor neuron survival, improved muscle function and extended the lifespan of G93A mice (Kieran et al., 2004b).

In this study, overexpression of wildtype but not mutant HspB8 suppresses mutant SOD1-mediated cell death indicating that autophagic clearance of mutant SOD1 aggregates is necessary for protection against mutant SOD1. As HspB8 mutations do not compound mutant SOD1 toxicity, it is possible that motor neuron cell death caused by mutations in HspB8 activates the same cell-death pathways as that of SOD1.

As many aggregate-prone proteins such as mutant SOD1 and HspB8 cause disease, therapeutic strategies that enhance autophagy may be beneficial. Moreover, as mitochondrial abnormalities and dysfunction are commonly observed in mutant SOD1 models, induction of autophagy by HspB8 can also help to eliminate these organelles before they activate the apoptotic programs.

4. Modelling accumulation of mutant SOD1 in the mitochondrial intermembrane space

4.1 Introduction

Mitochondria are indispensible eukaryotic organelles with important metabolic functions. In addition to providing the main source of cellular ATP by oxidative phosphorylation, mitochondria also have roles in calcium buffering and in regulating apoptotic cell death. Inside the mitochondria, SOD1 is concentrated in the intermembrane space (IMS) (Okado-Matsumoto and Fridovich, 2001, Sturtz et al., 2001, Higgins et al., 2002, Liu et al., 2004), but can also be found in the matrix and on the cytosolic face of the outer membrane. The roles of mitochondrial SOD1 have yet to be fully characterized, although SOD1 in the IMS is thought to protect against superoxides generated by the respiratory chain on the cytosolic side of the inner membrane.

The mechanisms of mitochondrial import of SOD1 are not yet fully understood. Known mitochondrial targeting signals or internal amino acid motifs that identify mitochondrial proteins have not been found in the SOD1 sequence. Studies in yeast have shown that import of SOD1 into the mitochondria can only occur if the protein is non-metallated and disulphide reduced (Field et al., 2003). Trapping and folding of SOD1 in the IMS is dependent on copper insertion and disulphide bridge formation facilitated by the copper chaperone for SOD1 (CCS). As CCS is, itself, distributed between the cytosol and mitochondria, the pool of CCS in the IMS at any given time will determine the amount of SOD1 inside the mitochondria (Sturtz et al., 2001, Field et al., 2003). Furthermore,

mitochondrial localization of CCS is regulated by oxygen status within the cell, thus allowing SOD1 uptake into the IMS to be physiologically regulated by oxygen concentration (Field et al., 2003, Kawamata and Manfredi, 2008). Upon import, folding of SOD1 by mitochondrial CCS traps wtSOD1 in the IMS. SOD1 import into the IMS is also regulated by the Mia40/Erv1 pathway – a disulphide relay system which in yeast allows import of CCS and other cysteine-rich proteins requiring oxidative folding into the IMS [reviewed in (Hell, 2008)]. Downregulation of Erv1 in yeast results in decreased SOD1 import (Mesecke et al., 2005).

Unlike wtSOD1, pathogenic ALS mutants demonstrate an increased propensity to misfold and aggregate and thus are not subjected to the same physiological regulation as wtSOD1. Enzymatically inactive mutant G85R was unresponsive to the physiological modulations of import by oxygen and the Mia40/Erv1 system, and its localization within the mitochondria was primarily dictated by the formation of aggregates (Kawamata and Manfredi, 2008). Import of G93A was only partially regulated by oxygen status and its localization in the mitochondria was also driven by aggregation formation (Kawamata and Manfredi, 2008). Thus misfolding and aggregation of SOD1 mutants in the mitochondria bypasses the mechanisms that regulate import into the mitochondria and may contribute to the mitochondrial dysfunction and cell toxicity that is observed in both cell and mouse models of ALS (Kawamata and Manfredi, 2008).

4.1.1 Aims of this chapter

Mitochondrial stress deriving from mitochondrial dysfunction and misfolded protein species has been linked to a number of debilitating neurodegenerative conditions. Since the majority of mutant SOD1 associated with the mitochondria resides in the IMS, the likelihood of finding a mitochondrial unfolded protein response to mutant SOD1 would be greatest for this compartment. Therefore, the primary aim for this chapter is to create a model for the accumulation of mutant SOD1 in the intermembrane space in motor neuron-like cells such that they could be used to identify proteins of the IMS stress response. Cells will also be characterized to determine if they can recapitulate some of the mitochondrial dysfunction observed in previous studies.

4.2 Results

4.2.1 Confirming expression of IMS-SOD1 constructs in NSC-34 cells

To model the accumulation of wildtype or mutant SOD1 within the intermembrane space, the bipartite signalling sequence from HtrA2 was incorporated N-terminal to the SOD1 cDNA sequence and the resulting construct was transfected into NSC-34 cells. The bipartite presequence will direct import of SOD1 through the OMM and into the IMS where it will be cleaved by an unknown IMS protease, leaving SOD1 trapped within the IMS (Fig. 4.1A). Comparisons of western blots of mitochondrial and cytosolic fractions derived from stable cell colonies revealed that hSOD1 was enriched in the mitochondrial fractions with both full length (~32kD, IMS-SOD1) and mature, processed hSOD1 (~22kDa) observed (Fig. 4.1B). The presence of this mature band also suggests localization

of hSOD1 within the intermembrane space since cleavage requires the IMS protease. The absence of full length bands for IMS-wtSOD1 clones 1 and 2 indicates that cleavage of the presequence is highly efficient in these cells (Fig. 4.1B). Localization of IMS-targeted hSOD1 in the mitochondria was also verified in these colonies by immunofluorescence after transfection with mito-DsRed2 (Clontech) (Fig. 4.1C). The immunofluorescence and western blot data also reveal that little IMS-SOD1 could be found in the cytosol thus confirming that the mitochondrial targeting was efficient.

4.2.1 Effects of IMS-targeted SOD1 on mitochondrial shape and content

Swollen, fragmented mitochondria have previously been observed in cell culture and in mouse models of SOD1-FALS (Kong and Xu, 1998, Menzies et al., 2002b, Raimondi et al., 2006). To determine if mitochondrial morphology was altered by continuous expression of mutant SOD1 in the IMS, live cell imaging was used. Mitochondrial structure was visualized by transfection of mito-DsRed2. In IMS-wtSOD1 expressing cells, mitochondrial morphology did not appear to be affected and mitochondria appeared as tubular structures in the cell soma and in the axons. In contrast, in cells overexpressing IMS-targeted G85R and G93A, the mitochondrial network appeared fragmented and mitochondria appeared as round, punctuate structures in the cytoplasm (Fig. 4.2). These results are consistent with the mitochondrial morphology observed in fixed cells (Fig. 4.1C). Abnormal mitochondrial morphology was observed in ~15% of cells expressing IMS-G85R and G93A; abnormalities were not observed in the wildtype cell line.

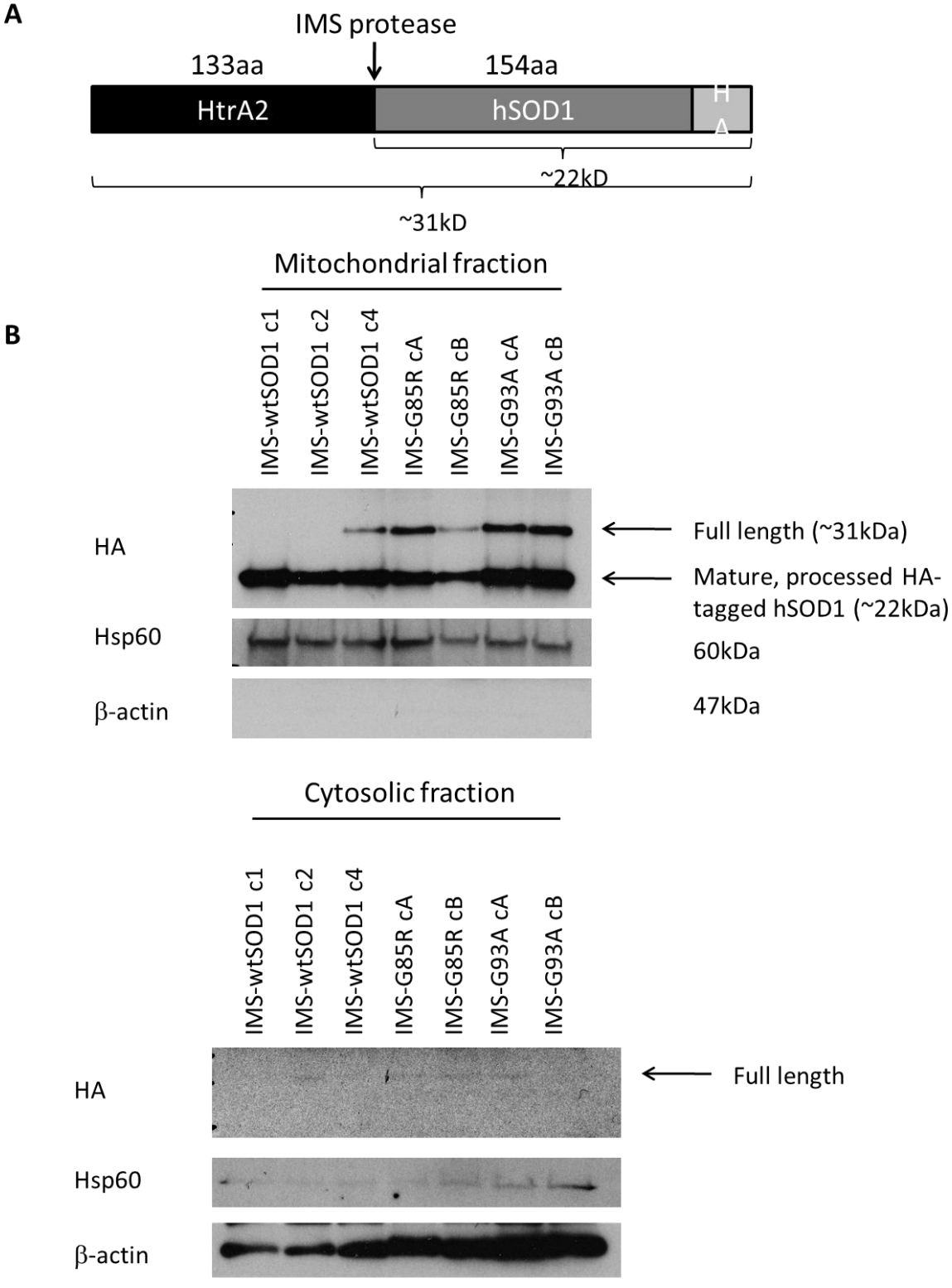
A
IMS protease
133aa
154aa
HtrA2
hSOD1
HA
~22kD
~31kD
B
Mitochondrial fraction
IMS-wtSOD1 c1
IMS-wtSOD1 c2
IMS-wtSOD1 c4
IMS-G85R cA
IMS-G85R cB
IMS-G93A cA
IMS-G93A cB
HA
Hsp60
β-actin
Full length (~31kDa)
Mature, processed HA-tagged hSOD1 (~22kDa)
60kDa
47kDa
Cytosolic fraction
IMS-wtSOD1 c1
IMS-wtSOD1 c2
IMS-wtSOD1 c4
IMS-G85R cA
IMS-G85R cB
IMS-G93A cA
IMS-G93A cB
HA
Hsp60
β-actin
Full length

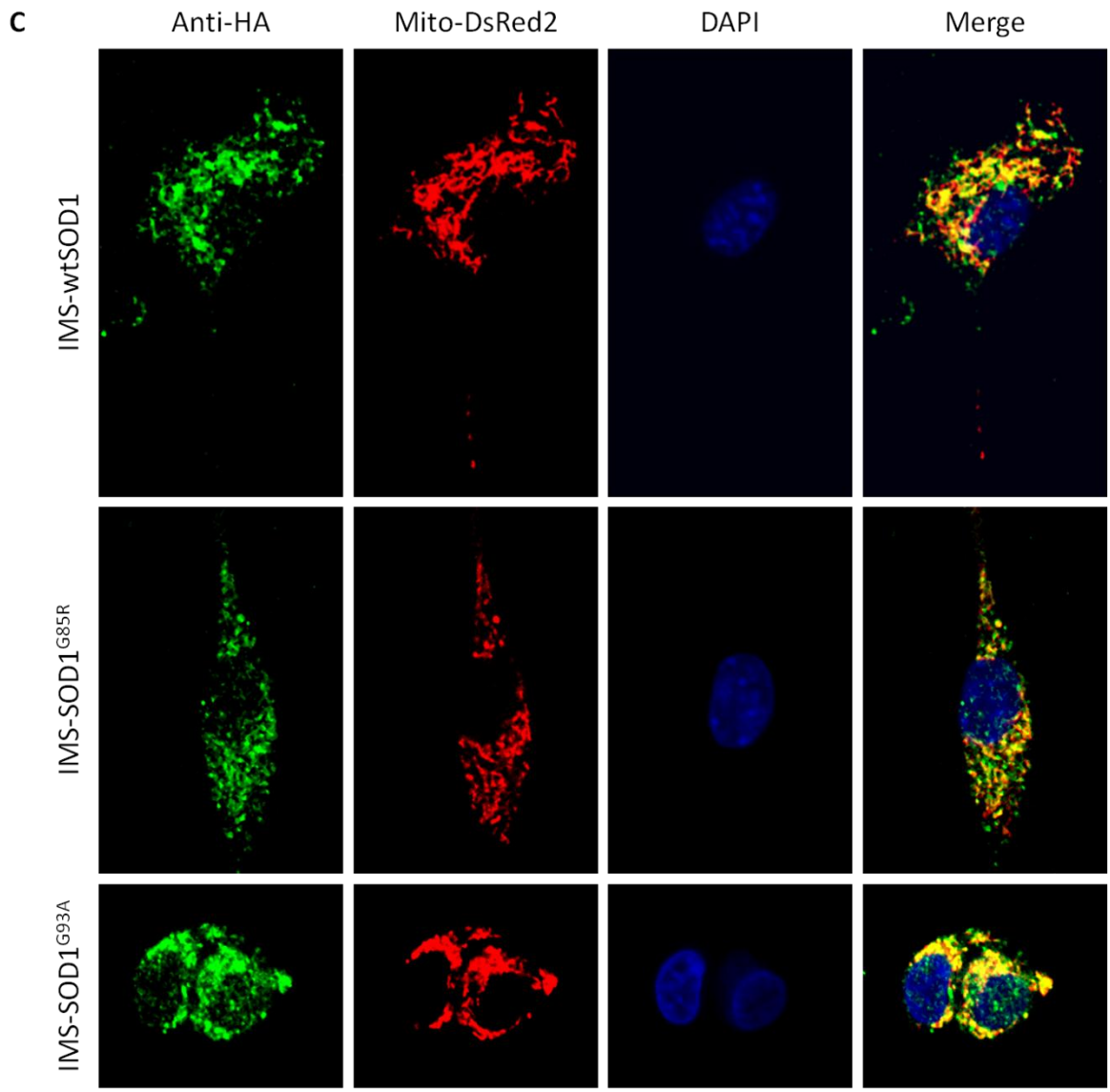

Fig 4.1 Targeting SOD1 into the mitochondrial intermembrane space. (A) Schematic of the IMS-hSOD1 construct. The 399nt bipartite signal sequence from HtrA2 was incorporated at the N-terminus of hSOD1 cDNA. A C-terminal HA tag was added to facilitate detection. (B) Confirming delivery of SOD1 into the IMS. NSC34 cell lines constitutively expressing IMS-SOD1 constructs were harvested and subcellular fractions analysed by western blotting. In the mitochondrial fraction, both unprocessed (~31KDa) and processed (~22KDa) hSOD1 bands were observed with the HA antibody. Only a faint unprocessed band was observed in the cytosolic fraction in each of the stable cell clones. Hsp60 and β-actin are markers of the mitochondria and cytosol respectively. (C) Representative images of NSC-34 cells co-transfected with IMS-SOD1 and mito-DsRed2 (Clontech) constructs to confirm localization of hSOD1 in the mitochondria. Cells were fixed and immunostained for the HA-epitope.

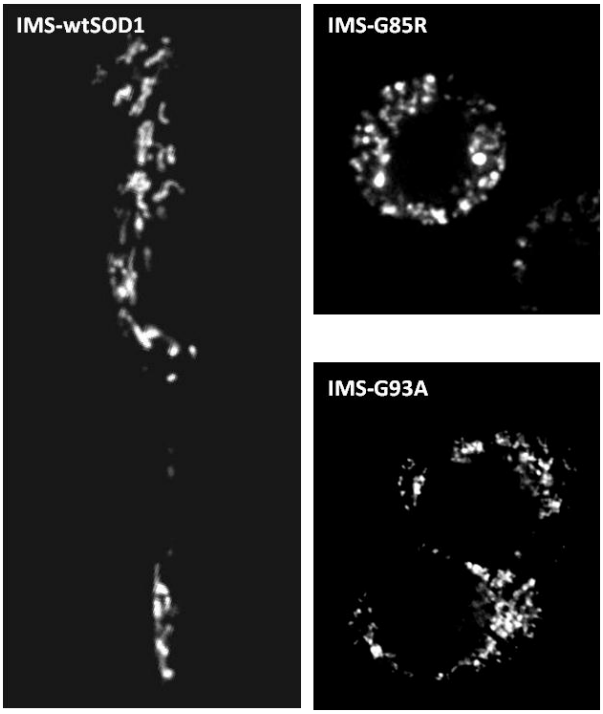

Fig. 4.2 Mitochondrial fragmentation in IMS-targeted mutant SOD1 expressing cells. NSC-34 cell lines were co-transfected with mito-Dsred2 and mitochondria were visualized by live cell imaging.

To address whether targeted expression of human SOD1 in the IMS has any effect on mitochondrial number, cell lines expressing IMS-targeted or untargeted SOD1 (pcDNA3-wtSOD1 and pcDNA3-G93A) were stained with Mitotracker Green (Invitrogen) for 1 h. Mitotracker Green is a fluorescent, vital dye that is specific for mitochondria and allows mitochondria to be quantified by fluorescence intensity in a flow cytometer (FACS). In basal culturing conditions (glucose), increased numbers of mitochondria were observed in all human SOD1 expressing cell lines although these differences were not significant when compared with the empty vector control. Interestingly, mitochondrial counts in IMS-

targeted G85R cell lines were much reduced compared to other human SOD1 expressing cell lines indicating that mitochondrial numbers may correlate with dismutase activity in the cell.

Subtle mitochondrial defects can often be masked in cells grown under basal conditions due to non-physiologically high amounts of glucose in the media that allows cells to generate ATP solely through glycolysis. Therefore, to stimulate oxidative phosphorylation in cultured cells, cells were grown in media in which glucose was replaced with glutamine. Under these conditions of metabolic stress, the differences in mitochondrial counts between cell lines were more pronounced with IMS-wtSOD1 exhibiting 8-fold more mitochondria compared to the pcDNA3 control. Consistent with findings in high glucose medium a significant reduction in mitochondria number was also observed in IMS-G85R cells when compared to IMS-wtSOD1. In general, mitochondrial counts in glutamine conditions was higher compared to cells grown in high glucose media and reflects the cells reliance on oxidative phosphorylation for ATP (Fig. 4.3).

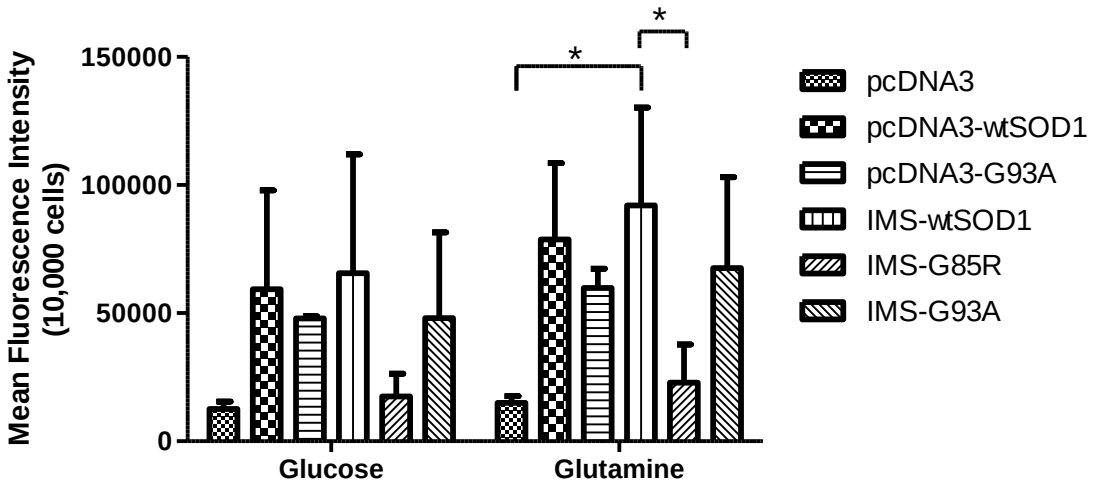

Fig. 4.3 Effects of mutant SOD1 on mitochondrial content. Cell lines constitutively expressing empty vector (pcDNA3), untagged wtSOD1 (pcDNA3-wtSOD1) and G93A (pcDNA3-G93A), and IMS-targeted wtSOD1, G85R and G93A were labelled with Mitotracker Green (Invitrogen) for 1h after which 10,000 cells were counted by flow cytometry. n=3, bars represent mean ± SD, *$p<0.05$

4.2.2 IMS-mutant SOD1 results in decreased respiratory chain activities under basal cell culture conditions and in conditions of metabolic stress

To investigate the effects of mutant SOD1 expression in the IMS on respiratory chain activities, oxygen consumption was measured with a Clark-type oxygen electrode in cells grown in basal conditions and in conditions of metabolic stress. Under normal conditions, oxygen consumption was halved in both IMS-targeted SOD1 mutants when compared with the empty vector control. Oxygen consumption was also reduced in IMS-wtSOD1 but this was not significant when compared with the control (Fig. 4.4). The removal of glucose stimulated oxygen consumption by ~20% in both pcDNA3 and IMS-wtSOD1 cell lines. A smaller increase in oxygen consumption was also observed in both IMS-G85R and IMS-G93A after culturing in glutamine-containing media, although this also was not significant. Again, significantly reduced respiratory chain activities were

observed in metabolically stressed-cells expressing either of the IMS-targeted SOD1 mutants (Fig. 4.4).

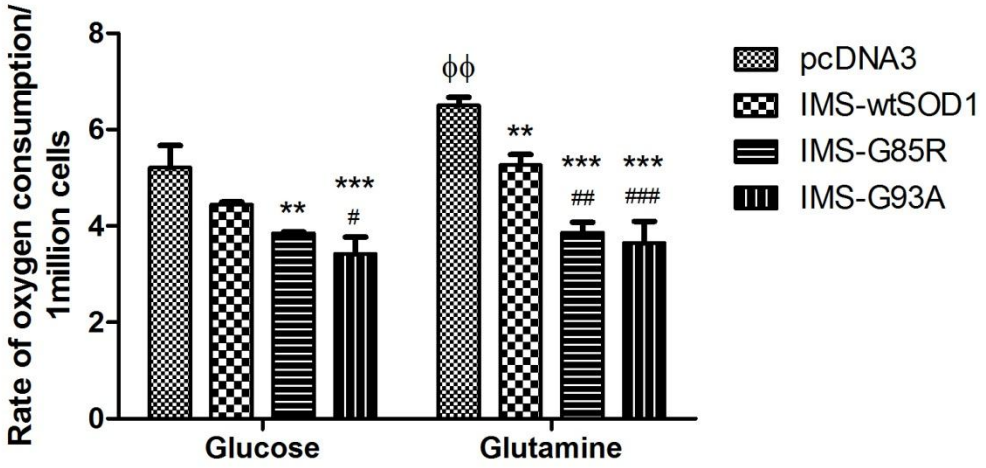

Fig. 4.4 Decreased respiratory chain activity in IMS-targeted mutant SOD1 expressing cells. Stable cell lines were cultured in normal glucose-containing media or in media where the glucose is replaced with glutamine for 4 days prior to the experiment. Rates of oxgygen consumption were measured at 37°C using the Clark electrode over a period of 30 minutes. n=2, data represents mean ± SD, ***$p<0.001$ vs pcDNA3, $^{###}p<0.001$ vs IMS-wtSOD1, $^{ΦΦ}p<0.01$ vs glucose

4.2.3 Expression of mutant SOD1 in the intermembrane space results in NSC34 cell death

To assess whether expression of wildtype or mutant SOD1 in the IMS causes toxicity, cell viability assays were performed 72h after cells were transiently transfected with IMS targeting constructs. Under normal conditions, both G85R and G93A expression in the IMS were toxic to cells with more than 40% cell death observed in both groups (Fig. 4.5A). Overexpression of IMS-wtSOD1 had little effect on NSC34 cell viability (Fig.

4.5A). The degree of toxicity associated with mutant SOD1 expression in the IMS compared to that of the cytosol was also studied. In this transient system, IMS mutant SOD1 constructs were ~15% more toxic compared to untagged constructs (Fig. 4.5A). Cell viability was also measured in NSC-34 cells constitutively expressing SOD1 in the IMS or cytosol. Consistent with the transient system, increased cell death was observed in cells stably expressing G85R and G93A mutants in the IMS. Constitutive expression of G93A in the cytosol also increased cell death by 15% compared to wildtype or control. Expression of wtSOD1 in either compartment had no effect on cell viability (Fig. 4.5B). Noxious effects of mutant SOD1 in the intermembrane space was cell type-specific, as HEK293 cells were largely unaffected after transfection of IMS-SOD1 (Fig. 4.5C).

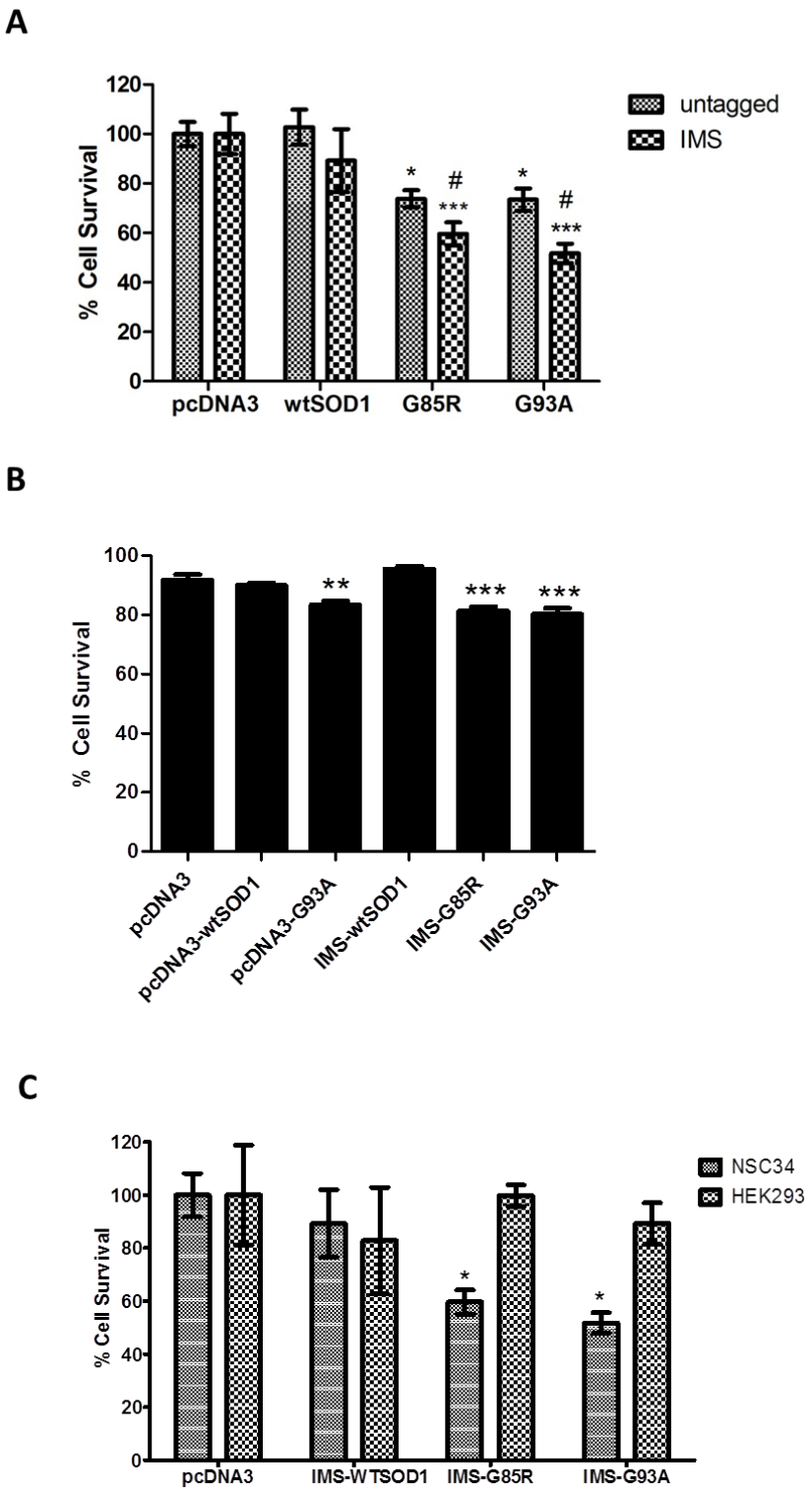

Fig 4.5 Expression of pathogenic SOD1 mutants in the IMS results in NSC34 cell death (A) Comparing the degree of toxicity associated with mutant SOD1 expression in the IMS to that of the cytosol. NSC34 cells were transiently transfected with IMS-targeted SOD1 constructs or untagged

(cytosolic) SOD1 constructs for 72h before Live/Dead cell viability assays were performed. (B) Assessing the degree of toxicity in NSC34 cells constitutively expressing untagged (pcDNA3) or IMS-targeted SOD1. (C) Pathogenic mutants are toxic to motor neuron-like cells but not HEK293 cells. NSC34 and HEK293 cells were transfected with IMS constructs for 72h after which Live/Dead cell viability assays were performed. Values are normalized to pcDNA3/NSC34 for each group. n=4 for each group, bars represent mean ± SD, #$p < 0.05$ vs untagged. *$p < 0.05$ vs pcDNA3

4.3 Discussion

This study took advantage of the well characterized mitochondrial import mechanism of HtrA2 and its highly conserved bipartite sequence to create NSC-34 cell lines that constitutively express wildtype, dismutase-inactive (G85R) and dismutase-active (G93A) SOD1 in the intermembrane space (IMS). Similar cell lines have also been created by Magrane et al. although a yeast cyt b_2 sequence was used to deliver SOD1 into the IMS in their study (Magrane et al., 2009). The main purpose of this study is to illustrate that human SOD1 can be effectively targeted to the mitochondrial IMS where it causes some of the well-known mitochondrial dysfunction that is observed in mouse models and in human FALS.

Mitochondrial fragmentation has previously been observed in motor neurons of transgenic SOD1 mice (De Vos et al., 2007), and in cell culture models transfected with untagged (cytosolic) mutant SOD1 (Menzies et al., 2002b, Raimondi et al., 2006), and IMS-targeted mutant SOD1 (Magrane et al., 2009). Consistent with these findings, small, punctuate mitochondria were also found in IMS-targeted G85R and G93A mutants in this study. In addition, this study also quantified mitochondria in the different cell lines. Under normal conditions, changes in mitochondrial content in the cell lines, compared to controls, were not significant. However, induction of metabolic stress resulted in significant increases in mitochondrial content in IMS-targeted wtSOD1. As mitochondrial numbers

were greatest in all cell lines exhibiting increased dismutase activity (either through overexpression of wtSOD1 or G93A) these preliminary results suggests that mitochondrial content may be influenced by SOD1 activity in cells. However, further studies will have to be done with other dismutase-inactive SOD1 mutants to test this hypothesis. A similar study analysing mitochondrial content after targeting SOD1 into the IMS also found no changes under normal conditions, but found reduced mitochondria number in mutant SOD1 expressing cells after inducing differentiation of the cells (Magrane et al., 2009). Thus, differences in results may arise from the different culturing conditions and the types of stress induced in the cells.

A balance between mitochondrial fission and fusion is thought to determine the shape and number of mitochondria in healthy and dying cells. Although mitochondrial fragmentation by mutant G93A has long been observed, the mechanism underlying this has not yet been determined. It is possible that the imbalance between fission and fusion rates may serve to accelerate removal of damaged mitochondrial proteins by autophagy. Mitochondrial fission is required for the selective removal of damaged mitochondrial components and increased fission is accompanied by increased mitochondrial autophagy (mitophagy) in primary cortical cultures (Barsoum et al., 2006). Alternatively, the disequilibrium between mitochondrial fission and fusion may arise through direct impairment of fission or fusion machinery by mutant SOD1. As both these processes are dependent on ATP, reduced respiratory chain activities in both IMS-targeted G85R and G93A cells can cause dysregulation of mitochondrial fusion and fission leading to alterations in mitochondrial shape. Reduced oxidative phosphorylation in these cells may occur through impairments in complex II and IV activities (Menzies et al., 2002b).

Impaired bioenergetics can also affect Ca^{2+} buffering capacity (Damiano et al., 2006), axonal transport (Miller and Sheetz, 2004, De Vos et al., 2007), protein degradation and other essential cellular functions. Mutant SOD1 has been found to selectively reduce mitochondrial anterograde movement resulting in the depletion of mitochondria from axonal terminals (Miller and Sheetz, 2004, De Vos et al., 2007). Therefore, the combined effects of mitochondrial redistribution and dysfunction is likely to place additional stress in synapses by further limiting the availability of ATP and reducing Ca^{2+} buffering capacity (De Vos et al., 2007).

Additional stress through mutant-SOD1 mediated mitochondrial damage can trigger apoptosis. In agreement with this theory, NSC-34 cells expressing IMS-targeted mutant SOD1 exhibit more cell death compared with their untagged counterparts. Mutant SOD1 toxicity also demonstrates cellular specificity, as HEK293 cells were unaffected by the expression of mutant SOD1 in the IMS. These results are also consistent with other studies in which extensive mitochondrial damage by G93A only occurred in motor neuron-like cells but not in MDCK cells (Raimondi et al., 2006). Over the years there has been speculation that mitochondria in motor neurons, and specifically in axonal and synaptic compartments, may be fundamentally different from other cell types and thus may not be able to cope with the additional burden of misfolded proteins. Thus, identifying components are that are involved in the processing of mutant SOD1 within this compartment may be an effective strategy in preventing mitochondrial dysfunction and stress associated with mutant SOD1.

5. Identifying potential components of an IMS-specific UPR by the targeted expression of mutant SOD1

5.1 Introduction

Protein quality control within organelles is essential to preserving their metabolic functions as well as cell survival. With the rare exception of respiratory chain complexes and mitochondrial ribosomes that are encoded by the mitochondrial genome, the vast majority of compartmental proteins are synthesized in the cytosol before their translocation as unfolded polypeptides to their destined subcompartments (as determined by the targeting sequences) [reviewed in (Tzagoloff and Myers, 1986, Schatz and Dobberstein, 1996)]. As such, organelles also require chaperones and proteases to monitor and facilitate the folding of imported polypeptides into their native conformation, and degrade those that are damaged or misfolded.

The unfolded protein responses (UPRs) comprise of a set of evolutionarily conserved signal transduction pathways aimed at minimizing the toxicity of misfolded proteins and restoring protein homeostasis during periods of cellular stress. Mutant SOD1 accumulation in the cytosol and ER has been found to induce Hsp (UPR^{cyt}) expression (Vleminckx et al., 2002, Kieran et al., 2004a, Crippa et al., 2010) and trigger UPR^{ER} respectively (Tobisawa et al., 2003, Wate et al., 2005, Atkin et al., 2006). Hitherto a mitochondrial UPR (UPR^{mt}) has been identified to operate in response to protein misfolding in the matrix compartment (Zhao et al., 2002, and reviewed in Haynes et al., 2010). As a majority of mutant SOD1 in mitochondria is concentrated in the IMS, it is

unlikely that the described UPR^{mt} can mitigate the effects of mSOD1 misfolding in the IMS. However, the prokaryotic origins of mitochondria raise the possibility that similar to the periplasmic compartment in bacteria the IMS may possess an independent UPR^{IMS} to counteract proteotoxic species in this compartment.

Like the UPR^{ER} and UPR^{mt}, adaptation to misfolded proteins in the IMS would require coordinated regulation and expression of genes involved in protein quality control in the IMS. Although little is known about how the PQC machinery operates in the IMS, stress mechanisms are highly conserved during evolution and it is possible that mammalian homologs of prokaryotic proteins involved in the periplasmic stress response retain the functions of their predecessors and thus may constitute components of the a *bona fide* UPR^{IMS}.

5.1.1 Protein import machinery

Protein import into the IMS is an essential feature of mitochondrial biogenesis and homeostasis. A large number of IMS proteins including SOD1 are catalytically or structurally reliant on disulphide bond formation allowing mitochondria to regulate the import and assembly of such proteins by controlling the redox environment in the IMS. The yeast mitochondrial intermembrane space assembly (MIA) pathway comprising the receptor protein, Mia40, and the sulphydryl oxidase, essential for respiration and viability 1 (Erv1), drives import of cysteine-rich proteins into the IMS and catalyses their folding through the formation of disulphide bonds (Fig. 5.1) (Chacinska et al., 2004). Since disulphide bond formation depends on the redox status of cytochrome c, import of proteins

through the MIA pathway is regulated by activities of the respiratory chain (Dabir et al., 2007). CCS is amongst the proteins and chaperones imported into the mitochondria via this pathway. As SOD1 levels in the mitochondria are determined by the amount of mitochondrial CCS, the MIA pathway indirectly acts as a regulator of SOD1 in this compartment (Field et al., 2003). Small Tim proteins and other chaperones are also imported via the MIA pathway [reviewed in (Hell, 2008)]. The presence of Mia40 and Erv1 orthologues in mammals (Chchd4 and Gfer, respectively) makes it likely that the same import mechanisms are also used in mammalian cells.

5.1.2 Chaperones

Small Tim proteins such as Tim8 and Tim9 function as chaperones that guide the import of pre-proteins through the outer and inner mitochondrial membranes (Fig. 5.1) (Sirrenberg et al., 1998, Wiedemann et al., 2004). Small Tim proteins are characterized by the presence of two pairs of cysteines, forming the 'twin Cx_3C' motif, and the formation of a disulphide bond between the cysteine residues via Mia40/Erv1 is essential for the hetero-oligomerization that is required for chaperone functions (Curran et al., 2002a, Curran et al., 2002b).

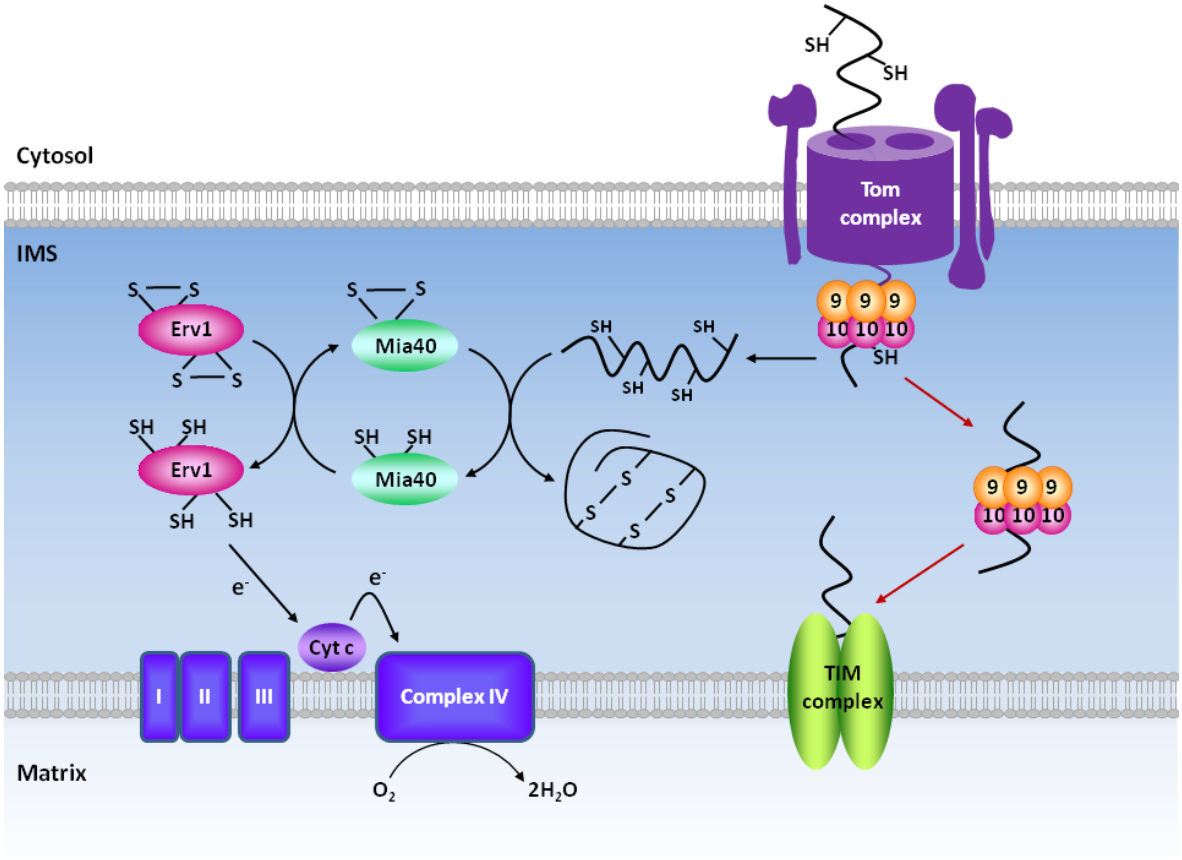

Fig. 5.1 Protein import and folding in the IMS. IMS proteins are imported in an unfolded conformation into the IMS through the translocases of the outer mitochondrial membrane (TOM complex). Vectorial translocation of substrates through the TOM complex may be assisted by small Tim proteins (e.g. Tim9 and Tim10), which assemble in hexameric complexes and bind to hydrophobic segments in the substrate, thus keeping proteins in an import-competent state. Once inside the IMS, proteins requiring oxidative folding are recognized and bound by the oxidized form of Mia40. Mia40 catalyses disulphide bond formation in the substrate protein; disulphide bond formation promotes folding of the protein thus trapping it in the IMS. Further rounds of import and disulphide bond formation require recycling of reduced Mia40 and this occurs via a series of steps. First, Mia40 is reoxidized by the sulphydryl oxidase, Erv1. Electrons from reduced Erv1 are subsequently shuttled to cytochrome c, which then passes the electrons to the final electron acceptor, oxygen, via complex IV. As such, the activities of the Mia40/Erv1 pathway are dependent on the activities of the respiratory chain. Inner membrane proteins are also guided to the translocase of the inner membrane (TIM complex) by small Tim proteins. Adapted from (Hell, 2008).

5.1.3 Proteolytic machinery

The elimination of misfolded/unfolded proteins in the IMS is critical to proper mitochondrial homeostasis and relies upon the action of proteases such as Yme1L1 and HtrA2. Yme1L1 is a protease of the i-AAA family and is involved in degradation of unassembled membrane complexes (Weber et al., 1996, Leonhard et al., 1999). A recent study has also shown that Yme1, the yeast orthologue of mammalian Yme1L1, is involved in protein translocation into the IMS (Rainey et al., 2006). Yme1 yeast mutants present abnormal mitochondrial function and morphology suggesting a key role for this protease in mitochondrial homeostasis (Campbell and Thorsness, 1998).

HtrA2 is a serine protease linked to Parkinson's disease (PD) and acts to limit the accumulation of mitochondrial IMS proteins following stress (Plun-Favreau et al., 2007). Loss of HtrA2 in the brain results in the accumulation of unfolded mitochondrial proteins and ROS which could signal activation of apoptosis through the activation of CHOP (Moisoi et al., 2009). As bacterial homologues of HtrA2, DegP and DegS, are components of a stress-activated proteolytic cascade that leads to the increased expression of genes encoding periplasmic chaperones and proteases [reviewed in (Schlieker et al., 2004)], this suggests that HtrA2 may also operate in an analogous fashion to protect cells against apoptosis under certain conditions in vertebrates. Although the mitochondrial substrates of HtrA2 are unknown, its activity within the IMS can be regulated by PTEN-induced kinase 1 (PINK1) (Plun-Favreau et al., 2007).

PINK1 kinase activity is required to protect cells from stress-induced mitochondrial dysfunction (Plun-Favreau et al., 2007). In addition to its role in activating HtrA2, PINK1 may also protect cells against the deleterious effects of mitochondrial damage by

promoting the elimination of dysfunctional mitochondria through autophagy (mitophagy) (Geisler et al., 2010, Narendra et al., 2010). Like HtrA2, mutations in PINK1 are also associated with Parkinson's disease (Valente et al., 2004).

5.1.4 Aims of Chapter 5

Age-dependent accumulation of mutant SOD1 occurs within the mitochondrial IMS in transgenic SOD1 mice (Liu et al., 2004). However, a homeostatic stress response mechanism has not yet been identified for this compartment. To address this issue, a model for the enhanced accumulation of misfolded mutant SOD1 within the IMS was created (Chapter 4). Changes in transcription and protein expression of PQC components in the IMS were determined to establish their ability to respond to mutant SOD1 misfolding in this compartment. Findings from the cell culture model were also validated in the SOD1 transgenic mouse.

5.2 Results

5.2.1 Effects of IMS-targeted mutant SOD1 on protein import and folding

Canonical UPRs result in an upregulation of chaperones and proteases to mitigate the effects of protein misfolding and aggregation. If mutant SOD1 misfolding and aggregation were to trigger a UPR^{IMS}, we speculated that it would upregulate IMS chaperones and components of the import machinery. CCS is a key chaperone involved in SOD1 folding, and CCS is imported into the IMS via the MIA pathway in yeast and mammals (Kawamata et al., 2008). This study assessed whether the components of this

pathway respond to mutant SOD1 misfolding in the IMS by monitoring mRNA transcript levels of Chchd4 and Gfer, the mammalian orthologues of Mia40 and Erv1. As shown in Fig. 5.2A, Gfer transcripts were significantly increased (>4fold) in IMS-G85R cells but not in G93A cells. As small Tim proteins also facilitate protein import and assembly in the IMS, transcript levels of Tim9 and Tim10 were also measured. Again, a significant increase in transcript levels for both the Tim proteins was observed in the IMS-G85R cell lines but not in the IMS-G93A cell lines. Levels of Tim transcripts for the other cell lines were slightly decreased relative to control although this was not statistically significant (Fig. 5.2B). qPCR results were also confirmed by immunoblotting of mitochondria-enriched fractions with a commercially available Gfer antibody. Again Gfer protein levels were much higher in IMS-G85R cells compared to the control (Fig. 5.2C).

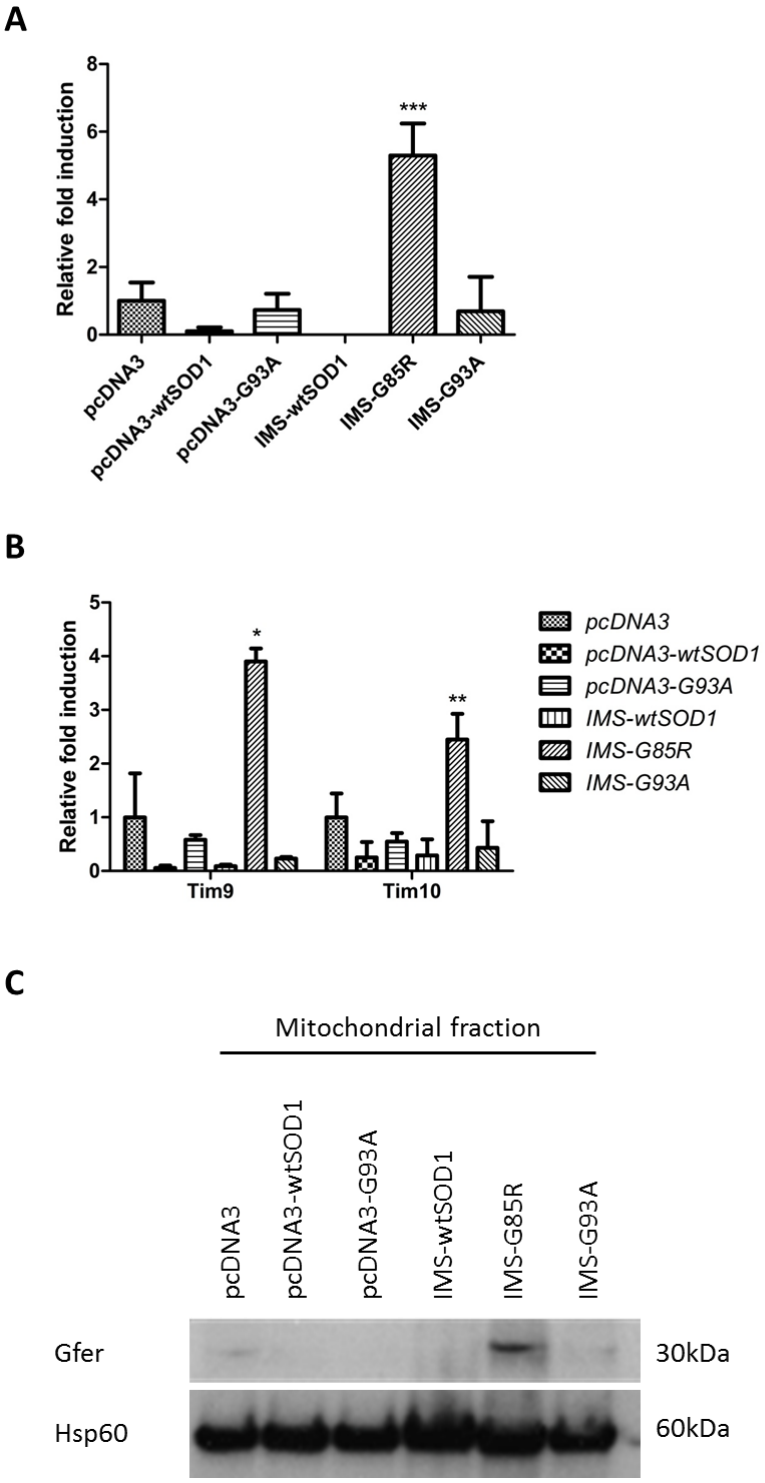

Fig. 5.2 Upregulation of genes encoding IMS chaperones and import machinery by mutant G85R. Cell lines constitutively expressing empty vector (pcDNA3), untagged wtSOD1 (pcDNA3-wtSOD1) and G93A (pcDNA3-G93A), and IMS-targeted SOD1 were grown under normal conditions. qPCR results show increased transcript levels of Gfer (A) and Tim9 and Tim10 (B).

Fold inductions for each gene are expressed relative to the amount present in pcDNA3-expressing cells. β-actin served as the endogenous control for each sample. Data represents mean ± SD for 3 independent experiments *p<0.05 vs pcDNA3 (C) Increased expression of Gfer was confirmed by western blotting of mitochondrial-enriched fractions.

5.2.1 Effects of IMS-targeted mutant SOD1 on the protein degradation machinery

To determine whether mutant SOD1 in the IMS alters the levels of proteases within the compartment, transcript levels of Yme1L1 and HtrA2 were also examine by qPCR. As shown in Fig. 5.3A, Yme1L1 transcripts were 3 fold greater in IMS-G85R compared to control. Levels of Yme1L1 transcript were comparable for all the other cell lines. In contrast, changes in HtrA2 levels were insignificant when compared to control (Fig. 5.3A). As PINK1 is known to phosphorylate HtrA2 and respond to mitochondrial stress, PINK1 transcript abundance was also measured. Levels of PINK1 transcript were 6 fold higher in IMS-G93A expressing cells and 3 fold higher in IMS-wtSOD1 expressing cells, although in the latter case, this was statistically insignificant when compared with the control. Interestingly, no changes were observed for the IMS-G85R mutant suggesting that responses to mutant SOD1 in the IMS may be variant specific (Fig. 5.3A). Changes in gene expression of Yme1L1 and PINK1 in IMS-G85R and IMS-G93A cell lines were also confirmed by western blotting. As shown in Fig. 5.3C, Yme1L1 levels were slightly increased in IMS-G85R cells and pcDNA3-wtSOD1 cell lines compared to control. In untagged and IMS-targeted G93A cell lines, Yme1L1 levels were similar to that of the control. Interestingly, Yme1L1 was not observed in IMS-targeted wtSOD1 cells indicating a very low level of expression for this protein (Fig. 5.3B).

PINK1 exists in two forms: a full length 63kDa form associated with the OMM which is relatively stable in depolarized mitochondria but which is rapidly cleaved into a

52kDa cytosolic fragment in normal mitochondria (Vives-Bauza et al., 2010). From western blotting analysis of total cell lysates, full length PINK1 protein was most abundant in IMS-G93A, IMS-wtSOD1, and pcDNA3-G93A expressing cells. In contrast, levels of cleaved PINK1 were greatest in IMS-G85R and pcDNA3-wtSOD1 expressing cells indicating that mitochondria are relatively stable in these cells (Fig. 5.3B).

As accumulation of PINK1 on the OMM is required for the selective degradation of mitochondria by the autophagosome-lysosome pathway (mitophagy) (Narendra et al., 2010, Vives-Bauza et al., 2010), mitophagy was assessed in IMS-targeted hSOD1 cell lines by imaging flow cytometry (Imagestream; Amnis). For each sample, cells were labeled with anti-Hsp60 (mitochondrial marker), anti-LC3A and Lyso-ID (lysosome marker). Colocalization between all three markers, as measured using the bright detailed similarity parameter provided by the IDEAS software (IDEAS; Amnis), indicates mitophagy. Under normal conditions (pCAGGs), mitophagy was greatest in IMS-targeted G93A cells. Mitophagy was also significantly enhanced in IMS-wtSOD1 expressing cells although this was 20% lower compared to IMS-G93A. Levels of mitophagy were comparable between IMS-G85R and control cell lines. Altogether, these results indicate that PINK1 accumulation is responsible for bringing about enhanced mitophagy in IMS-wtSOD1 and IMS-G93A cell lines (Fig. 5.4).

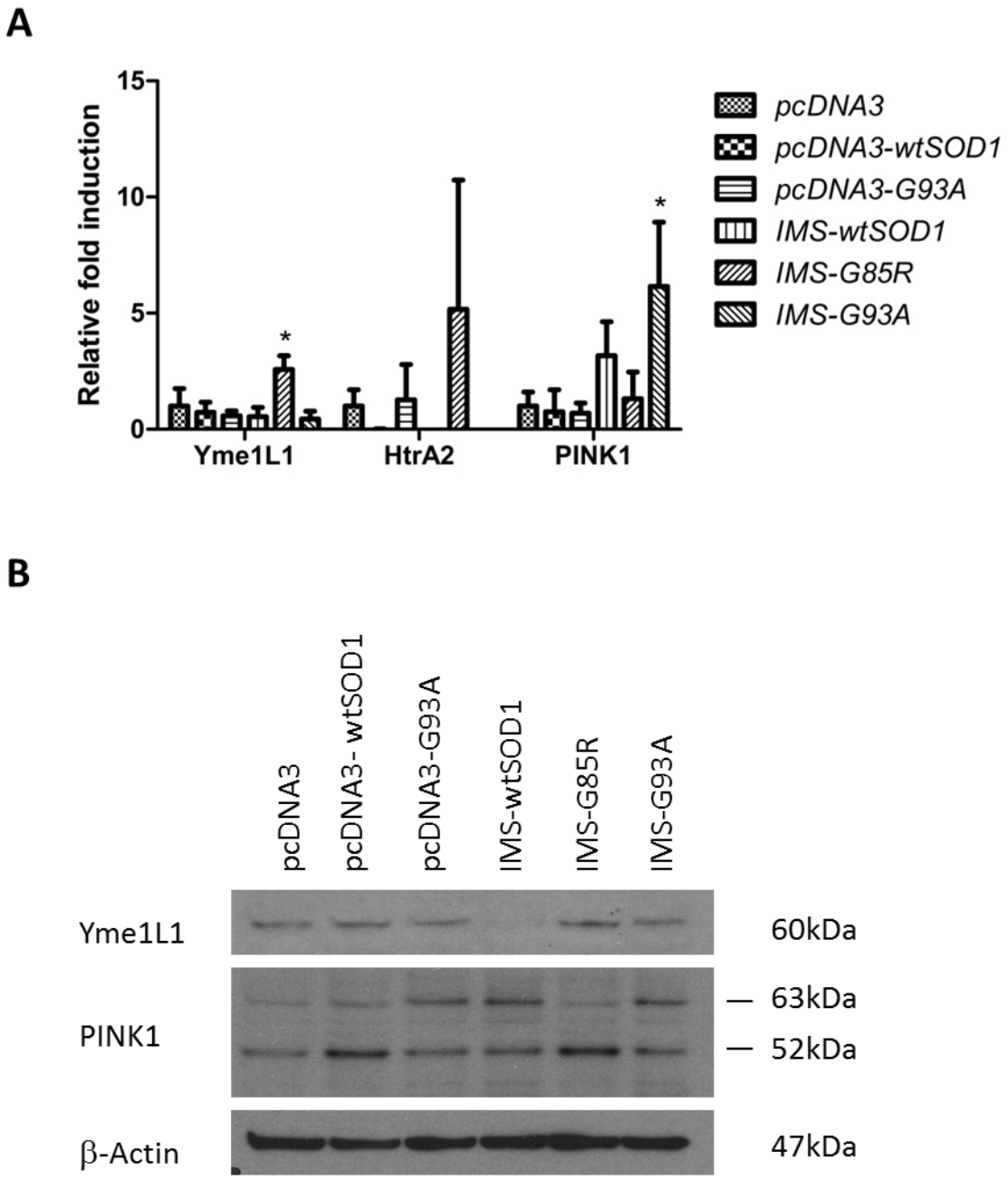

Fig. 5.3 Effects of IMS-targeted mutant SOD1 on IMS proteolytic machinery. Cell lines constitutively expressing empty vector (pcDNA3), untagged wtSOD1 (pcDNA3-wtSOD1) and G93A (pcDNA3-G93A), and IMS-targeted SOD1 were grown under normal conditions. (A) qPCR results show increased levels of Yme1L1 and PINK1 transcripts in IMS-G85R and IMS-G93A cell lines respectively. Fold inductions for each gene are expressed relative to the amount of transcript present in the pcDNA3 sample. β-actin served as the endogenous control. Data represents mean ± SD for 3 independent experiments *$p<0.05$ vs pcDNA3 (B) Western blot analysis of Yme1L1 and PINK1 in whole cell lysates.

Cytosolic chaperones can impede SOD1 import into the mitochondria and thus alleviate mitochondrial dysfunction. To determine if HspB8 has any effect on mitophagy, NSC34 cell lines were co-transfected with HspB8. Although high levels of mitophagy was still observed in IMS-G93A after HspB8 overexpression, these levels were significantly reduced compared to IMS-G93A cells co-transfected with the vector control. Mitophagy was also similarly reduced in IMS-wtSOD1 and HspB8 co-expressing cells thus suggesting the beneficial effect of HspB8 overexpression on mitochondrial functions and homeostasis (Fig. 5.4). This may be attributed to HspB8's effects on promoting general macroautophagy (Chapter 3); HspB8-mediated macroautophagy of mutant SOD1 in the cytosol will likely decrease the import of IMS-targeted mutant SOD1, thereby reducing mitochondrial stress and mitophagy.

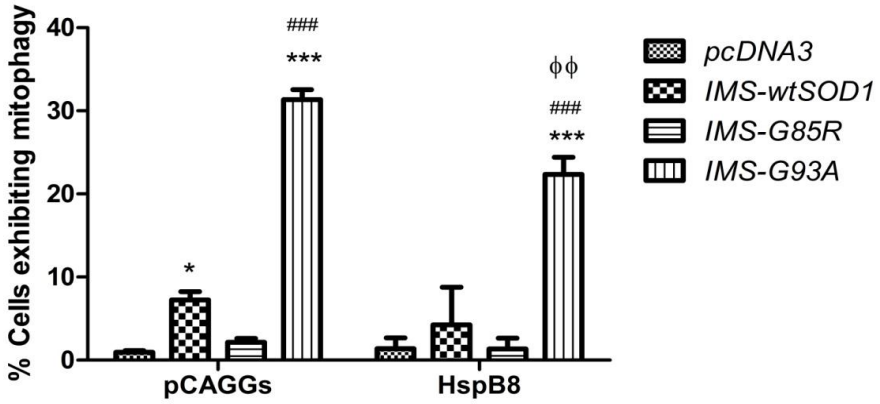

Fig. 5.4 Increased mitophagy in IMS-G93A cell lines. Stable cell lines expressing IMS-targeted wildtype and mutant SOD1 and transiently co-transfected with empty or HspB8 constructs were treated with LysoID prior to fixation and permeabilization. Fixed cells were subsequently immunostained with Hsp60 (mitochondrial marker) and LC3A antibodies prior to analysis by ImageStream. 25,000 cells were counted for each sample. Mitophagy was assessed by counting cells that displayed colocalization (as assessed by the bright detailed similarity feature) between the Hsp60, LC3A and LysoID signals (Top panel). Representative images for each sample (Bottom panel). Data represent means ± SD for 4 independent experiments. *$p<0.05$ vs pcDNA3, $^{###}p<0.001$ vs IMS-wtSOD1, $^{\varphi\varphi}p<0.01$ vs pCAGGs.

5.2.1 Changes in IMS proteases *in vivo*

To determine if the stress responsive expression of Yme1L1, PINK1 and Gfer observed *in vitro* is relevant *in vivo*, western blots were performed on spinal cord and brain lysates from G93A mice at pre-symptomatic (P30), symptomatic (P100), and end stage (P150) of the disease. In spinal cords, levels of Yme1L1 changed with disease progression in G93A mice with Yme1L1 peaking at symptomatic stage (Fig. 5.5A and B). By end stage, levels of Yme1L1 were similar to that at pre-symptomatic stages. Compared with age-matched Ntg or WT mice, Yme1L1 levels at symptomatic stage were higher in G93A mice but much reduced at the terminal stage (Fig. 5.5A and B). A similar trend was also observed for PINK1 in spinal cord lysates. Full-length PINK1 isoforms increased with disease in G93A mice with levels peaking at symptomatic stage. By end stage, full-length PINK1 was much reduced in the G93A spinal cords, with levels below that observed at presymptomatic stage (Fig. 5.5A and B). Levels of 63kDa PINK1 at end stage were also reduced when compared to age-matched WT or Ntg controls. Interestingly, cleaved 52kDa PINK1 steadily increased with disease in G93A mice with levels peaking at end stage (Fig. 5.5A and B). Gfer levels decreased steadily after disease-onset in G93A and Ntg mice indicating this may be a natural consequence of aging. Gfer proteins in G93A mice were comparable with their age-matched Ntg counterparts (Fig. 5.5A and B).

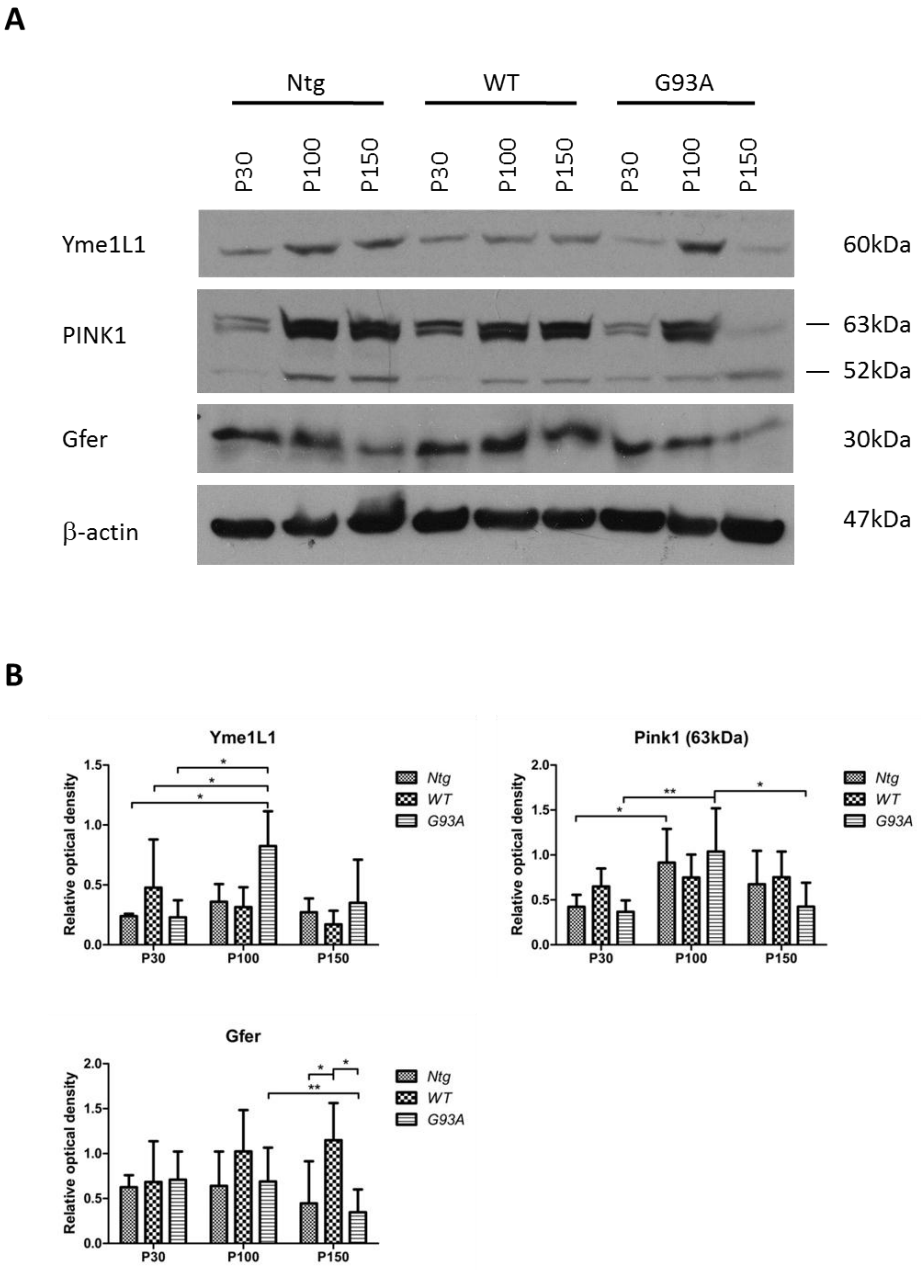

Fig. 5.5 Changes in expression of Yme1L1, PINK1 and Gfer proteins in spinal cord from G93A mice. (A) Immunoblotting analysis of Yme1L1, PINK1 and Gfer proteins in spinal cords of pre-symptomatic (P30), symptomatic (P100), and end-stage (P150) transgenic SOD1 mice. (B) Levels of Yme1L1, PINK1, and Gfer proteins were quantified in the spinal cord by densitometry. Optical densities for Yme1L1, PINK1 and Gfer proteins were expressed relative to the amount of β-actin present in each sample. Data represents mean ± SD of three independent experiments, *$p<0.05$ vs Ntg unless where indicated.

To determine if similar fluctuations in Yme1L1, PINK1 and Gfer proteins also occurred in brains of SOD1 transgenic mice, western blotting was performed. In contrast with spinal cords, Yme1L1 and full-length PINK1 proteins declined with disease in G93A mice (Fig. 5.6A and B). This observation is also in sharp contrast with brain lysates from Ntg mice, where both Yme1L1 and 63kDa proteins increased with age. Gfer proteins also declined with age in brain lysates from G93A mice but increased with age in Ntg mice (Fig. 5.6A and B).

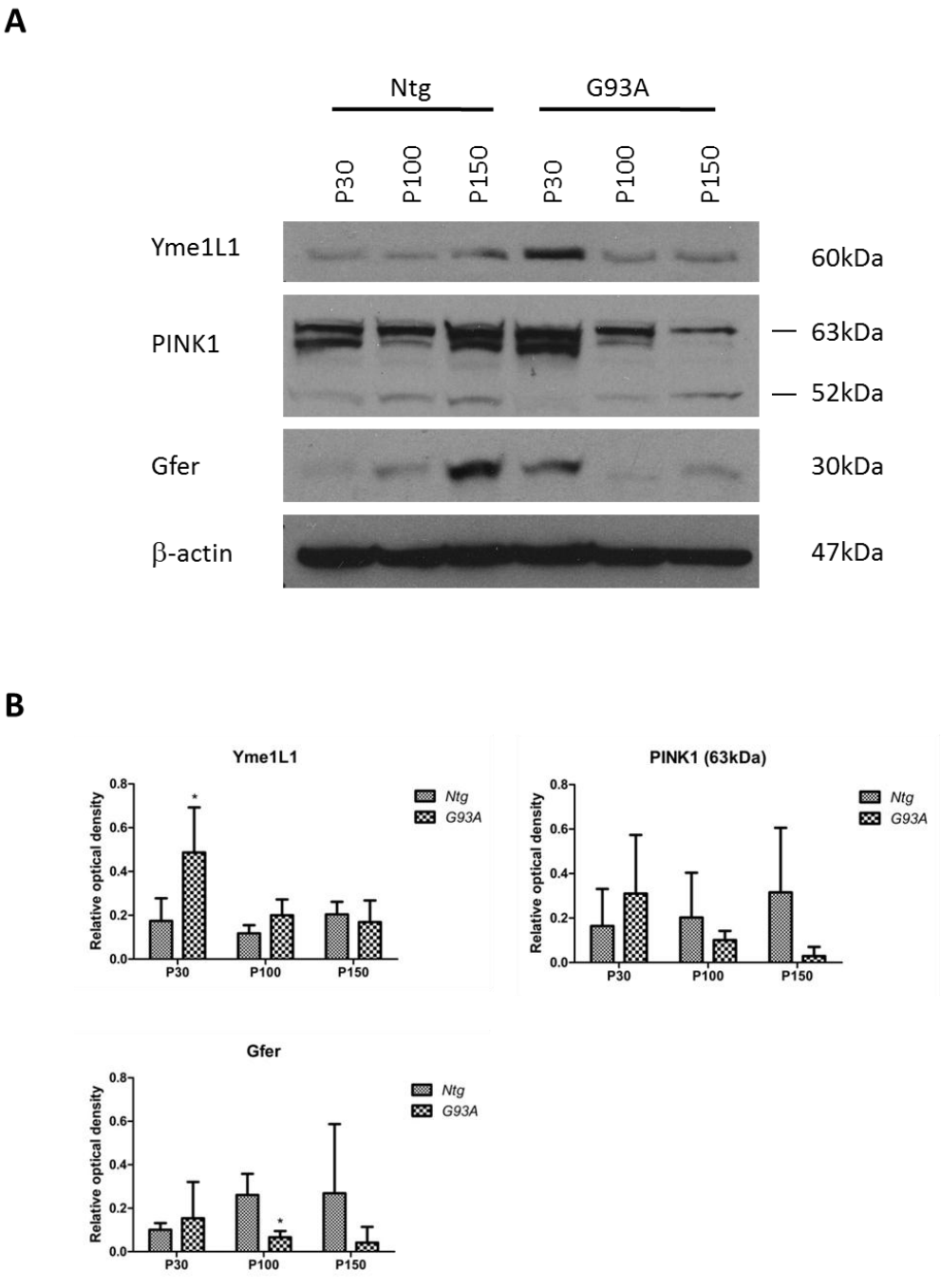

Fig. 5.6 Changes in expression of Yme1L1, PINK1 and Gfer proteins in brain tissue from G93A mice. (A) Immunoblotting analysis of Yme1L1, PINK1 and Gfer proteins in brains of pre-symptomatic (P30), symptomatic (P100), and end-stage (P150) transgenic SOD1 mice. (B) Levels of Yme1L1, PINK1, and Gfer proteins were quantified by densitometry. Optical densities for Yme1L1, PINK1 and Gfer proteins were expressed relative to the amount of β-actin present in each sample. Data represents mean ± SD of three independent experiments, *$p<0.05$ vs Ntg unless where indicated.

5.3 Discussion

A stress response mechanism to misfolded proteins in the IMS has not yet been identified in mammalian cells. In this study, candidate proteins for a potential IMS-specific UPR response were examined based on the following two assumptions: (i) well-established stress response mechanisms in the cytosol and the ER require chaperones, proteases and translocation machinery (ER only) to facilitate the folding and degradation of misfolded proteins, and (ii) key components of stress tolerance programs must be conserved throughout evolution to enable cell survival. Due to its endosymbiotic origins, as much as half of the proteins found in prokaryotes have eukaryotic counterparts in the mitochondria (Karlberg et al., 2000). In some cases, the functions of these mitochondrial proteins have also been retained from their prokaryotic ancestors.

A role for Chchd4 and Gfer, mammalian homologues of yeast Mia 40 and Erv1 respectively, in facilitating import of SOD1 in the mitochondria has not yet been described in the literature. Furthermore, it is only speculated that Chchd4 and Gfer will function in an analogous manner to Mia 40 and Erv1 – that is, to drive the import of chaperones and IMS proteins requiring oxidative folding into the IMS. This *in vitro* study has found that Gfer, Tim9, and Tim10 proteins are upregulated concurrently in IMS-G85R cells, reflecting the need to increase protein import and folding capacities within the IMS during proteotoxic stress. As mitochondrial localization of CCS in yeast requires Mia40 and Erv1, elevated Gfer levels in IMS-G85R expressing cells raises the possibility that mitochondrial CCS levels are also increased to assist in the folding of mutant SOD1. Although SOD1-Tim interactions have not yet been identified, Tim proteins might also assist the folding of SOD1 in the IMS.

Upregulation of Yme1L1 was also observed in IMS-G85R cell lines indicating an increase in protein degradation capacities in response to the accumulation of mutant SOD1 in the compartment. Therefore in IMS-G85R cells, the combination of increased chaperones, import machinery and proteases may constitute part of the adaptation mechanism to cell stress for this particular SOD1 variant. Interestingly, induction of Yme1L1, small Tim proteins and Gfer were not observed in IMS-targeted G93A cells; rather PINK1 was the only transcript upregulated in IMS-G93A cells suggesting a variant specific response to protein misfolding. PINK1 is a kinase embedded in the OMM where it has a role in maintaining mitochondrial integrity (Zhou et al., 2008). In previous studies, elevated levels of PINK1 have been found to protect mitochondria from oxidative damage in senescent cells (Mai et al., 2010) which suggests that upregulation of PINK1 might also be protective in IMS-G93A cell lines. Protection might be procured through PINK1-activation of HtrA2 protease activities (Plun-Favreau et al., 2007) leading to increased turnover of mutant SOD1 in the compartment. However, the lack of induction of HtrA2 transcripts in IMS-G93A cells suggests that HtrA2 might not participate in SOD1 degradation and that PINK1 might serve a different purpose. Full-length PINK1 accumulates on the outer mitochondrial membranes of depolarized mitochondria where it acts as a signal for Parkin recruitment and mitophagy (Narendra et al., 2010, Vives-Bauza et al., 2010). In this study, full length PINK1 was elevated in IMS-targeted G93A but not G85R. Furthermore, this coincided with increased mitophagy in IMS-G93A cells suggesting that PINK1 is involved in promoting mitophagy in these cells. Interestingly, recognition of mitochondria by the autophagosome-lysosome pathway also requires Parkin-mediated ubiquitination of VDAC (Geisler et al., 2010), an anion channel whose

activities are also impaired by SOD1 mutants (Israelson et al., 2010). It has not yet been shown whether G93A-mediated inhibition of VDAC functions directly affects mitophagy.

The difference between mitophagy levels in G85R and G93A mutants (3% and 30% respectively) is also particularly striking as mitophagy is often viewed as a last resort strategy for cells to restore homeostasis and occurs after UPR mechanisms have failed to control protein misfolding. As increased mitophagy was also observed in IMS-wtSOD1 expressing cells, and both IMS-wtSOD1 and IMS-G93A cells share the common feature of high mitochondrial content (Chapter 4), the contrasting responses to IMS stress exhibited by G85R and G93A mutants may simply be the result of differences in mitochondria abundance in these cells. Alternatively, the absence of elevated levels of IMS proteases and chaperones in IMS-G93A cells indicates that these cells are more reliant on alternative degradation strategies such as mitophagy rather than intrinsic proteases for the elimination of mutant SOD1.

The mechanism by which stress originating in the IMS is transmitted to the nucleus is unknown. The JUN/JNK signaling pathway has been implicated in the stress response for the mitochondrial matrix (Horibe and Hoogenraad, 2007). A similar signaling mechanism may operate for the UPR in the IMS whereby PINK1 accumulation on the OMM results in activation of a similar phosphorylation cascade and culminates in the increased transcription of autophagy-related genes and IMS chaperones. With the exception of PINK1 and HtrA2, Yme1L1, Gfer, Tim8 and Tim9 transcripts are induced concurrently in IMS-G85R cells potentially indicating common regulatory elements upstream of these genes.

A limitation of this study is that whole spinal cords were analysed rather than motor neurons and may explain why changes in Gfer and PINK1 levels observed *in vitro* were not reflected *in vivo*. All the proteins studied here are ubiquitously expressed and thus any subtle changes occurring in spinal motor neurons are likely to be masked by signals coming from all the other cells in the spinal cord. Despite these limitations, Yme1L1 appears to be a promising candidate for the IMS-specific stress response.

Protein quality control machinery in the IMS is very important for maintaining mitochondrial homeostasis in neurons. Mutations in the twin Cx_3C motif of a human homolog of Tim protein (deafness dystonia peptide 1) are associated with the neurodegenerative disorder, Mohr-Tranebjaerg syndrome (Hofmann et al., 2002, Roesch et al., 2002). Likewise, mutations in PINK1 and HtrA2 are associated with the degeneration of nigrostriatal neurons in Parkinson's Disease (Valente et al., 2004, Strauss et al., 2005). Although Yme1L1 mutants are not yet associated with any neurological disease, mutations in the Yme1L1 paralog, Paraplegin, are associated with hereditary spastic paraplegia (HSP) (Casari et al., 1998). Paraplegin is a protease localized within the inner mitochondrial membrane and is required for quality control of the electron transport chain as well as mitochondrial ribosomes within the matrix (Nolden et al., 2005). Therefore, impairments in mitochondrial PQC proteins add to mitochondrial stress leading to apoptosis.

A potentially effective strategy in reducing mitochondrial stress associated with mutant SOD1 is to prevent its import into the mitochondria. Cytosolic chaperones such as HspB8 can bind to mutant SOD1 in the cytosol and therefore intercept mutant SOD1 before it can be imported into the mitochondria. As shown in this study, upregulation of HspB8 significantly reduced mitophagy in IMS-G93A cell lines indicating that HspB8-

mediated autophagy of SOD1 mutants in the cytosol can reduce mitochondrial damage. Thus coordinated induction of UPRs in several compartments may be an effective strategy in alleviating mutant SOD1-mediated toxicity.

6. Discussion

Cellular stress responses are important in suppressing the toxicity of misfolded mutant proteins. The broad aims of this thesis were to understand the roles of stress mechanisms in the pathogenesis of fALS deriving from SOD1 mutations. Under this general theme, this thesis has explored how SOD1 aggregates elicit stress responses in the cytosol and mitochondrial IMS, leading to the upregulation of chaperones and proteolytic machinery involved in the processing of mutant SOD1 within these compartments. In the cytosol, this study has shown that HspB8 is upregulated by SOD1 mutants where it induced the clearance of aggregates by macroautophagy. As overexpression of HspB8 suppresses mutant-SOD1 mediated toxicity, this indicates that HspB8 induction *in vivo* may act as a protective mechanism to counteract the toxicity of mutant SOD1 aggregates. HspB8 mutants associated with dHMN and CMT are defective in macroautophagy, thus indicating the crucial roles of this chaperone in motor and sensory neuron survival. The mechanisms for the IMS-UPR have not been previously identified but are expected to provide similar neuroprotective functions. Preliminary results revealed some possible candidates that may have a role in the adaptation to mitochondrial stress. Interestingly, increased mitophagy was also found in IMS-G93A expressing cells and advocates the central role of macroautophagy in eliminating protein aggregates and damaged mitochondria in SOD1-FALS (Fig. 6.1).

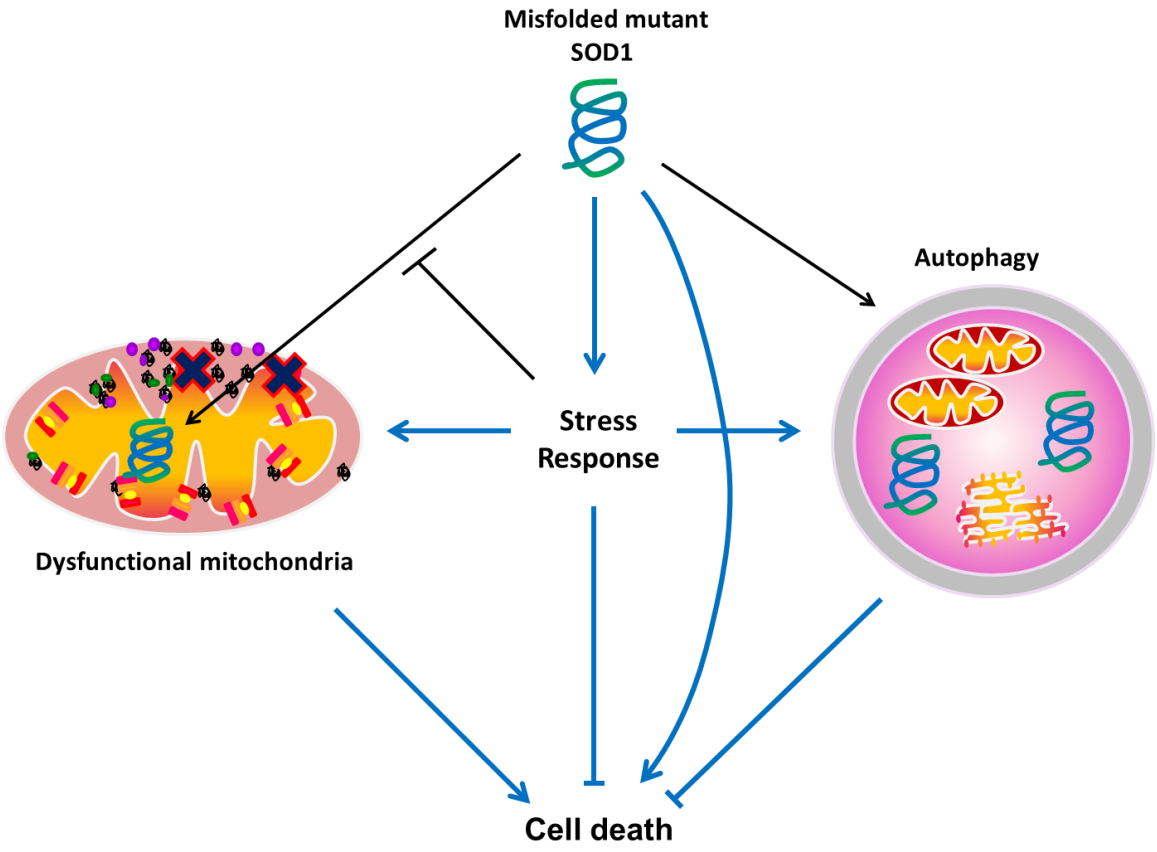

Fig. 6.1 Stress response mechanisms in mutant SOD1-mediated motor neuron cell death. Mutant SOD1 misfolds and aggregates in the cytosol and mitochondria causing motor neuron cell death. To protect against mutant SOD1-mediated neurotoxicity, cellular stress response programs are induced in both these compartments. In particular, HspB8 upregulation in the cytosol through the heat shock response promotes autophagy of mutant SOD1 aggregates and dysfunctional mitochondria (mitophagy). Furthermore, upregulation of HspB8 can further limit mitochondrial damage in cells by binding to mutant SOD1 species and thus preventing their import into the mitochondria. As mutant SOD1 in the IMS negatively affects mitochondrial morphology and bioenergetics, upregulation of stress response programs within this compartment can help to limit mitochondrial damage and thereby prevent apoptosis. Putative candidates of this IMS stress response include PINK1, Yme1l1 and Gfer.

An emerging theme in the study of UPRs is the understanding of how different stress pathways are integrated to allow cells to efficiently eliminate mutant SOD1 and prevent apoptosis. Both ER and mitochondria house pro-apoptotic mediators that can be activated and released as a result of prolonged stress in these compartments (Nakagawa et al., 2000, Urano et al., 2000, Mayer and Oberbauer, 2003, Nishitoh et al., 2008). Therefore cells must be able to couple UPR^{mt} and UPR^{ER} signaling mechanisms with the induction of autophagy machinery if it is to successfully sequester damaged organelles and avoid apoptosis during times of chronic stress. Some of the components of the signaling pathway for UPR^{ER}-induced autophagy have already been identified and involve PERK-eIF2α-dependent upregulation of a number of transcription factors including Atg12, CHOP, and ATF4 (Carracedo et al., 2006, Kouroku et al., 2007). It is not known how these transcription factors promote autophagy but one possibility is through enhancing LC3 expression, which is required for sustained induction of autophagy (Milani et al., 2009). CHOP signaling also plays a key role in UPR^{mt} and it is possible that mitochondrial UPR may induce autophagy via a similar mechanism (Zhao et al., 2002, Horibe and Hoogenraad, 2007). Activation of the cytosolic heat shock response through UPR^{ER} and UPR^{mt} pathways can also relieve stress and damage in this compartment by inducing chaperones which bind to cytosolic mutant SOD1 and prevent its import into the ER or mitochondria. This was suggested in chapter 5, where overexpression of HspB8 reduced mitophagy in IMS-G93A cell lines.

Autophagy is an important homeostatic mechanism in neurons and impairments in this pathway have been observed in a growing number of neurodegenerative disorders. In Alzheimer's Disease, large numbers of autophagic vacuoles accumulate within distended,

atrophic neurites in affected neurons as a result of impaired clearance of autophagosomes (Nixon et al., 2005, Boland et al., 2008, Lee et al., 2010). Deregulation of macroautophagy, mitophagy and chaperone-mediated autophagy (CMA) has been implicated in the pathogenesis of Parkinson's Disease (Webb et al., 2003, Cuervo et al., 2004, Kabuta et al., 2008, Dagda et al., 2009). This study has shown that mutations in the HspB8 chaperone also disrupt macroautophagy, and indicates that the impaired clearance of proteins and organelles from synaptic terminals is essential for the maintenance of motor and sensory neurons, and may contribute to the pathogenesis of distal motor neuropathies. Although this study and others have found increased macroautophagy in SOD1 transgenic mice, the latency of the autophagic response – arising at symptomatic rather than early stages in G93A mice – means that motor neurons can do little to reverse the damage caused by mutant SOD1 (Morimoto et al., 2007, Li et al., 2008, Crippa et al., 2010). Therefore, the timing, amplitude and duration of the autophagic responses are important in determining whether neurons die from the toxicity of misfolded proteins.

One of the least understood aspects of neurodegeneration is why protein aggregation and pathology occurs only in a selected subset of neurons. Proteostatic mechanisms are ubiquitous and highly conserved between all cells yet, in SOD1-FALS motor neurons are selectively targeted by the mutant protein. One possibility is that the complement of molecular chaperones and the efficiency of the proteolytic machinery are deficient in motor neurons making them less able to face proteotoxic insults. The differences in expression profiles of chaperones are likely to occur via post-transcriptional or post-translational mechanisms rather than transcript abundance as only a small number of chaperone transcripts vary significantly between neuronal populations in adult mice

(Tebbenkamp and Borchelt, 2010). Selective vulnerability of motor neurons to proteotoxic stress can also be attributed to the high thresholds required to activate Hsf1 (Batulan et al., 2003). However, as disease does not manifest until later on in life, this also suggests that misfolded mutant SOD1 is only problematic when combined with age-dependent waning of Hsf1 and chaperone activities (Rabek et al., 2003, Shamovsky and Gershon, 2004, Hussain and Ramaiah, 2007, Kayani et al., 2008, Naidoo et al., 2008). Furthermore, several arms of the UPR^{ER} are not activated in aged tissue and may compromise the ability of the ER to efficiently process mutant SOD1 (Paz Gavilan et al., 2006, Naidoo et al., 2008). Therefore, insufficient activation of UPRs leading to reduced SOD1 turnover is likely to contribute to ALS pathogenesis.

Numerous studies have shown that pharmacological induction of UPRs and autophagy is neuroprotective in SOD1 transgenic mice. The mechanism of action for riluzole is not yet known, however, a recent study suggests that riluzole may exert protective effects by interfering with degradation of Hsf1 thereby prolonging the heat shock response (Yang et al., 2008). Another Hsf1 inducer, arimoclomol, is currently in clinical trials after demonstrating efficacy in transgenic G93A mice (Kieran et al., 2004a). Neuroprotection by arimoclomol was attributed to upregulated Hsp70 levels – upregulation of sHsps such as HspB1 was not observed (Kieran et al., 2004a). Lithium administration was shown to slow disease progression in ALS patients and in transgenic mice in one study (Fornai et al., 2008). These neuroprotective effects are attributed to the ability of lithium to promote autophagy through the inhibition of inositol-monophosphatase. Lithium also reduced mitochondrial vacuolization and increased mitochondrial content in G93A spinal cords suggesting that autophagy is crucial to alleviating the toxicity posed by mutant SOD1

in the cytosol and in the mitochondria (Fornai et al., 2008). Although this is an attractive hypothesis, larger and better conducted clinical trials have been negative, suggesting that more complex mechanisms operate in ALS (Aggarwal et al., 2010, Chiò et al., 2010).

A large number of studies on the protective effects of individual Hsps have concentrated on the major inducible heat shock protein, Hsp70. However, a variety of evidence suggests that HspB1 may have more potent protective capacities in the nervous system. In contrast to Hsp70 or Hsp90, HspB1 is able to protect neurons against certain apoptosis-inducing stimuli such as serum or nerve growth factor withdrawal (Mailhos et al., 1993, Lewis et al., 1999, Wagstaff et al., 1999). Furthermore, HspB1 is a strong neuroprotectant in models of ischemia (Badin et al., 2005, Stetler et al., 2008) and acute nerve injury (Benn et al., 2002). However, the neuroprotective functions of HspB1 in SOD1-FALS are not as clear. HspB1 is upregulated in spinal cord homogenates of transgenic ALS mice in late stages of the disease (Vleminckx et al., 2002) but reduced in motor neurons preceding disease-onset (Maatkamp et al., 2004) suggesting that HspB1 is involved in guarding these cells from mutant SOD1-mediated toxicity. However, overexpression of HspB1 had no effect in preventing motor neuron loss, nor did it delay disease onset or progression in G93A transgenic mice (Krishnan et al., 2008). Similarly, overexpression of HspB1 did not alleviate oxidative stress or delay disease onset in the mouse model Huntington's Disease (Zourlidou et al., 2007) indicating that HspB1 may not be as effective protecting neurons from chronic stress, as it is in protecting against neuronal cell death during acute cellular stress (Benn et al., 2002, Akbar et al., 2003, Sharp et al., 2006). Nevertheless, a rare mutation in the heat shock element of HspB1 has been found in a single patient with ALS; this mutation attenuates stress-induced HspB1 transcription and

hence supports the role of HspB1 as an essential survival factor in motor neurons during cellular stress (Dierick et al., 2007). Therefore, a greater understanding of the diverse functions of individual sHsps, as well as the regulatory mechanisms and circumstances under which they are induced, is required to further our understanding into the mechanisms underlying motor neuron degeneration and to potentially use sHsps as therapeutic drug targets in motor neuron disorders.

6.1 Conclusions and Future Directions

The results in this thesis provide valuable insight into the contribution of unfolded protein responses and autophagy in mutant SOD1-pathogenesis and the importance of these mechanisms in maintaining motor neuron homeostasis. Further studies are required to determine whether overexpression or induction of HspB8 at earlier stages of the disease is sufficient to delay motor neuron degeneration and extend survival of G93A mice. Moreover, as HspB8 mutants are associated with dHMN, more work is required to elucidate the mechanism by which macroautophagy is impaired in motor and sensory neurons. The last chapter provided some preliminary results for the involvement of a potential IMS-specific UPR in mutant SOD1-mediated ALS. However, to determine whether the findings can be replicated in motor neurons *in vivo*, laser capture micro-dissection of motor neurons followed by qPCR of selected transcripts is required. Alternatively, *in-situ* hybridization and immunofluorescence labelling of spinal cord sections can be employed to compare differences in the expression of these proteins in motor neurons with neighbouring cells. Knockdown of candidate proteins by siRNA in cell

lines could also be carried to confirm their involvement in the IMS-stress response. Commonly, genes involved in the same stress response also share promoter elements. Future studies into the mechanism of the IMS-UPR will also require identification of these promoter element(s). Finally, studies are also required to understand how mitochondrial stress is perceived by the nucleus and other compartments and how stress mechanisms are coordinated to allow efficient removal of mutant SOD1.

7. References

Ackerley S, James PA, Kalli A, French S, Davies KE, Talbot K (2006) A mutation in the small heat-shock protein HSPB1 leading to distal hereditary motor neuronopathy disrupts neurofilament assembly and the axonal transport of specific cellular cargoes. Hum Mol Genet 15:347-354.

Aggarwal SP, Zinman L, Simpson E, McKinley J, Jackson KE, Pinto H, Kaufman P, Conwit RA, Schoenfeld D, Shefner J, Cudkowicz M (2010) Safety and efficacy of lithium in combination with riluzole for treatment of amyotrophic lateral sclerosis: a randomised, double-blind, placebo-controlled trial. The Lancet Neurology 9:481-488.

Akbar MT, Lundberg AM, Liu K, Vidyadaran S, Wells KE, Dolatshad H, Wynn S, Wells DJ, Latchman DS, de Belleroche J (2003) The neuroprotective effects of heat shock protein 27 overexpression in transgenic animals against kainate-induced seizures and hippocampal cell death. J Biol Chem 278:19956-19965.

Al-Chalabi A, Andersen PM, Chioza B, Shaw C, Sham PC, Robberecht W, Matthijs G, Camu W, Marklund SL, Forsgren L, Rouleau G, Laing NG, Hurse PV, Siddique T, Leigh PN, Powell JF (1998) Recessive amyotrophic lateral sclerosis families with the D90A SOD1 mutation share a common founder: evidence for a linked protective factor. Hum Mol Genet 7:2045-2050.

Aldridge JE, Horibe T, Hoogenraad NJ (2007) Discovery of genes activated by the mitochondrial unfolded protein response (mtUPR) and cognate promoter elements. Plos One 2:e874.

Alexander MD, Traynor BJ, Miller N, Corr B, Frost E, McQuaid S, Brett FM, Green A, Hardiman O (2002) "True" sporadic ALS associated with a novel SOD-1 mutation. Ann Neurol 52:680-683.

Andersen PM, Forsgren L, Binzer M, Nilsson P, Ala-Hurula V, Keranen ML, Bergmark L, Saarinen A, Haltia T, Tarvainen I, Kinnunen E, Udd B, Marklund SL (1996) Autosomal recessive adult-onset amyotrophic lateral sclerosis associated with homozygosity for Asp90Ala CuZn-superoxide dismutase mutation. A clinical and genealogical study of 36 patients. Brain 119 (Pt 4):1153-1172.

Andersen PM, Nilsson P, Ala-Hurula V, Keranen ML, Tarvainen I, Haltia T, Nilsson L, Binzer M, Forsgren L, Marklund SL (1995) Amyotrophic lateral sclerosis associated with homozygosity for an Asp90Ala mutation in CuZn-superoxide dismutase. Nat Genet 10:61-66.

Andersen PM, Nilsson P, Keranen ML, Forsgren L, Hagglund J, Karlsborg M, Ronnevi LO, Gredal O, Marklund SL (1997) Phenotypic heterogeneity in motor neuron disease patients with CuZn-superoxide dismutase mutations in Scandinavia. Brain 120 (Pt 10):1723-1737.

Anderson LG, Meeker RB, Poulton WE, Huang DY (2010) Abnormal interaction of motor neuropathy-associated mutant HspB8 (Hsp22) forms with the RNA helicase Ddx20 (gemin3). Cell Stress Chaperon 15:487-495.

Arisato T, Okubo R, Arata H, Abe K, Fukada K, Sakoda S, Shimizu A, Qin XH, Izumo S, Osame M, Nakagawa M (2003) Clinical and pathological studies of familial amyotrophic lateral sclerosis (FALS) with SOD1 H46R mutation in large Japanese families. Acta Neuropathol 106:561-568.

Arndt V, Dick N, Tawo R, Dreiseidler M, Wenzel D, Hesse M, Furst DO, Saftig P, Saint R, Fleischmann BK, Hoch M, Hohfeld J (2010) Chaperone-Assisted Selective Autophagy Is Essential for Muscle Maintenance. Curr Biol.

Arnold A, Edgren DC, Palladino VS (1953) Amyotrophic Lateral Sclerosis- 50 cases observed on Guam. J Nerv Ment Dis 117:135-139.

Atkin JD, Farg MA, Turner BJ, Tomas D, Lysaght JA, Nunan J, Rembach A, Nagley P, Beart PM, Cheema SS, Horne MK (2006) Induction of the Unfolded Protein Response in Familial Amyotrophic Lateral Sclerosis and Association of Protein-disulfide Isomerase with Superoxide Dismutase 1. J Biol Chem 281:30152-30165.

Audet JN, Gowing G, Julien JP (2010) Wild-type human SOD1 overexpression does not accelerate motor neuron disease in mice expressing murine Sod1^{G86R}. Neurobiol Dis 40:245-250.

Badin RA, Lythgoe MF, van der Weerd L, Thomas DL, Gadian DG, Latchman DS (2005) Neuroprotective effects of virally delivered HSPs in experimental stroke. J Cereb Blood Flow Metab 26:371-381.

Barsoum MJ, Yuan H, Gerencser AA, Liot G, Kushnareva Y, Graber S, Kovacs I, Lee WD, Waggoner J, Cui J, White AD, Bossy B, Martinou J-C, Youle RJ, Lipton SA, Ellisman MH, Perkins GA, Bossy-Wetzel E (2006) Nitric oxide-induced mitochondrial fission is regulated by dynamin-related GTPases in neurons. EMBO J 25:3900-3911.

Battistoni A, Mazzetti AP, Rotilio G (1999) In vivo formation of Cu,Zn superoxide dismutase disulfide bond in Escherichia coli. Febs Letters 443:313-316.

Batulan Z, Shinder GA, Minotti S, He BP, Doroudchi M, Nalbantoglu J, Strong MJ, Durham HD (2003) High threshold for induction of the stress response in motor neurons is associated with failure to activate HSF1. Journal of Neuroscience 23:5789-5798.

Beleza-Meireles A, Al-Chalabi A (2009) Genetic studies of amyotrophic lateral sclerosis: controversies and perspectives. Amyotroph Lateral Scler 10:1-14.

Benn SC, Perrelet D, Kato AC, Scholz J, Decosterd I, Mannion RJ, Bakowska JC, Woolf CJ (2002) Hsp27 upregulation and phosphorylation is required for injured sensory and motor neuron survival. Neuron 36:45-56.

Benndorf R, Sun XK, Gilmont RR, Biedermann KJ, Molloy MP, Goodmurphy CW, Cheng H, Andrews PC, Welsh MJ (2001) HSP22, a new member of the small heat shock protein superfamily, interacts with mimic of phosphorylated HSP27 ((3D)HSP27). J Biol Chem 276:26753-26761.

Berg TO, Fengsrud M, Strømhaug PE, Berg T, Seglen PO (1998) Isolation and Characterization of Rat Liver Amphisomes. J Biol Chem 273:21883-21892.

Bergemalm D, Jonsson PA, Graffmo KS, Andersen PM, Brannstrom T, Rehnmark A, Marklund SL (2006) Overloading of stable and exclusion of unstable human superoxide dismutase-1 variants in mitochondria of murine amyotrophic lateral sclerosis models. J Neurosci 26:4147-4154.

Bernales S, McDonald KL, Walter P (2006) Autophagy counterbalances endoplasmic reticulum expansion during the unfolded protein response. PLoS Biol 4:e423.

Berridge MJ (2002) The endoplasmic reticulum: a multifunctional signaling organelle. Cell Calcium 32:235-249.

Bertini I, Mangani S, Viezzoli MS (1998) Structure and properties of copper-zinc superoxide dismutases. Adv Inorg Chem 45:127-250.

Boland B, Kumar A, Lee S, Platt FM, Wegiel J, Yu WH, Nixon RA (2008) Autophagy Induction and Autophagosome Clearance in Neurons: Relationship to Autophagic Pathology in Alzheimer's Disease. J Neurosci 28:6926-6937.

Borchelt DR, Lee MK, Slunt HS, Guarnieri M, Xu ZS, Wong PC, Brown RH, Price DL, Sisodia SS, Cleveland DW (1994) Superoxide-Dismutase-1 with Mutations Linked to Familial Amyotrophic-Lateral-Sclerosis Possesses Significant Activity. Proceedings of the National Academy of Sciences of the United States of America 91:8292-8296.

Bordo D, Djinovic K, Bolognesi M (1994) Conserved patterns in the Cu,Zn superoxide-dismutase family. J Mol Biol 238:366-386.

Bortoff GA, Strick PL (1993) Corticospinal Terminations in 2 New-World Primates - Further Evidence That Corticomotoneuronal Connections Provide Part of the Neural Substrate for Manual Dexterity. Journal of Neuroscience 13:5105-5118.
Bowling AC, Barkowski EE, Mckennayasek D, Sapp P, Horvitz HR, Beal MF, Brown RH (1995) Superoxide-Dismutase Concentration and Activity in Familial Amyotrophic-Lateral-Sclerosis. Journal of Neurochemistry 64:2366-2369.
Bruening W, Roy J, Giasson B, Figlewicz DA, Mushynski WE, Durham HD (1999) Up-regulation of protein chaperones preserves viability of cells expressing toxic Cu/Zn-superoxide dismutase mutants associated with amyotrophic lateral sclerosis. Journal of Neurochemistry 72:693-699.
Bruijn LI, Becher MW, Lee MK, Anderson KL, Jenkins NA, Copeland NG, Sisodia SS, Rothstein JD, Borchelt DR, Price DL, Cleveland DW (1997) ALS-linked SOD1 mutant G85R mediates damage to astrocytes and promotes rapidly progressive disease with SOD1-containing inclusions. Neuron 18:327-338.
Bruijn LI, Houseweart MK, Kato S, Anderson KL, Anderson SD, Ohama E, Reaume AG, Scott RW, Cleveland DW (1998) Aggregation and motor neuron toxicity of an ALS-linked SOD1 mutant independent from wild-type SOD1. Science 281:1851-1854.
Byrne S, Walsh C, Lynch C, Bede P, Elamin M, Kenna K, McLaughlin R, Hardiman O (2010) Rate of familial amyotrophic lateral sclerosis: a systematic review and meta-analysis. Journal of Neurology, Neurosurgery & Psychiatry [e-pub ahead of print].
Campbell CL, Thorsness PE (1998) Escape of mitochondrial DNA to the nucleus in yme1 yeast is mediated by vacuolar-dependent turnover of abnormal mitochondrial compartments. Journal of Cell Science 111:2455-2464.
Carra S, Brunsting JF, Lambert H, Landry J, Kampinga HH (2009) HspB8 Participates in Protein Quality Control by a Non-chaperone-like Mechanism That Requires eIF2 alpha Phosphorylation. J Biol Chem 284:5523-5532.
Carra S, Sivilotti M, Zobel ATC, Lambert H, Landry J (2005) HspB8, a small heat shock protein mutated in human neuromuscular disorders, has in vivo chaperone activity in cultured cells. Human Molecular Genetics 14:1659-1669.
Carracedo A, Gironella M, Lorente M, Garcia S, Guzman M, Velasco G, Iovanna JL (2006) Cannabinoids induce apoptosis of pancreatic tumor cells via endoplasmic reticulum stress-related genes. Cancer Res 66:6748-6755.
Casari G, De Fusco M, Ciarmatori S, Zeviani M, Mora M, Fernandez P, De Michele G, Filla A, Cocozza S, Marconi R, Durr A, Fontaine B, Ballabio A (1998) Spastic paraplegia and OXPHOS impairment caused by mutations in paraplegin, a nuclear-encoded mitochondrial metalloprotease. Cell 93:973-983.
Chacinska A, Pfannschmidt S, Wiedemann N, Kozjak V, Sanjua?n Szklarz LK, Schulze-Specking A, Truscott KN, Guiard B, Meisinger C, Pfanner N (2004) Essential role of Mia40 in import and assembly of mitochondrial intermembrane space proteins. EMBO Journal 23:3735-3746.
Chance B, Sies H, Boveris A (1979) Hydroperoxide metabolism in mammalian organs. Physiol Rev 59:527-605.
Chen YZ, Bennett CL, Huynh HM, Blair IP, Puls I, Irobi J, Dierick I, Abel A, Kennerson ML, Rabin BA, Nicholson GA, Auer-Grumbach M, Wagner K, De Jonghe P, Griffin JW, Fischbeck KH, Timmerman V, Cornblath DR, Chance PF (2004) DNA/RNA helicase gene mutations in a form of juvenile amyotrophic lateral sclerosis (ALS4). Am J Hum Genet 74:1128-1135.
Cheroni C, Marino M, Tortarolo M, Veglianese P, De Biasi S, Fontana E, Zuccarello LV, Maynard CJ, Dantuma NP, Bendotti C (2009) Functional alterations of the ubiquitin-proteasome system in motor neurons of a mouse model of familial amyotrophic lateral sclerosis dagger. Human Molecular Genetics 18:82-96.

Chiò A, Borghero G, Calvo A, Capasso M, Caponnetto C, Corbo M, Giannini F, Logroscino G, Mandrioli J, Marcello N, Mazzini L, Moglia C, Monsurrò MR, Mora G, Patti F, Perini M, Pietrini V, Pisano F, Pupillo E, Sabatelli M, Salvi F, Silani V, Simone IL, Sorarù G, Tola MR, Volanti P, Beghi E, Group ObotLS (2010) Lithium carbonate in amyotrophic lateral sclerosis. Neurology 75:619-625.

Cleveland DW, Rothstein JD (2001) From charcot to lou gehrig: deciphering selective motor neuron death in als. Nat Rev Neurosci 2:806-819.

Crippa V, Sau D, Rusmini P, Boncoraglio A, Onesto E, Bolzoni E, Galbiati M, Fontana E, Marino M, Carra S, Bendotti C, De Biasi S, Poletti A (2010) The Small Heat Shock Protein B8 (HspB8) promotes autophagic removal of misfolded proteins involved in Amyotrophic Lateral Sclerosis (ALS). Hum Mol Genet 19:3440-3456.

Crow JP, Sampson JB, Zhuang YX, Thompson JA, Beckman JS (1997) Decreased zinc affinity of amyotrophic lateral sclerosis-associated superoxide dismutase mutants leads to enhanced catalysis of tyrosine nitration by peroxynitrite. Journal of Neurochemistry 69:1936-1944.

Cudkowicz ME, McKennaYasek D, Sapp PE, Chin W, Geller B, Hayden DL, Schoenfeld DA, Hosler BA, Horvitz HR, Brown RH (1997) Epidemiology of mutations in superoxide dismutase in amyotrophic lateral sclerosis. Annals of Neurology 41:210-221.

Cuervo AM, Stefanis L, Fredenburg R, Lansbury PT, Sulzer D (2004) Impaired degradation of mutant alpha-synuclein by chaperone-mediated autophagy. Science 305:1292-1295.

Culotta VC, Strain J, Klomp LWJ, Casareno RLB, Gitlin JD (1997) The copper chaperone for superoxide dismutase. Mol Biol Cell 8:574-574.

Dabir DV, Leverich EP, Kim SK, Tsai FD, Hirasawa M, Knaff DB, Koehler CM (2007) A role for cytochrome c and cytochrome c peroxidase in electron shuttling from Erv1. EMBO J 26:4801-4811.

Dagda RK, Cherra SJ, Kulich SM, Tandon A, Park D, Chu CT (2009) Loss of PINK1 Function Promotes Mitophagy through Effects on Oxidative Stress and Mitochondrial Fission. J Biol Chem 284:13843-13855.

Dalcanto MC, Gurney ME (1994) Development of Central-Nervous-System Pathology in a Murine Transgenic Model of Human Amyotrophic-Lateral-Sclerosis. American Journal of Pathology 145:1271-1279.

Damiano M, Starkov AA, Petri S, Kipiani K, Kiaei M, Mattiazzi M, Flint Beal M, Manfredi G (2006) Neural mitochondrial Ca^{2+} capacity impairment precedes the onset of motor symptoms in G93A Cu/Zn-superoxide dismutase mutant mice. J Neurochem 96:1349-1361.

De Vos KJ, Chapman AL, Tennant ME, Manser C, Tudor EL, Lau KF, Brownlees J, Ackerley S, Shaw PJ, McLoughlin DM, Shaw CE, Leigh PN, Miller CC, Grierson AJ (2007) Familial amyotrophic lateral sclerosis-linked SOD1 mutants perturb fast axonal transport to reduce axonal mitochondria content. Hum Mol Genet 16:2720-2728.

Deng HX, Shi Y, Furukawa Y, Zhai H, Fu R, Liu E, Gorrie GH, Khan MS, Hung WY, Bigio EH, Lukas T, Dal Canto MC, O'Halloran TV, Siddique T (2006) Conversion to the amyotrophic lateral sclerosis phenotype is associated with intermolecular linked insoluble aggregates of SOD1 in mitochondria. Proc Natl Acad Sci U S A 103:7142-7147.

Derman AI, Prinz WA, Belin D, Beckwith J (1993) Mutations That Allow Disulfide Bond Formation in the Cytoplasm of Escherichia-Coli. Science 262:1744-1747.

Dierick I, Irobi J, Janssens S, Theuns J, Lemmens R, Jacobs A, Corsmit E, Hersmus N, Van Den Bosch L, Robberecht W, De Jonghe P, Van Broeckhoven C, Timmerman V (2007) Genetic variant in the HSPB1 promoter region impairs the HSP27 stress response. Hum Mutat 28:830.

Ding X, Patel M, Shen D, Herzlich AA, Cao X, Villasmil R, Klupsch K, Tuo J, Downward J, Chan C-C (2009) Enhanced HtrA2/Omi Expression in Oxidative Injury to Retinal Pigment Epithelial Cells and Murine Models of Neurodegeneration. Invest Ophthalmol Vis Sci 50:4957-4966.

Dion PA, Daoud H, Rouleau GA (2009) Genetics of motor neuron disorders: new insights into pathogenic mechanisms. 10:769-782.
Durham HD, Roy J, Dong L, Figlewicz DA (1997) Aggregation of mutant Cu/Zn superoxide dismutase proteins in a culture model of ALS. J Neuropath Exp Neur 56:523-530.
Dyck PJ, Lambert EH (1968a) Lower motor and primary sensory neuron diseases with peroneal muscular atrophy. I. Neurologic, genetic, and electrophysiologic findings in hereditary polyneuropathies. Arch Neurol 18:603-618.
Dyck PJ, Lambert EH (1968b) Lower motor and primary sensory neuron diseases with peroneal muscular atrophy. II. Neurologic, genetic, and electrophysiologic findings in various neuronal degenerations. Arch Neurol 18:619-625.
Ehrnsperger M, Graber S, Gaestel M, Buchner J (1997) Binding of non-native protein to Hsp25 during heat shock creates a reservoir of folding intermediates for reactivation. Embo Journal 16:221-229.
Eisen A (2009) Amyotrophic lateral sclerosis—Evolutionary and other perspectives. Muscle & Nerve 40:297-304.
Evgrafov OV, Mersiyanova I, Irobi J, Van Den Bosch L, Dierick I, Leung CL, Schagina O, Verpoorten N, Van Impe K, Fedotov V, Dadali E, Auer-Grumbach M, Windpassinger C, Wagner K, Mitrovic Z, Hilton-Jones D, Talbot K, Martin JJ, Vasserman N, Tverskaya S, Polyakov A, Liem RKH, Gettemans J, Robberecht W, De Jonghe P, Timmerman V (2004) Mutant small heat-shock protein 27 causes axonal Charcot-Marie-Tooth disease and distal hereditary motor neuropathy. Nature Genetics 36:602-606.
Field LS, Furukawa Y, O'Halloran TV, Culotta VC (2003) Factors controlling the uptake of yeast copper/zinc superoxide dismutase into mitochondria. J Biol Chem 278:28052-28059.
Fischer LR, Culver DG, Tennant P, Davis AA, Wang MS, Castellano-Sanchez A, Khan J, Polak MA, Glass JD (2004) Amyotrophic lateral sclerosis is a distal axonopathy: evidence in mice and man. Experimental Neurology 185:232-240.
Fontaine JM, Sun X, Hoppe AD, Simon S, Vicart P, Welsh MJ, Benndorf R (2006) Abnormal small heat shock protein interactions involving neuropathy-associated HSP22 (HSPB8) mutants. FASEB J 20:2168-2170.
Forman HJ, Fridovic.I (1973) Stability of Bovine Superoxide Dismutase - Effects of Metals. J Biol Chem 248:2645-2649.
Fornai F, Longone P, Cafaro L, Kastsiuchenka O, Ferrucci M, Manca ML, Lazzeri G, Spalloni A, Bellio N, Lenzi P, Modugno N, Siciliano G, Isidoro C, Murri L, Ruggieri S, Paparelli A (2008) Lithium delays progression of amyotrophic lateral sclerosis. Proc Natl Acad Sci U S A 105:2052-2057.
Franks PW, Scheele C, Loos RJF, Nielsen AR, Finucane FM, Wahlestedt C, Pedersen BK, Wareham NJ, Timmons JA (2008) Genomic variants at the PINK1 locus are associated with transcript abundance and plasma nonesterified fatty acid concentrations in European whites. FASEB J 22:3135-3145.
Fuchs M, Poirier DJ, Seguin SJ, Lambert H, Carra S, Charette SJ, Landry J (2010) Identification of the key structural motifs involved in HspB8/HspB6-Bag3 interaction. Biochem J 425:245-255.
Gajdusek DC (1963) Motor-neuron disease in natives of New Guinea. N Engl J Med 268:474-476.
Gajdusek DC (1982) Foci of motor neuron disease in high incidence in isolated populations of East Asia and the Western Pacific. Adv Neurol 36:363-393.
Gajdusek DC, Salazar AM (1982) Amyotrophic lateral sclerosis and parkinsonian syndromes in high incidence among the Auyu and Jakai people of West New Guinea. Neurology 32:107-126.
Geisler S, Holmstrom KM, Skujat D, Fiesel FC, Rothfuss OC, Kahle PJ, Springer W (2010) PINK1/Parkin-mediated mitophagy is dependent on VDAC1 and p62/SQSTM1. Nat Cell Biol 12:119-131.

Glick D, Barth S, Macleod KF (2010) Autophagy: cellular and molecular mechanisms. J Pathol 221:3-12.
Gould TW, Buss RR, Vinsant S, Prevette D, Sun W, Knudson CM, Milligan CE, Oppenheim RW (2006) Complete dissociation of motor neuron death from motor dysfunction by Bax deletion in a mouse model of ALS. J Neurosci 26:8774-8786.
Greenway MJ, Andersen PM, Russ C, Ennis S, Cashman S, Donaghy C, Patterson V, Swingler R, Kieran D, Prehn J, Morrison KE, Green A, Acharya KR, Brown RH, Hardiman O (2006) ANG mutations segregate with familial and 'sporadic' amyotrophic lateral sclerosis. Nature Genetics 38:411-413.
Guegan C, Vila M, Rosoklija G, Hays AP, Przedborski S (2001) Recruitment of the mitochondrial-dependent apoptotic pathway in amyotrophic lateral sclerosis. J Neurosci 21:6569-6576.
Gurney ME, Pu H, Chiu AY, Dal Canto MC, Polchow CY, Alexander DD, Caliendo J, Hentati A, Kwon YW, Deng HX, et al. (1994) Motor neuron degeneration in mice that express a human Cu,Zn superoxide dismutase mutation. Science 264:1772-1775.
Hadano S, Hand CK, Osuga H, Yanagisawa Y, Otomo A, Devon RS, Miyamoto N, Showguchi-Miyata J, Okada Y, Singaraja R, Figlewicz DA, Kwiatkowski T, Hosler BA, Sagie T, Skaug J, Nasir J, Brown RH, Scherer SW, Rouleau GA, Hayden MR, Ikeda J-E (2001) A gene encoding a putative GTPase regulator is mutated in familial amyotrophic lateral sclerosis 2. 29:166-173.
Halawani D, Latterich M (2006) p97: The cell's molecular purgatory? Mol Cell 22:713-717.
Hand CK, Khoris J, Salachas F, Gros-Louis F, Lopes AA, Mayeux-Portas V, Brewer CG, Brown RH, Jr., Meininger V, Camu W, Rouleau GA (2002) A novel locus for familial amyotrophic lateral sclerosis, on chromosome 18q. Am J Hum Genet 70:251-256.
Hara T, Nakamura K, Matsui M, Yamamoto A, Nakahara Y, Suzuki-Migishima R, Yokoyama M, Mishima K, Saito I, Okano H, Mizushima N (2006) Suppression of basal autophagy in neural cells causes neurodegenerative disease in mice. Nature 441:885-889.
Harding AE (1993) Inherited neuronal atrophy and degeneration predominantly of lower motor neurons. In: Peripheral Neuropathy, vol. 2 (Dyck PJ, T. P., Griffin JW, Low PA, Poduslo JF, ed), pp 1051-1064 Philadelphia: W.B. Saunders Company.
Harding AE, Thomas PK (1980) Genetic aspects of hereditary motor and sensory neuropathy (types I and II). J Med Genet 17:329-336.
Hartl FU, Hayer-Hartl M (2002) Molecular Chaperones in the Cytosol: from Nascent Chain to Folded Protein. Science 295:1852-1858.
Haynes CM, Yang Y, Blais SP, Neubert TA, Ron D (2010) The matrix peptide exporter HAF-1 signals a mitochondrial UPR by activating the transcription factor ZC376.7 in C. elegans. Mol Cell 37:529-540.
Hayward LJ, Rodriguez JA, Kim JW, Tiwari A, Goto JJ, Cabelli DE, Valentine JS, Brown RH, Jr. (2002) Decreased metallation and activity in subsets of mutant superoxide dismutases associated with familial amyotrophic lateral sclerosis. J Biol Chem 277:15923-15931.
Heffner R, Masterton B (1975) Variation in form of the pyramidal tract and its relationship to digital dexterity. Brain Behav Evol 12:161-200.
Heffner RS, Masterton RB (1983) The role of the corticospinal tract in the evolution of human digital dexterity. Brain Behav Evol 23:165-183.
Hell K (2008) The Erv1-Mia40 disulfide relay system in the intermembrane space of mitochondria. Biochim Biophys Acta 1783:601-609.
Hentati A, Ouahchi K, Pericak-Vance MA, Nijhawan D, Ahmad A, Yang Y, Rimmler J, Hung W, Schlotter B, Ahmed A, Ben Hamida M, Hentati F, Siddique T (1998) Linkage of a commoner form of recessive amyotrophic lateral sclerosis to chromosome 15q15-q22 markers. Neurogenetics 2:55-60.

Hetz C, Thielen P, Matus S, Nassif M, Court F, Kiffin R, Martinez G, Cuervo AM, Brown RH, Glimcher LH (2009) XBP-1 deficiency in the nervous system protects against amyotrophic lateral sclerosis by increasing autophagy. Genes Dev 23:2294-2306.
Higgins CMJ, Jung CW, Ding HL, Xu ZS (2002) Mutant Cu, Zn superoxide dismutase that causes motoneuron degeneration is present in mitochondria in the CNS. Journal of Neuroscience 22.
Hirano A, Donnenfeld H, Sasaki S, Nakano I (1984) Fine structural observations of neurofilamentous changes in amyotrophic lateral sclerosis. J Neuropathol Exp Neurol 43:461-470.
Hirano A, Malamud N, Elizan TS, Kurland LT (1966) Amyotrophic lateral sclerosis and Parkinsonism-dementia complex on Guam. Further pathologic studies. Arch Neurol 15:35-51.
Hofmann S, Rothbauer U, Muhlenbein N, Neupert W, Gerbitz KD, Brunner M, Bauer MF (2002) The C66W mutation in the deafness dystonia peptide 1 (DDP1) affects the formation of functional DDP1 center dot TIM13 complexes in the mitochondrial intermembrane space. J Biol Chem 277:23287-23293.
Horibe T, Hoogenraad NJ (2007) The Chop Gene Contains an Element for the Positive Regulation of the Mitochondrial Unfolded Protein Response. Plos One 2:e835.
Horwitz J (1992) Alpha-crystallin can function as a molecular chaperone. Proceedings of the National Academy of Sciences of the United States of America 89:10449-10453.
Hussain SG, Ramaiah KV (2007) Reduced eIF2alpha phosphorylation and increased proapoptotic proteins in aging. Biochem Biophys Res Commun 355:365-370.
Ikemoto A, Hirano A, Akiguchi I (2000) Neuropathology of amyotrophic lateral sclerosis with extra-motor system degeneration: Characteristics and differences in the molecular pathology between ALS with dementia and Guamanian ALS. Amyotrophic Lateral Sclerosis 1:97-104.
Ince PG, Tomkins J, Slade JY, Thatcher NM, Shaw PJ (1998) Amyotrophic lateral sclerosis associated with genetic abnormalities in the gene encoding Cu/Zn superoxide dismutase: Molecular pathology of five new cases, and comparison with previous reports and 73 sporadic cases of ALS. J Neuropath Exp Neur 57:895-904.
Irobi J, Almeida-Souza L, Asselbergh B, De Winter V, Goethals S, Dierick I, Krishnan J, Timmermans JP, Robberecht W, De Jonghe P, Van Den Bosch L, Janssens S, Timmerman V (2010) Mutant HSPB8 causes motor neuron-specific neurite degeneration. Hum Mol Genet 19:3254-3265.
Irobi J, Van Impe K, Seeman P, Jordanova A, Dierick I, Verpoorten N, Michalik A, De Vriendt E, Jacobs A, Van Gerwen V, Vennekens K, Mazanec R, Tournev I, Hilton-Jones D, Talbot K, Kremensky N, Van Den Bosch L, Robberecht W, Vandekerckhove J, Van Broeckhoven C, Gettemans J, De Jonghe P, Timmerman V (2004) Hot-spot residue in small heat-shock protein 22 causes distal motor neuropathy. Nature Genetics 36:597-601.
Ishigaki S, Liang Y, Yamamoto M, Niwa J, Ando Y, Yoshihara T, Takeuchi H, Doyu M, Sobue G (2002) X-Linked inhibitor of apoptosis protein is involved in mutant SOD1-mediated neuronal degeneration. Journal of Neurochemistry 82:576-584.
Israelson A, Arbel N, Da Cruz S, Ilieva H, Yamanaka K, Shoshan-Barmatz V, Cleveland DW (2010) Misfolded mutant SOD1 directly inhibits VDAC1 conductance in a mouse model of inherited ALS. Neuron 67:575-587.
Johnson JO, Mandrioli J, Benatar M, Abramzon Y, Van Deerlin VM, Trojanowski JQ, Gibbs JR, Brunetti M, Gronka S, Wuu J, Ding J, McCluskey L, Martinez-Lage M, Falcone D, Hernandez DG, Arepalli S, Chong S, Schymick JC, Rothstein J, Landi F, Wang Y-D, Calvo A, Mora G, Sabatelli M, Monsurrò MR, Battistini S, Salvi F, Spataro R, Sola P, Borghero G, Galassi G, Scholz SW, Taylor JP, Restagno G, Chiò A, Traynor BJ (2010)

Exome Sequencing Reveals VCP Mutations as a Cause of Familial ALS. Neuron 68:857-864.
Johnston JA, Dalton MJ, Gurney ME, Kopito RR (2000) Formation of high molecular weight complexes of mutant Cu, Zn-superoxide dismutase in a mouse model for familial amyotrophic lateral sclerosis. Proc Natl Acad Sci U S A 97:12571-12576.
Ju JS, Fuentealba RA, Miller SE, Jackson E, Piwnica-Worms D, Baloh RH, Weihl CC (2009) Valosin-containing protein (VCP) is required for autophagy and is disrupted in VCP disease. J Cell Biol 187:875-888.
Jung CW, Higgins CMJ, Xu ZS (2002) A quantitative histochemical assay for activities of mitochondrial electron transport chain complexes in mouse spinal cord sections. J Neurosci Methods 114:165-172.
Kabashi E, Agar JN, Taylor DM, Minotti S, Durham HD (2004) Focal dysfunction of the proteasome: a pathogenic factor in a mouse model of amyotrophic lateral sclerosis. J Neurochem 89:1325-1335.
Kabashi E, Valdmanis PN, Dion P, Spiegelman D, McConkey BJ, Velde CV, Bouchard JP, Lacomblez L, Pochigaeva K, Salachas F, Pradat PF, Camu W, Meininger V, Dupre N, Rouleau GA (2008) TARDBP mutations in individuals with sporadic and familial amyotrophic lateral sclerosis. Nature Genetics 40:572-574.
Kabuta T, Setsuie R, Mitsui T, Kinugawa A, Sakurai M, Aoki S, Uchida K, Wada K (2008) Aberrant molecular properties shared by familial Parkinson's disease-associated mutant UCH-L1 and carbonyl-modified UCH-L1. Hum Mol Genet 17:1482-1496.
Kabuta T, Suzuki Y, Wada K (2006) Degradation of amyotrophic lateral sclerosis-linked mutant Cu,Zn-superoxide dismutase proteins by macroautophagy and the proteasome. J Biol Chem 281:30524-30533.
Kappe G, Verschuure P, Philipsen RL, Staalduinen AA, Van de Boogaart P, Boelens WC, De Jong WW (2001) Characterization of two novel human small heat shock proteins: protein kinase-related HspB8 and testis-specific HspB9. Biochim Biophys Acta 1520:1-6.
Karlberg O, Canback B, Kurland CG, Andersson SG (2000) The dual origin of the yeast mitochondrial proteome. Yeast (Chichester, England) 17:170-187.
Kato S, Horiuchi S, Nakashima K, Hirano A, Shibata N, Nakano I, Saito M, Kato M, Asayama K, Ohama E (1999) Astrocytic hyaline inclusions contain advanced glycation endproducts in familial amyotrophic lateral sclerosis with superoxide dismutase 1 gene mutation: immunohistochemical and immunoelectron microscopical analyses. Acta Neuropathol 97:260-266.
Kaufman RJ (1999) Stress signaling from the lumen of the endoplasmic reticulum: coordination of gene transcriptional and translational controls (vol 13, pg 1211, 1999). Gene Dev 13:1898-1898.
Kawamata H, Magrane J, Kunst C, King MP, Manfredi G (2008) Lysyl-tRNA synthetase is a target for mutant SOD1 toxicity in mitochondria. J Biol Chem 283:28321-28328.
Kawamata H, Manfredi G (2008) Different regulation of wild-type and mutant Cu,Zn superoxide dismutase localization in mammalian mitochondria. Hum Mol Genet 17:3303-3317.
Kawamoto Y, Ito H, Kobayashi Y, Suzuki Y, Akiguchi I, Fujimura H, Sakoda S, Kusaka H, Hirano A, Takahashi R (2010) HtrA2/Omi-immunoreactive intraneuronal inclusions in the anterior horn of patients with sporadic and Cu/Zn superoxide dismutase (SOD1) mutant amyotrophic lateral sclerosis. Neuropathol Appl Neurobiol 36:331-344.
Kayani AC, Morton JP, McArdle A (2008) The exercise-induced stress response in skeletal muscle: failure during aging. Appl Physiol Nutr Metab 33:1033-1041.
Kiaei M, Kipiani K, Petri S, Chen J, Calingasan NY, Beal MF (2005) Celastrol blocks neuronal cell death and extends life in transgenic mouse model of amyotrophic lateral sclerosis. Neurodegener Dis 2:246-254.

Kieran D, Kalmar B, Dick JR, Riddoch-Contreras J, Burnstock G, Greensmith L (2004a) Treatment with arimoclomol, a coinducer of heat shock proteins, delays disease progression in ALS mice. Nat Med 10:402-405.
Kieran D, Kalmar B, Dick JRT, Riddoch-Contreras J, Burnstock G, Greensmith L (2004b) Treatment with arimoclomol, a coinducer of heat shock proteins, delays disease progression in ALS mice. Nature Medicine 10:402-405.
Kijima K, Numakura C, Goto T, Takahashi T, Otagiri T, Umetsu K, Hayasaka K (2005) Small heat shock protein 27 mutation in a Japanese patient with distal hereditary motor neuropathy. J Hum Genet 50:473-476.
Kikuchi H, Almer G, Yamashita S, Guegan C, Nagai M, Xu Z, Sosunov AA, McKhann GM, 2nd, Przedborski S (2006) Spinal cord endoplasmic reticulum stress associated with a microsomal accumulation of mutant superoxide dismutase-1 in an ALS model. Proc Natl Acad Sci U S A 103:6025-6030.
Kim I, Rodriguez-Enriquez S, Lemasters JJ (2007) Selective degradation of mitochondria by mitophagy. Arch Biochem Biophys 462:245-253.
Kim KK, Kim R, Kim SH, Yn (1998) Crystal structure of a small heat-shock protein. Nature 394:595-599.
Kirkinezos IG, Bacman SR, Hernandez D, Oca-Cossio J, Arias LJ, Perez-Pinzon MA, Bradley WG, Moraes CT (2005) Cytochrome c Association with the Inner Mitochondrial Membrane Is Impaired in the CNS of G93A-SOD1 Mice. J Neurosci 25:164-172.
Kiselyov K, Jennigs JJ, Rbaibi Y, Chu CT (2007) Autophagy, mitochondria and cell death in lysosomal storage diseases. Autophagy 3:259-262.
Klionsky DJ (2007) Autophagy: from phenomenology to molecular understanding in less than a decade. Nat Rev Mol Cell Bio 8:931-937.
Koerner DR (1952) Amyotrophic Lateral Sclerosis on Guam - a Clinical Study and Review of the Literature. Ann Intern Med 37:1204-1220.
Kokubo Y, Kuzuhara S, Narita Y, Kikugawa K, Nakano R, Inuzuka T, Tsuji S, Watanabe M, Miyazaki T, Murayama S, Ihara Y (1999) Accumulation of neurofilaments and SOD1-immunoreactive products in a patient with familial amyotrophic lateral sclerosis with I113T SOD1 mutation. Arch Neurol 56:1506-1508.
Komatsu M, Waguri S, Chiba T, Murata S, Iwata J-i, Tanida I, Ueno T, Koike M, Uchiyama Y, Kominami E, Tanaka K (2006) Loss of autophagy in the central nervous system causes neurodegeneration in mice. Nature 441:880-884.
Kong JM, Xu ZS (1998) Massive mitochondrial degeneration in motor neurons triggers the onset of amyotrophic lateral sclerosis in mice expressing a mutant SOD1. Journal of Neuroscience 18:3241-3250.
Kostic V, Jackson-Lewis V, de Bilbao F, Dubois-Dauphin M, Przedborski S (1997) Bcl-2: prolonging life in a transgenic mouse model of familial amyotrophic lateral sclerosis. Science 277:559-562.
Kouroku Y, Fujita E, Tanida I, Ueno T, Isoai A, Kumagai H, Ogawa S, Kaufman RJ, Kominami E, Momoi T (2007) ER stress (PERK/eIF2alpha phosphorylation) mediates the polyglutamine-induced LC3 conversion, an essential step for autophagy formation. Cell Death Differ 14:230-239.
Kovacs AL, Reith A, Seglen PO (1982) Accumulation of auto-phagosomes after inhibition of hepatocytic protein-degradation by vinblastine, leupeptin or a lysosomotropic amine. Exp Cell Res 137:191-201.
Koyama S, Arawaka S, Chang-Hong R, Wada M, Kawanami T, Kurita K, Kato M, Nagai M, Aoki M, Itoyama Y, Sobue G, Chan PH, Kato T (2006) Alteration of familial ALS-linked mutant SOD1 solubility with disease progression: Its modulation by the proteasome and Hsp70. Biochem Bioph Res Co 343:719-730.

Krishnan J, Vannuvel K, Andries M, Waelkens E, Robberecht W, Van Den Bosch L (2008) Over-expression of Hsp27 does not influence disease in the mutant SOD1(G93A) mouse model of amyotrophic lateral sclerosis. Journal of Neurochemistry 106:2170-2183.

Kurland LT, Mulder DW (1954) Epidemiologic Investigations of Amyotrophic Lateral Sclerosis .1. Preliminary Report on Geographic Distribution, with Special Reference to the Mariana Islands, Including Clinical and Pathologic Observations. Neurology 4:438-448.

Kwiatkowski TJ, Bosco DA, LeClerc AL, Tamrazian E, Vanderburg CR, Russ C, Davis A, Gilchrist J, Kasarskis EJ, Munsat T, Valdmanis P, Rouleau GA, Hosler BA, Cortelli P, de Jong PJ, Yoshinaga Y, Haines JL, Pericak-Vance MA, Yan J, Ticozzi N, Siddique T, McKenna-Yasek D, Sapp PC, Horvitz HR, Landers JE, Brown RH (2009) Mutations in the FUS/TLS Gene on Chromosome 16 Cause Familial Amyotrophic Lateral Sclerosis. Science 323:1205-1208.

Lee GJ, Roseman AM, Saibil HR, Vierling E (1997) A small heat shock protein stably binds heat-denatured model substrates and can maintain a substrate in a folding-competent state. Embo Journal 16:659-671.

Lee JH, Yu WH, Kumar A, Lee S, Mohan PS, Peterhoff CM, Wolfe DM, Martinez-Vicente M, Massey AC, Sovak G, Uchiyama Y, Westaway D, Cuervo AM, Nixon RA (2010) Lysosomal proteolysis and autophagy require presenilin 1 and are disrupted by Alzheimer-related PS1 mutations. Cell 141:1146-1158.

Leonhard K, Stiegler A, Neupert W, Langer T (1999) Chaperone-like activity of the AAA domain of the yeast Yme1 AAA protease. Nature 398:348-351.

Lewis SE, Mannion RJ, White FA, Coggeshall RE, Beggs S, Costigan M, Martin JL, Dillmann WH, Woolf CJ (1999) A Role for HSP27 in Sensory Neuron Survival. J Neurosci 19:8945-8953.

Li L, Zhang X, Le W (2008) Altered macroautophagy in the spinal cord of SOD1 mutant mice. Autophagy 4:290-293.

Li MW, Ona VO, Guegan C, Chen MH, Jackson-Lewis V, Andrews LJ, Olszewski AJ, Stieg PE, Lee JP, Przedborski S, Friedlander RM (2000) Functional role of caspase-1 and caspase-3 in an ALS transgenic mouse model. Science 288:335-339.

Lindberg MJ, Bystrom R, Boknas N, Andersen PM, Oliveberg M (2005) Systematically perturbed folding patterns of amyotrophic lateral sclerosis (ALS)-associated SOD1 mutants. Proceedings of the National Academy of Sciences of the United States of America 102:9754-9759.

Liu J, Lillo C, Jonsson PA, Vande Velde C, Ward CM, Miller TM, Subramaniam JR, Rothstein JD, Marklund S, Andersen PM, Brannstrom T, Gredal O, Wong PC, Williams DS, Cleveland DW (2004) Toxicity of familial ALS-linked SOD1 mutants from selective recruitment to spinal mitochondria. Neuron 43:5-17.

Liu J, Shinobu LA, Ward CM, Young D, Cleveland DW (2005a) Elevation of the Hsp70 chaperone does not effect toxicity in mouse models of familial amyotrophic lateral sclerosis. Journal of Neurochemistry 93:875-882.

Liu XM, Tang BS, Zhao GH, Xia K, Zhang FF, Pan Q, Cai F, Hu ZM, Zhang C, Chen B, Shen L, Zhang RX, Jiang H (2005b) [Mutation analysis of small heat shock protein 27 gene in Chinese patients with Charcot-Marie-Tooth disease]. Zhonghua Yi Xue Yi Chuan Xue Za Zhi 22:510-513.

Liu Y, Chang A (2008) Heat shock response relieves ER stress. EMBO J 27:1049-1059.

Maatkamp A, Vlug A, Haasdijk E, Troost D, French PJ, Jaarsma D (2004) Decrease of Hsp25 protein expression precedes degeneration of motoneurons in ALS-SOD1 mice. European Journal of Neuroscience 20:14-28.

Mackenzie IRA, Bigio EH, Ince PG, Geser F, Neumann M, Cairns NJ, Kwong LK, Forman MS, Ravits J, Stewart H, Eisen A, Mcclusky L, Kretzschmar HA, Monoranu CM, Highley JR, Kirby J, Siddique T, Shaw PJ, Lee VMY, Trojanowski JQ (2007) Pathological TDP-43

distinguishes sporadic amyotrophic lateral sclerosis from amyotrophic lateral sclerosis with SOD1 mutations. Annals of Neurology 61:427-434.
Magrane J, Hervias I, Henning MS, Damiano M, Kawamata H, Manfredi G (2009) Mutant SOD1 in neuronal mitochondria causes toxicity and mitochondrial dynamics abnormalities. Hum Mol Genet 18:4552-4564.
Mai S, Klinkenberg M, Auburger G, Bereiter-Hahn J, Jendrach M (2010) Decreased expression of Drp1 and Fis1 mediates mitochondrial elongation in senescent cells and enhances resistance to oxidative stress through PINK1. J Cell Sci 123:917-926.
Mailhos C, Howard MK, Latchman DS (1993) Heat shock protects neuronal cells from programmed cell death by apoptosis. Neuroscience 55:621-627.
Manfredi G, Xu Z (2005) Mitochondrial dysfunction and its role in motor neuron degeneration in ALS. Mitochondrion 5:77-87.
Martins LM, Morrison A, Klupsch K, Fedele V, Moisoi N, Teismann P, Abuin A, Grau E, Geppert M, Livi GP, Creasy CL, Martin A, Hargreaves I, Heales SJ, Okada H, Brandner S, Schulz JB, Mak T, Downward J (2004) Neuroprotective role of the Reaper-related serine protease HtrA2/Omi revealed by targeted deletion in mice. Mol Cell Biol 24:9848-9862.
Maruyama H, Morino H, Ito H, Izumi Y, Kato H, Watanabe Y, Kinoshita Y, Kamada M, Nodera H, Suzuki H, Komure O, Matsuura S, Kobatake K, Morimoto N, Abe K, Suzuki N, Aoki M, Kawata A, Hirai T, Kato T, Ogasawara K, Hirano A, Takumi T, Kusaka H, Hagiwara K, Kaji R, Kawakami H (2010) Mutations of optineurin in amyotrophic lateral sclerosis. Nature advance online publication.
Mattiazzi M, D'Aurelio M, Gajewski CD, Martushova K, Kiaei M, Beal MF, Manfredi G (2002) Mutated human SOD1 causes dysfunction of oxidative phosphorylation in mitochondria of transgenic mice. J Biol Chem 277:29626-29633.
Mayer B, Oberbauer R (2003) Mitochondrial Regulation of Apoptosis. News Physiol Sci 18:89-94.
McCord JM, Fridovich I (1969) Superoxide dismutase. An enzymic function for erythrocuprein (hemocuprein). J Biol Chem 244:6049-6055.
McGeer PL, McGeer EG (2002) Inflammatory processes in amyotrophic lateral sclerosis. Muscle & Nerve 26:459-470.
Meikle ADS, Martin AH (1981) A Rapid Method for Removal of the Spinal Cord. Biotechnic & Histochemistry 56:235-237.
Menzies FM, Cookson MR, Taylor RW, Turnbull DM, Chrzanowska-Lightowlers ZM, Dong L, Figlewicz DA, Shaw PJ (2002a) Mitochondrial dysfunction in a cell culture model of familial amyotrophic lateral sclerosis. Brain 125:1522-1533.
Menzies FM, Cookson MR, Taylor RW, Turnbull DM, Chrzanowska-Lightowlers ZMA, Dong LC, Figlewicz DA, Shaw PJ (2002b) Mitochondrial dysfunction in a cell culture model of familial amyotrophic lateral sclerosis. Brain 125:1522-1533.
Mesecke N, Terziyska N, Kozany C, Baumann F, Neupert W, Hell K, Herrmann JM (2005) A disulfide relay system in the intermembrane space of mitochondria that mediates protein import. Cell 121:1059-1069.
Milani M, Rzymski T, Mellor HR, Pike L, Bottini A, Generali D, Harris AL (2009) The role of ATF4 stabilization and autophagy in resistance of breast cancer cells treated with Bortezomib. Cancer Res 69:4415-4423.
Miller KE, Sheetz MP (2004) Axonal mitochondrial transport and potential are correlated. J Cell Sci 117:2791-2804.
Miller RG, Mitchell JD, Lyon M, Moore DH (2003) Riluzole for amyotrophic lateral sclerosis (ALS)/motor neuron disease (MND). Amyotroph Lateral Scler Other Motor Neuron Disord 4:191-206.
Moisoi N, Klupsch K, Fedele V, East P, Sharma S, Renton A, Plun-Favreau H, Edwards RE, Teismann P, Esposti MD, Morrison AD, Wood NW, Downward J, Martins LM (2009)

Mitochondrial dysfunction triggered by loss of HtrA2 results in the activation of a brain-specific transcriptional stress response. Cell Death Differ 16:449-464.
Monastyrska I, Klionsky DJ (2006) Autophagy in organelle homeostasis: peroxisome turnover. Mol Aspects Med 27:483-494.
Morimoto N, Nagai M, Ohta Y, Miyazaki K, Kurata T, Morimoto M, Murakami T, Takehisa Y, Ikeda Y, Kamiya T, Abe K (2007) Increased autophagy in transgenic mice with a G93A mutant SOD1 gene. Brain Res 1167:112-117.
Morimoto RI (1998) Regulation of the heat shock transcriptional response: cross talk between a family of heat shock factors, molecular chaperones, and negative regulators. Gene Dev 12:3788-3796.
Morimoto RI, Kline MP, Bimston DN, Cotto JJ (1997) The heat-shock response: regulation and function of heat-shock proteins and molecular chaperones. Essays in Biochemistry, Vol 32, 1997 32:17-29.
Naidoo N, Ferber M, Master M, Zhu Y, Pack AI (2008) Aging impairs the unfolded protein response to sleep deprivation and leads to proapoptotic signaling. J Neurosci 28:6539-6548.
Nakagawa T, Zhu H, Morishima N, Li E, Xu J, Yankner BA, Yuan J (2000) Caspase-12 mediates endoplasmic-reticulum-specific apoptosis and cytotoxicity by amyloid-beta. Nature 403:98-103.
Nakai A, Yamaguchi O, Takeda T, Higuchi Y, Hikoso S, Taniike M, Omiya S, Mizote I, Matsumura Y, Asahi M, Nishida K, Hori M, Mizushima N, Otsu K (2007) The role of autophagy in cardiomyocytes in the basal state and in response to hemodynamic stress. Nat Med 13:619-624.
Narendra DP, Jin SM, Tanaka A, Suen DF, Gautier CA, Shen J, Cookson MR, Youle RJ (2010) PINK1 Is Selectively Stabilized on Impaired Mitochondria to Activate Parkin. Plos Biology 8:-.
Neumann M, Sampathu DM, Kwong LK, Truax AC, Micsenyi MC, Chou TT, Bruce J, Schuck T, Grossman M, Clark CM, McCluskey LF, Miller BL, Masliah E, Mackenzie IR, Feldman H, Feiden W, Kretzschmar HA, Trojanowski JQ, Lee VMY (2006) Ubiquitinated TDP-43 in frontotemporal lobar degeneration and amyotrophic lateral sclerosis. Science 314:130-133.
Neutzner A, Benard G, Youle RJ, Karbowski M (2008) Role of the Ubiquitin Conjugation System in the Maintenance of Mitochondrial Homeostasis. Annals of the New York Academy of Sciences 1147:242-253.
Nicholson SJ, Witherden AS, Hafezparast M, Martin JE, Fisher EMC (2000) Mice, the motor system, and human motor neuron pathology. Mamm Genome 11:1041-1052.
Nishimura AL, Mitne-Neto M, Silva HCA, Oliveira JRM, Vainzof M, Zatz M (2004) A novel locus for late onset amyotrophic lateral sclerosis/motor neurone disease variant at 20q13. J Med Genet 41:315-320.
Nishitoh H, Kadowaki H, Nagai A, Maruyama T, Yokota T, Fukutomi H, Noguchi T, Matsuzawa A, Takeda K, Ichijo H (2008) ALS-linked mutant SOD1 induces ER stress- and ASK1-dependent motor neuron death by targeting Derlin-1. Genes Dev 22:1451-1464.
Nixon RA, Wegiel J, Kumar A, Yu WH, Peterhoff C, Cataldo A, Cuervo AM (2005) Extensive involvement of autophagy in Alzheimer disease: an immuno-electron microscopy study. J Neuropathol Exp Neurol 64:113-122.
Nolden M, Ehses S, Koppen M, Bernacchia A, Rugarli EI, Langer T (2005) The m-AAA protease defective in hereditary spastic paraplegia controls ribosome assembly in mitochondria. Cell 123:277-289.
Okado-Matsumoto A, Fridovich I (2001) Subcellular Distribution of Superoxide Dismutases (SOD) in Rat Liver. J Biol Chem 276:38388-38393.
Okado-Matsumoto A, Fridovich I (2002) Amyotrophic lateral sclerosis: A proposed mechanism. Proceedings of the National Academy of Sciences of the United States of America 99:9010-9014.

Orrell RW (2000) Amyotrophic lateral sclerosis: copper/zinc superoxide dismutase (SOD1) gene mutations. Neuromuscul Disord 10:63-68.
Pardo CA, Xu ZS, Borchelt DR, Price DL, Sisodia SS, Cleveland DW (1995) Superoxide-Dismutase Is an Abundant Component in Cell-Bodies, Dendrites, and Axons of Motor-Neurons and in a Subset of Other Neurons. Proceedings of the National Academy of Sciences of the United States of America 92:954-958.
Parton MJ, Broom W, Andersen PM, Al-Chalabi A, Nigel Leigh P, Powell JF, Shaw CE (2002) D90A-SOD1 mediated amyotrophic lateral sclerosis: a single founder for all cases with evidence for a Cis-acting disease modifier in the recessive haplotype. Hum Mutat 20:473.
Pasinelli P, Belford ME, Lennon N, Bacskai BJ, Hyman BT, Trotti D, Brown RH, Jr. (2004) Amyotrophic lateral sclerosis-associated SOD1 mutant proteins bind and aggregate with Bcl-2 in spinal cord mitochondria. Neuron 43:19-30.
Patel YJK, Payne Smith MD, de Belleroche J, Latchman DS (2005a) Hsp27 and Hsp70 administered in combination have a potent protective effect against FALS-associated SOD1-mutant-induced cell death in mammalian neuronal cells. Brain Res Mol Brain Res 134:256-274.
Patel YJK, Smith MDP, de Belleroche J, Latchman DS (2005b) Hsp27 and Hsp70 administered in combination have a potent protective effect against FALS-associated SOD1-mutant-induced cell death in mammalian neuronal cells. Molecular Brain Research 134:256-274.
Paz Gavilan M, Vela J, Castano A, Ramos B, del Rio JC, Vitorica J, Ruano D (2006) Cellular environment facilitates protein accumulation in aged rat hippocampus. Neurobiol Aging 27:973-982.
Plun-Favreau H, Klupsch K, Moisoi N, Gandhi S, Kjaer S, Frith D, Harvey K, Deas E, Harvey RJ, McDonald N, Wood NW, Martins LM, Downward J (2007) The mitochondrial protease HtrA2 is regulated by Parkinson's disease-associated kinase PINK1. Nat Cell Biol 9:1243-1252.
Prudencio M, Hart PJ, Borchelt DR, Andersen PM (2009) Variation in aggregation propensities among ALS-associated variants of SOD1: Correlation to human disease. Hum Mol Genet 18:3217-3226.
Puls I, Jonnakuty C, LaMonte BH, Holzbaur EL, Tokito M, Mann E, Floeter MK, Bidus K, Drayna D, Oh SJ, Brown RH, Jr., Ludlow CL, Fischbeck KH (2003) Mutant dynactin in motor neuron disease. Nat Genet 33:455-456.
Puttaparthi K, Wojcik C, Rajendran B, DeMartino GN, Elliott JL (2003) Aggregate formation in the spinal cord of mutant SOD1 transgenic mice is reversible and mediated by proteasomes. Journal of Neurochemistry 87:851-860.
Rabek JP, Boylston WH, 3rd, Papaconstantinou J (2003) Carbonylation of ER chaperone proteins in aged mouse liver. Biochem Biophys Res Commun 305:566-572.
Raimondi A, Mangolini A, Rizzardini M, Tartari S, Massari S, Bendotti C, Francolini M, Borgese N, Cantoni L, Pietrini G (2006) Cell culture models to investigate the selective vulnerability of motoneuronal mitochondria to familial ALS-linked G93ASOD1. Eur J Neurosci 24:387-399.
Rainey RN, Glavin JD, Chen HW, French SW, Teitell MA, Koehler CM (2006) A new function in translocation for the mitochondrial i-AAA protease Yme1: Import of polynucleotide phosphorylase into the intermembrane space. Mol Cell Biol 26:8488-8497.
Ravits J, Paul P, Jorg C (2007) Focality of upper and lower motor neuron degeneration at the clinical onset of ALS. Neurology 68:1571-1575.
Ravits JM, La Spada AR (2009) ALS motor phenotype heterogeneity, focality, and spread Deconstructing motor neuron degeneration. Neurology 73:805-811.
Reaume AG, Elliott JL, Hoffman EK, Kowall NW, Ferrante RJ, Siwek DF, Wilcox HM, Flood DG, Beal MF, Brown RH, Jr., Scott RW, Snider WD (1996) Motor neurons in Cu/Zn

superoxide dismutase-deficient mice develop normally but exhibit enhanced cell death after axonal injury. Nat Genet 13:43-47.
Rideout HJ, Lang-Rollin IC, Stefanis L (2004) Involvement of macroautophagy in the dissolution of neuronal inclusions. Movement Disord 19:S30-S30.
Roe JA, Butler A, Scholler DM, Valentine JS, Marky L, Breslauer KJ (1988) Differential Scanning Calorimetry of Cu,Zn-Superoxide Dismutase, the Apoprotein, and Its Zinc-Substituted Derivatives. Biochemistry-Us 27:950-958.
Roesch K, Curran SP, Tranebjaerg L, Koehler CM (2002) Human deafness dystonia syndrome is caused by a defect in assembly of the DDP1/TIMM8a-TIMM13 complex. Human Molecular Genetics 11:477-486.
Rosen DR (1993) Mutations in Cu/Zn superoxide dismutase gene are associated with familial amyotrophic lateral sclerosis. Nature 364:362.
Rosen DR, Bowling AC, Patterson D, Usdin TB, Sapp P, Mezey E, Mckennayasek D, Oregan J, Rahmani Z, Ferrante RJ, Brownstein MJ, Kowall NW, Beal MF, Horvitz HR, Brown RH (1994) A Frequent Ala-4 to Val Superoxide Dismutase-1 Mutation Is Associated with a Rapidly Progressive Familial Amyotrophic-Lateral-Sclerosis. Human Molecular Genetics 3:981-987.
Rutkowski DT, Kaufman RJ (2004) A trip to the ER: coping with stress. Trends Cell Biol 14:20-28.
Sanbe A, Yamauchi J, Miyamoto Y, Fujiwara Y, Murabe M, Tanoue A (2007) Interruption of CryAB-Amyloid oligomer formation by HSP22. J Biol Chem 282:555-563.
Santti H, Mikkonen L, Anand A, Hirvonen-Santti S, Toppari J, Panhuysen M, Vauti F, Perera M, Corte G, Wurst W, Janne OA, Palvimo JJ (2005) Disruption of the murine PIASx gene results in reduced testis weight. J Mol Endocrinol 34:645-654.
Sapp PC, Hosler BA, McKenna-Yasek D, Chin W, Gann A, Genise H, Gorenstein J, Huang M, Sailer W, Scheffler M, Valesky M, Haines JL, Pericak-Vance M, Siddique T, Horvitz HR, Brown RH, Jr. (2003) Identification of two novel loci for dominantly inherited familial amyotrophic lateral sclerosis. Am J Hum Genet 73:397-403.
Sasaki S, Iwata M (1996) Dendritic synapses of anterior horn neurons in amyotrophic lateral sclerosis: an ultrastructural study. Acta Neuropathol 91:278-283.
Sasaki S, Iwata M (2007) Mitochondrial alterations in the spinal cord of patients with sporadic amyotrophic lateral sclerosis. J Neuropathol Exp Neurol 66:10-16.
Sassa H, Takaishi Y, Terada H (1990) The Triterpene Celastrol as a Very Potent Inhibitor of Lipid-Peroxidation in Mitochondria. Biochem Bioph Res Co 172:890-897.
Saxena S, Cabuy E, Caroni P (2009) A role for motoneuron subtype-selective ER stress in disease manifestations of FALS mice. Nat Neurosci 12:627-636.
Schatz G, Dobberstein B (1996) Common principles of protein translocation across membranes. Science 271:1519-1526.
Schlieker C, Mogk A, Bukau B (2004) A PDZ Switch for a Cellular Stress Response. Cell 117:417-419.
Schymick JC, Talbot K, Traynor BJ (2007) Genetics of sporadic amyotrophic lateral sclerosis. Human Molecular Genetics 16:R233-R242.
Shamovsky I, Gershon D (2004) Novel regulatory factors of HSF-1 activation: facts and perspectives regarding their involvement in the age-associated attenuation of the heat shock response. Mech Ageing Dev 125:767-775.
Sharp P, Krishnan M, Pullar O, Navarrete R, Wells D, de Belleroche J (2006) Heat shock protein 27 rescues motor neurons following nerve injury and preserves muscle function. Exp Neurol 198:511-518.
Shaw BF, Valentine JS (2007) How do ALS-associated mutations in superoxide dismutase 1 promote aggregation of the protein? Trends in Biochemical Sciences 32:78-85.
Shaw P, Eggett C (2000) Molecular factors underlying selective vulnerability of motor neurons to neurodegeneration in amyotrophic lateral sclerosis. Journal of Neurology 247:I17-I27.

Shibata N, Hirano A, Kobayashi M, Siddique T, Deng HX, Hung WY, Kato T, Asayama K (1996) Intense superoxide dismutase-1 immunoreactivity in intracytoplasmic hyaline inclusions of familial amyotrophic lateral sclerosis with posterior column involvement. J Neuropath Exp Neur 55:481-490.

Shinder GA, Lacourse MC, Minotti S, Durham HD (2001) Mutant Cu/Zn-superoxide dismutase proteins have altered solubility and interact with heat shock/stress proteins in models of amyotrophic lateral sclerosis. J Biol Chem 276:12791-12796.

Stetler RA, Cao G, Gao Y, Zhang F, Wang S, Weng Z, Vosler P, Zhang L, Signore A, Graham SH, Chen J (2008) Hsp27 Protects against Ischemic Brain Injury via Attenuation of a Novel Stress-Response Cascade Upstream of Mitochondrial Cell Death Signaling. J Neurosci 28:13038-13055.

Strauss KM, Martins LM, Plun-Favreau H, Marx FP, Kautzmann S, Berg D, Gasser T, Wszolek Z, Muller T, Bornemann A, Wolburg H, Downward J, Riess O, Schulz JB, Kruger R (2005) Loss of function mutations in the gene encoding Omi/HtrA2 in Parkinson's disease. Hum Mol Genet 14:2099-2111.

Sturtz LA, Diekert K, Jensen LT, Lill R, Culotta VC (2001) A fraction of yeast Cu,Zn-superoxide dismutase and its metallochaperone, CCS, localize to the intermembrane space of mitochondria. A physiological role for SOD1 in guarding against mitochondrial oxidative damage. J Biol Chem 276:38084-38089.

Sun XK, Fontaine JM, Rest JS, Shelden EA, Welsh MJ, Benndorf R (2004) Interaction of human HSP22 (HSPB8) with other small heat shock proteins. J Biol Chem 279:2394-2402.

Tainer JA, Getzoff ED, Beem KM, Richardson JS, Richardson DC (1982) Determination and analysis of the 2 A-structure of copper, zinc superoxide dismutase. J Mol Biol 160:181-217.

Takeshige K, Baba M, Tsuboi S, Noda T, Ohsumi Y (1992) Autophagy in yeast demonstrated with proteinase-deficient mutants and conditions for its induction. The Journal of Cell Biology 119:301-311.

Takeuchi H, Kobayashi Y, Ishigaki S, Doyu M, Sobue G (2002a) Mitochondrial localization of mutant superoxide dismutase 1 triggers caspase-dependent cell death in a cellular model of familial amyotrophic lateral sclerosis. J Biol Chem 277:50966-50972.

Takeuchi H, Kobayashi Y, Yoshihara T, Niwa J, Doyu M, Ohtsuka K, Sobue G (2002b) Hsp70 and Hsp40 improve neurite outgrowth and suppress intracytoplasmic aggregate formation in cultured neuronal cells expressing mutant SOD1. Brain Res 949:11-22.

Talbot K (2002) Motor neurone disease. Postgraduate Medical Journal 78:513-519.

Talbot K (2009) Motor neuron disease. Practical Neurology 9:303-309.

Tanaka F, Niwa J, Ishigaki S, Katsuno M, Waza M, Yamamoto M, Doyu M, Sobue G (2006) Gene expression profiling toward understanding of ALS pathogenesis. Integrated Molecular Medicine for Neuronal and Neoplastic Disorders 1086:1-10.

Tang BS, Luo W, Xia K, Xiao JF, Jiang H, Shen L, Tang JG, Zhao GH, Cai F, Pan Q, Dai HP, Yang QD, Xia JH, Evgrafov OV (2004) A new locus for autosomal dominant Charcot-Marie-Tooth disease type 2 (CMT2L) maps to chromosome 12q24. Hum Genet 114:527-533.

Tang BS, Zhao GH, Luo W, Xia K, Cai F, Pan Q, Zhang RX, Zhang FF, Liu XM, Chen B, Zhang C, Shen L, Jiang H, Long ZG, Dai HP (2005) Small heat-shock protein 22 mutated in autosomal dominant Charcot-Marie-Tooth disease type 2L. Hum Genet 116:222-224.

Tanida I, Minematsu-Ikeguchi N, Ueno T, Kominami E (2005) Lysosomal turnover, but not a cellular level, of endogenous LC3 is a marker for autophagy. Autophagy 1:84-91.

Tebbenkamp ATN, Borchelt DR (2010) Analysis of Chaperone mRNA Expression in the Adult Mouse Brain by Meta Analysis of the Allen Brain Atlas. Plos One 5:e13675.

Tiwari A, Hayward LJ (2003) Familial amyotrophic lateral sclerosis mutants of copper/zinc superoxide dismutase are susceptible to disulfide reduction. J Biol Chem 278:5984-5992.

Tobisawa S, Hozumi Y, Arawaka S, Koyama S, Wada M, Nagai M, Aoki M, Itoyama Y, Goto K, Kato T (2003) Mutant SOD1 linked to familial amyotrophic lateral sclerosis, but not wild-type SOD1, induces ER stress in COS7 cells and transgenic mice. Biochem Bioph Res Co 303:496-503.

Traynor BJ, Alexander M, Corr B, Frost E, Hardiman O (2003) An outcome study of riluzole in amyotrophic lateral sclerosis--a population-based study in Ireland, 1996-2000. J Neurol 250:473-479.

Tummala H, Jung C, Tiwari A, Higgins CMJ, Hayward LJ, Xu ZS (2005) Inhibition of chaperone activity is a shared property of several Cu,Zn-superoxide dismutase mutants that cause amyotrophic lateral sclerosis. J Biol Chem 280:17725-17731.

Turner BJ, Talbot K (2008) Transgenics, toxicity and therapeutics in rodent models of mutant SOD1-mediated familial ALS. Prog Neurobiol 85:94-134.

Tzagoloff A, Myers AM (1986) Genetics of Mitochondrial Biogenesis. Annual review of biochemistry 55:249-285.

Urano F, Wang XZ, Bertolotti A, Zhang YH, Chung P, Harding HP, Ron D (2000) Coupling of stress in the ER to activation of JNK protein kinases by transmembrane protein kinase IRE1. Science 287:664-666.

Urushitani M, Kurisu J, Tateno M, Hatakeyama S, Nakayama KI, Kato S, Takahashi R (2004) CHIP promotes proteasomal degradation of familial ALS-linked mutant SOD1 by ubiquitinating Hsp/Hsc70. Journal of Neurochemistry 90:231-244.

Urushitani M, Kurisu J, Tsukita K, Takahashi R (2002) Proteasomal inhibition by misfolded mutant superoxide dismutase 1 induces selective motor neuron death in familial amyotrophic lateral sclerosis. J Neurochem 83:1030-1042.

Valente EM, Abou-Sleiman PM, Caputo V, Muqit MM, Harvey K, Gispert S, Ali Z, Del Turco D, Bentivoglio AR, Healy DG, Albanese A, Nussbaum R, Gonzalez-Maldonado R, Deller T, Salvi S, Cortelli P, Gilks WP, Latchman DS, Harvey RJ, Dallapiccola B, Auburger G, Wood NW (2004) Hereditary early-onset Parkinson's disease caused by mutations in PINK1. Science 304:1158-1160.

Van Montfort R, Slingsby C, Vierling E (2002) Structure and function of the small heat shock protein/alpha-crystallin family of molecular chaperones. Protein Folding in the Cell 59:105-156.

van Montfort RLM, Basha E, Friedrich KL, Slingsby C, Vierling E, Rm (2001) Crystal structure and assembly of a eukaryotic small heat shock protein. Nat Struct Biol 8:1025-1030.

Vance C, Rogelj B, Hortobagyi T, De Vos KJ, Nishimura AL, Sreedharan J, Hu X, Smith B, Ruddy D, Wright P, Ganesalingam J, Williams KL, Tripathi V, Al-Saraj S, Al-Chalabi A, Leigh PN, Blair IP, Nicholson G, de Belleroche J, Gallo JM, Miller CC, Shaw CE (2009) Mutations in FUS, an RNA Processing Protein, Cause Familial Amyotrophic Lateral Sclerosis Type 6. Science 323:1208-1211.

Vande Velde C, Miller TM, Cashman NR, Cleveland DW (2008) Selective association of misfolded ALS-linked mutant SOD1 with the cytoplasmic face of mitochondria. Proc Natl Acad Sci U S A 105:4022-4027.

Vives-Bauza C, Zhou C, Huang Y, Cui M, de Vries RLA, Kim J, May J, Tocilescu MA, Liu WC, Ko HS, Magrane J, Moore DJ, Dawson VL, Grailhe R, Dawson TM, Li CJ, Tieu K, Przedborski S (2010) PINK1-dependent recruitment of Parkin to mitochondria in mitophagy. Proceedings of the National Academy of Sciences of the United States of America 107:378-383.

Vleminckx V, Van Damme P, Goffin K, Delye H, Van den Bosch L, Robberecht W (2002) Upregulation of HSP27 in a transgenic model of ALS. J Neuropath Exp Neur 61:968-974.

Vukosavic S, Dubois-Dauphin M, Romero N, Przedborski S (1999) Bax and Bcl-2 interaction in a transgenic mouse model of familial amyotrophic lateral sclerosis. J Neurochem 73:2460-2468.

Wagstaff MJD, CollaÃ§o-Moraes Y, Smith J, de Belleroche JS, Coffin RS, Latchman DS (1999) Protection of Neuronal Cells from Apoptosis by Hsp27 Delivered with a Herpes Simplex Virus-based Vector. Journal of Biological Chemistry 274:5061-5069.
Wang J, Slunt H, Gonzales V, Fromholt D, Coonfield M, Copeland NG, Jenkins NA, Borchelt DR (2003) Copper-binding-site-null SOD1 causes ALS in transgenic mice: aggregates of non-native SOD1 delineate a common feature. Hum Mol Genet 12:2753-2764.
Wang J, Xu G, Borchelt DR (2002) High molecular weight complexes of mutant superoxide dismutase 1: Age-dependent and tissue-specific accumulation. Neurobiol Dis 9:139-148.
Wate R, Ito H, Zhang JH, Ohnishi S, Nakano S, Kusaka H (2005) Expression of an endoplasmic reticulum-resident chaperone, glucose-regulated stress protein 78, in the spinal cord of a mouse model of amyotrophic lateral sclerosis. Acta Neuropathol 110:557-562.
Webb JL, Ravikumar B, Atkins J, Skepper JN, Rubinsztein DC (2003) alpha-synuclein is degraded by both autophagy and the proteasome. J Biol Chem 278:25009-25013.
Weber ER, Hanekamp T, Thorsness PE (1996) Biochemical and functional analysis of the YME1 gene product, an ATP and zinc-dependent mitochondrial protease from S. cerevisiae. Mol Biol Cell 7:307-317.
Weisiger RA, Fridovich I (1973) Superoxide dismutase. Organelle specificity. J Biol Chem 248:3582-3592.
Wilhelmus MMM, Boelens WC, Otte-Holler I, Kamps B, Kusters B, Maat-Schieman MLC, Waal RMW, Verbeek MM (2006) Small heat shock protein HspB8: its distribution in Alzheimer's disease brains and its inhibition of amyloid-beta protein aggregation and cerebrovascular amyloid-beta toxicity. Acta Neuropathol 111:139-149.
Wong PC, Pardo CA, Borchelt DR, Lee MK, Copeland NG, Jenkins NA, Sisodia SS, Cleveland DW, Price DL (1995) An adverse property of a familial ALS-linked SOD1 mutation causes motor-neuron disease characterized by vacuolar degeneration of mitochondria. Neuron 14:1105-1116.
Wootz H, Weber E, Korhonen L, Lindholm D (2006) Altered distribution and levels of cathepsind and cystatins in amyotrophic lateral sclerosis transgenic mice: Possible roles in motor neuron survival. Neuroscience 143:419-430.
Yang J, Bridges K, Chen KY, Liu AYC (2008) Riluzole Increases the Amount of Latent HSF1 for an Amplified Heat Shock Response and Cytoprotection. Plos One 3:e2864.
Yang Y, Hentati A, Deng H-X, Dabbagh O, Sasaki T, Hirano M, Hung W-Y, Ouahchi K, Yan J, Azim AC, Cole N, Gascon G, Yagmour A, Ben-Hamida M, Pericak-Vance M, Hentati F, Siddique T (2001) The gene encoding alsin, a protein with three guanine-nucleotide exchange factor domains, is mutated in a form of recessive amyotrophic lateral sclerosis. 29:160-165.
Yonashiro R, Sugiura A, Miyachi M, Fukuda T, Matsushita N, Inatome R, Ogata Y, Suzuki T, Dohmae N, Yanagi S (2009) Mitochondrial Ubiquitin Ligase MITOL Ubiquitinates Mutant SOD1 and Attenuates Mutant SOD1-induced Reactive Oxygen Species Generation. Mol Biol Cell 20:4524-4530.
Young JC, Hartl FU (2003) A stress sensor for the bacterial periplasm. Cell 113:1-2.
Zhao Q, Wang JH, Levichkin IV, Stasinopoulos S, Ryan MT, Hoogenraad NJ (2002) A mitochondrial specific stress response in mammalian cells. Embo Journal 21:4411-4419.
Zhou C, Huang Y, Shao Y, May J, Prou D, Perier C, Dauer W, Schon EA, Przedborski S (2008) The kinase domain of mitochondrial PINK1 faces the cytoplasm. Proc Natl Acad Sci U S A 105:12022-12027.
Zhu S, Stavrovskaya IG, Drozda M, Kim BY, Ona V, Li M, Sarang S, Liu AS, Hartley DM, Wu DC, Gullans S, Ferrante RJ, Przedborski S, Kristal BS, Friedlander RM (2002) Minocycline inhibits cytochrome c release and delays progression of amyotrophic lateral sclerosis in mice. Nature 417:74-78.

Zourlidou A, Gidalevitz T, Kristiansen M, Landles C, Woodman B, Wells DJ, Latchman DS, de Belleroche J, Tabrizi SJ, Morimoto RI, Bates GP (2007) Hsp27 overexpression in the R6/2 mouse model of Huntington's disease: chronic neurodegeneration does not induce Hsp27 activation. Hum Mol Genet 16:1078-1090.